

UNIVERSIDAD MIGUEL HERNANDEZ DE ELCHE
INSTITUTO DE BIOLOGIA MOLECULAR Y CELULAR

**TRPV1 STRUCTURE-
FUNCTION STUDY: ROLE
OF THE TRP DOMAIN IN
TRPV1 ALLOSTERIC
GATING**

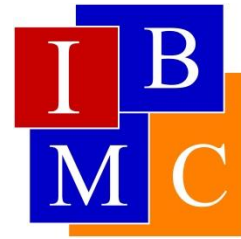
DOCTORAL THESIS

LUCIA GREGORIO TERUEL

Elche, 2013

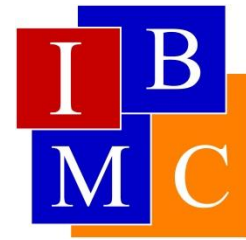
SUPERVISOR:

ANTONIO FERRER MONTIEL



Dr. Antonio Ferrer Montiel, Catedrático y Director del Instituto de Biología Molecular y Celular de la Universidad Miguel Hernández de Elche.

DA SU CONFORMIDAD a la lectura de tesis doctoral titulada: “TRPV1 Structure-Function study: Role of TRP domain in TRPV1 allosteric gating”, presentada por Dña. Lucía Gregorio Teruel.



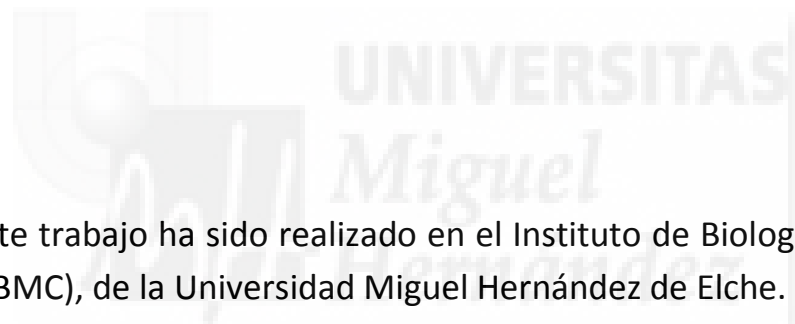
Dr. Antonio Ferrer Montiel, Catedrático de la Universidad Miguel Hernández de Elche.

CERTIFICA que el trabajo de investigación que lleva por título “TRPV1 Structure-Function study: Role of TRP domain in TRPV1 allosteric gating”, presentado por Dña. Lucía Gregorio Teruel para optar al grado de Doctor, ha sido realizado bajo su dirección en el Instituto de Biología Molecular y Celular de la Universidad Miguel Hernández de Elche.

Y para que así conste a los efectos oportunos, se expide el presente escrito.

Elche, Noviembre 2013

Dr. Antonio Ferrer Montiel



El presente trabajo ha sido realizado en el Instituto de Biología Molecular y Celular (IBMC), de la Universidad Miguel Hernández de Elche.

Lucía Gregorio Teruel ha sido beneficiaria de una beca predoctoral del Instituto de Salud Carlos III, perteneciente al Ministerio de Economía y Competitividad, PFIS- 2008.

Este trabajo se ha desarrollado gracias a la financiación procedente de Ministerio de Economía y competitividad, CONSOLIDER-INGENIO 2010 de Ministerio de Ciencia e Inovación, PROMETEO-GVA, ISIC-GVA

Small changes make a big difference.



TRPV1 STRUCTURE-FUNCTION STUDY: ROLE OF THE TRP DOMAIN IN TRPV1 ALLOSTERIC GATING

DOCTORAL THESIS

LUCIA GREGORIO TERUEL

ABSTRACT

Transient receptor potential vanilloid receptor subtype I (TRPV1) is a polymodal sensory receptor gated by chemical and physical stimuli. Akin to other TRP channels, TRPV1 contains in its C-terminus, adjacent to the pore, a highly conserved domain referred to as TRP domain. This region is necessary for both channel multimerization and correct coupling of activating sensors and channel gate. Centered in this region it appears a 6-mer sequence called TRP box which is also preserved in other TRP channels members. Previous studies have identified that changes in this area, and specifically in TRP box residues, drastically affect the channel response to all activating stimuli, thus implying a pivotal role of these residues in channel gating. We have further interrogated the role of this domain in TRPV1 function by using two complementary approaches based on site-directed mutagenesis. On one hand, we performed sequential mutations to recover the original sequence of TRP domain in TRPV1 from a non-functional chimera containing the cognate sequence from TRPV2 (TRPV1-AD2). Minor changes in this region severely affected channel response to voltage, capsaicin and heating temperatures. In turn, protein structure was also impaired by these mutations since we detected a dramatic decrease in protein expression level. Furthermore, we studied the involvement of TRP box residues I696 and W697 in TRPV1 by incorporating 18 natural L-amino acids and evaluating their impact on voltage and capsaicin gating. Analysis of the experimental data from both approaches with an allosteric model of activation indicates that mutations in this region primarily affected the equilibrium constant of gate opening and the allosteric coupling constants of ligand, voltage and temperature sensors to the channel pore. Taken together, our findings substantiate the notion that inter- and/or intra-subunit interactions at the level of the TRP box, and TRP domain, are critical for efficient coupling of stimulus sensing and gate opening. Perturbation of these interactions has a drastic impact on the efficacy and potency of the activating stimuli. Furthermore, our results signal to these interactions as potential sites for pharmacological intervention.

TRPV1 STRUCTURE-FUNCTION STUDY: ROLE OF THE TRP DOMAIN IN TRPV1 ALLOSTERIC GATING

DOCTORAL THESIS

LUCIA GREGORIO TERUEL



TRPV1 STRUCTURE-FUNCTION STUDY: ROLE OF THE TRP DOMAIN IN TRPV1 ALLOSTERIC GATING

DOCTORAL THESIS

LUCIA GREGORIO TERUEL

INDICE

ABSTRACT	1
1. INTRODUCTION	7
1.1. PAIN AND NOCICEPTION	9
1.2. TRP CHANNELS	15
1.2.1. TRPC SUBFAMILY	17
1.2.2. TRPP SUBFAMILY	18
1.2.3. TRPML SUBFAMILY	18
1.2.4. TRPN SUBFAMILY	18
1.3. TRP NOCISENSORS.....	19
1.3.1. TRPA SUBFAMILY	19
1.3.2. TRPM SUBFAMILY	20
1.3.3. TRPV SUBFAMILY	21
Calcium selective TRPV channels.	22
TRPV channels as thermoreceptors.	23
1.4. TRPV1 AND PAIN	27
1.4.1. TRPV1 AS A THERAPEUTIC TARGET	28
1.5. STRUCTURE-FUNCTION RELATIONSHIP IN TRPV1.....	31
1.5.1. PORE REGION	32
1.5.2. CAPSAICIN BINDING SITE	34
1.5.3. TEMPERATURE SENSITIVITY	34
1.5.4. AMINO TERMINAL DOMAIN	35
1.5.5. CARBOXY TERMINAL DOMAIN	36
2. OBJECTIVES	39
3. RESULTS	43
3.1. CHARACTERIZATION OF TRP BOX IN TRPV1	45
3.1.1. MUTAGENESIS STRATEGY	45

TRPV1 STRUCTURE-FUNCTION STUDY: ROLE OF THE TRP DOMAIN IN TRPV1 ALLOSTERIC GATING

DOCTORAL THESIS

LUCIA GREGORIO TERUEL

3.1.2. FUNCTIONAL CHARACTERIZATION OF TRP BOX MUTANTS	46
3.1.3. I696X MUTANTS CHARACTERIZATION	50
Protein expression level	50
Voltage response	52
Capsaicin response	55
Allosteric model	60
3.1.4. W697 MUTANTS CHARACTERIZATION	68
Protein expression level	68
Voltage response	70
Capsaicin response	71
Allosteric model	74
3.1.5. STRUCTURAL FEATURES OF TRP BOX	78
3.2. CHARACTERIZATION OF TRP DOMAIN IN TRPV1	81
3.2.1. MUTAGENESIS STRATEGY	81
3.2.2. FUNCTIONAL CHARACTERIZATION OF CHIMERIC CHANNELS	83
AD2 chimeras expression level	83
Calcium assay screening method.	85
Voltage response	89
Temperature response and THERMODYNAMIC ANALYSIS	91
Allosteric model	101
3.2.3. STRUCTURAL FEATURES OF TRP DOMAIN	107
4. DISCUSSION	111
4.1. CHARACTERIZATION OF TRP box IN TRPV1	114
4.2. CHARACTERIZATION OF TRP domain IN TRPV1	117
4.3. STRUCTURAL FEATURES OF TRP DOMAIN AND IMPLICATION IN CHANNEL GATING.	120
5. CONCLUSIONS	123

TRPV1 STRUCTURE-FUNCTION STUDY: ROLE OF THE TRP DOMAIN IN TRPV1 ALLOSTERIC GATING

DOCTORAL THESIS

LUCIA GREGORIO TERUEL

6. MATERIAL AND METHODS	127
MOLECULAR BIOLOGY.....	129
PLASMIDS AND CHIMERIC CONSTRUCTS	129
SITE-DIRECTED MUTAGENESIS	129
TRANSFORMATION AND PLASMIDIC DNA EXTRACTION	130
FUNCTIONAL ASSESMENT.....	131
CELL CULTURE AND TRANSFECTION	131
CALCIUM MICROFLUOROGRAPHIC ASSAY	131
PATCH-CLAMP RECORDINGS, DATA ACQUISITION AND ANALYSIS	132
PATCH-CLAMP RECORDINGS AND LASER DIODE HEATING (Yao et al., 2009, 121) ..	134
BIOCHEMICAL APPROACHES.....	137
BIOTINYLATION ASSAY	137
SODIUM DODECYL SULFATE POLYACRYLAMIDE GEL ELECTROPHORESIS (SDS-PAGE) 138	
WESTERN IMMUNOBLOTTING	138
BIONFORMATICS.....	140
SECONDARY STRUCTURE PREDICTION	140
MODELLING FULL-LENGTH TRPV1 CHANNEL	140
7. REFERENCES	143
8. ACKNOWLEDGMENT	163
9. APPENDIX	169
9.1 ABBREVIATION LIST.....	171
9.2 ARTICLES.....	173

TRPV1 STRUCTURE-FUNCTION STUDY: ROLE OF THE TRP DOMAIN IN TRPV1 ALLOSTERIC GATING

DOCTORAL THESIS

LUCIA GREGORIO TERUEL



**TRPV1 STRUCTURE-FUNCTION STUDY: ROLE OF THE TRP DOMAIN IN
TRPV1 ALLOSTERIC GATING**

DOCTORAL THESIS

LUCIA GREGORIO TERUEL



1. INTRODUCTION



1.1. PAIN AND NOCICEPTION

Pain is one of the most common complains with a worldwide 20% prevalence, thus, generating a tremendous cost to global economy. Surprisingly, an effective treatment for this pathology has not been discovered yet. This fact is basically due to the lack of knowledge about the molecular and cellular mechanisms implicated in the physiology of this pathological process. Therefore, development of new therapeutic strategies is still a challenge in modern biomedicine. Nowadays, one of the most outstanding approaches for pain intervention and drug development is the characterization of molecular, biochemical and cellular mechanisms involved in **NOCICEPTION**. This process is described as the molecular mechanism whereby primary sensory neurons detect pain-producing stimuli or noxious stimuli [1].

Pain is defined as *“an unpleasant sensory and emotional experience associated with actual or potential tissue damage, or described in terms of such damage”* according to the IASP (International Association for the Study of Pain). The concept of pain can be classified based on different aspects of this affection:

- Intensity (mild-moderate-severe; 0-10 numeric pain rating scale)
- Time course (acute, chronic)
- Type of tissue involved (skin, muscles, viscera, joints, tendons, bones)
- Syndromes (cancer, fibromyalgia, migraine, others)
- Special considerations (psychological state, age, gender, culture)
- Pain physiology (nociceptive, inflammatory, neuropathic)

(<http://projects.hsl.wisc.edu/GME/PainManagement/tables.html?panel=0>)

As it is mentioned above pain physiology can be divided into three main categories:

- **NEUROPATHIC PAIN**. Neuropathic pain syndromes are chronic pain disorders caused as a direct consequence of a lesion or by disease of the parts of the nervous system that normally signal pain ([2], [3]).

- **INFLAMMATORY PAIN**. It is associated with tissue injury and inflammation characterized by reduced threshold and increased responsiveness [4].

1. INTRODUCTION

- **NOCICEPTIVE PAIN.** Affection that arises from actual or threatened damage to non-neuronal tissue and it evokes the activation of nociceptors. (IASP, International association for the Study of Pain)

In figure I1 we can see some characteristics of those three types of pain [4].

	Nociceptive pain	Inflammatory pain	Neuropathic pain
Stimulus	Noxious	Inflammation	Neural damage and ectopic firing
Sensory neuron	Nociceptor	Nociceptor and non-nociceptor	Nociceptor and non-nociceptor
Site	PNS	PNS and CNS	PNS and CNS
Involvement of TRP channels	TRP	TRP	TRP?
Clinical setting	• Acute trauma	• Post-operative pain • Arthritis	• PNS and CNS lesions • Diabetic neuropathy • Lumbar radiculopathy • Spinal-cord injury
Function	Protective	Healing/repair	Pathological
Pain sensitivity	High threshold	Low threshold	Low threshold

Figure I1. Physiological classification of pain. [4]

The three major pain syndromes are triggered by different causes (noxious stimulus for nociceptive pain, inflammation for inflammatory pain or neural damage for neuropathic pain), being nociceptor excitability a common factor in all pain pathways. The term **NOCICEPTOR** was described a century ago by Charles Sherrington as “*the neural apparatus responsible for detecting a noxious stimulus*” where noxious stimulus was defined as “*stimulus with an intensity and quality sufficient to trigger reflex withdrawal, autonomic responses and pain*” (Sherrington, 1906). The concept of nociceptor has evolved since then and, nowadays we know nociceptors as high-threshold sensory receptor of the peripheral nervous system that are capable of transducing and encoding stimulus intensities within the noxious range (IASP; [4], [5]). However, there are two relevant features defining a nociceptor that Charles Sherrington already described a hundred years ago; i) nociceptor was a specialized noxious stimulus detector; and ii) those

TRPV1 STRUCTURE-FUNCTION STUDY: ROLE OF THE TRP DOMAIN IN TRPV1 ALLOSTERIC GATING

DOCTORAL THESIS

LUCIA GREGORIO TERUEL

specific neurons had a high threshold and were only activated by stimuli with energy enough to potentially or actually damage tissue. Taking into consideration these properties we comprehend that the process of nociception allows us to detect potentially damaging stimuli and to learn the necessary reactions to avoid them. This phenomenon has been crucial for living organisms to recognize and discern potentially harmful noxious stimuli from innocuous stimuli and, consequently, for the maintenance of life.

As mentioned, nociceptors are implicated not only in nociception but also in inflammatory and neuropathic pain. Inflammatory responses evoked by tissue injury and/or inflammation produced by trauma, infection, surgery, burns or diseases sensitize nociceptors so that their threshold for activation is decreased and, consequently, their responsiveness rise ([4], [6], [7], [8]). Besides, in the presence of peripheral nervous system damage, nociceptors may fire ectopically producing a response from non-damaged axons and modulating neurotransmitter release [4], and enhancing pain sensation.

The sensitization process might give rise to alterations of the pain pathway producing hypersensitivity. As a consequence of this altered pain sensation some innocuous stimuli can provoke a painful reaction (phenomenon referred to as Allodynia) or normally mild painful stimuli may elicit pain of higher intensity (referred to as Hyperalgesia). On the one hand, these processes may be seen, somehow, as part of the healing process where the hyperactivity of nociceptors promoted to keep safe the damaged area [8]. Furthermore, it may occur that the sensitization process becomes permanently evolving to a situation of chronic pain. In this case the painful sensation may persist long after an acute injury and represent non-adaptive pathological situation, such as that accompanying numerous diseases like arthritis, migraine, neuralgias or cancer ([7], [8]).

The fact that nociceptors appear at different levels of pain signaling pathway confers to these sensory neurons the property of being a potential targets for developing novel pain relief drugs. Up to now, pharmacological compounds designed for pain reduction produce analgesia by diminishing excitation or increasing inhibition in the central nervous system (CNS). The main problem attributed to these drugs is they act against target receptors/channels located in the brain. Therefore, those centrally acting drugs cause unpleasant side effects such as sedation,

1. INTRODUCTION

dizziness, somnolence or loss of cognitive. As an alternative, new strategies for drug development are being investigated where the target molecule is positioned at the beginning of the pain pathway function [4]. These molecules correspond to receptors or ion channels which are located in the membrane of primary afferent sensory neurons (nociceptors) of the Peripheral Nervous System (PNS). In these peripheral neurons the noxious stimuli is detected and encoded by the mentioned receptors/channels into nerve impulses that enclose the information about this triggering initial stimulus. Consequently, this neural activity is processed at different levels of the CNS and interpreted finally by the brain as pain (Fig. I2) [9].

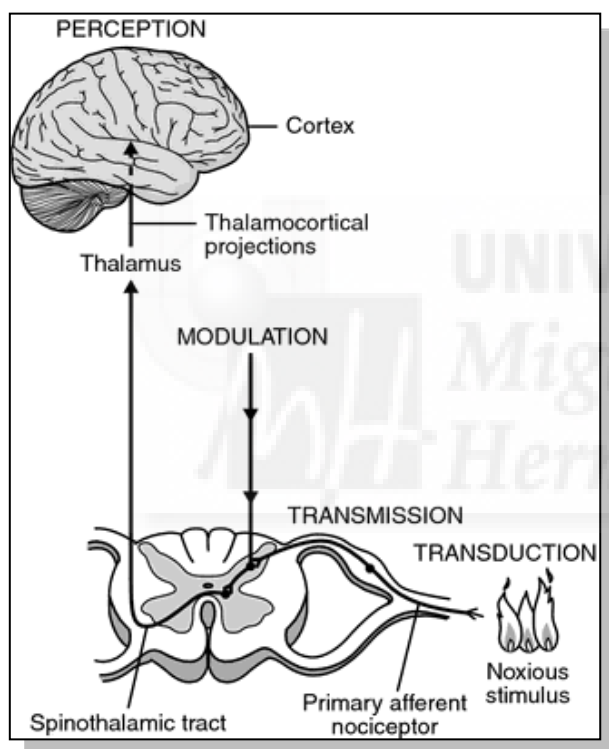


Figure I2. Anatomy of the pain pathway. (Ferrante and VadeBoncouer, 1993)

The primary afferent sensory neurons can be divided in three groups attending to anatomical and functional criteria [1]:

- $A\alpha$ and $A\beta$ fibers, myelinated, rapidly conducting, with large diameter and mainly implicated in proprioception.
- $A\delta$ fibers, lightly myelinated, medium diameter, medium rapidly conducting and participate in nociception.
- C fibers, unmyelinated, small diameter, slow conduction and involve in nociception.

TRPV1 STRUCTURE-FUNCTION STUDY: ROLE OF THE TRP DOMAIN IN TRPV1 ALLOSTERIC GATING

DOCTORAL THESIS

LUCIA GREGORIO TERUEL

Some nociceptors correspond to A δ fibers but the majority of them belong to the group of C fibers. The structure of those primary sensory neurons is described as follow (Fig 13A) [10]:

- *Cell bodies*, which are grouped in dorsal root (DRG) or trigeminal ganglia (TG).
- *Axon*, that conducts action potentials from the periphery to the CNS and bifurcates into:
 - *Peripheral terminal*, which innervates peripheral target tissue and transduces noxious stimuli.
 - *Central terminal*, where information is transferred to second order neurons at central synapses.

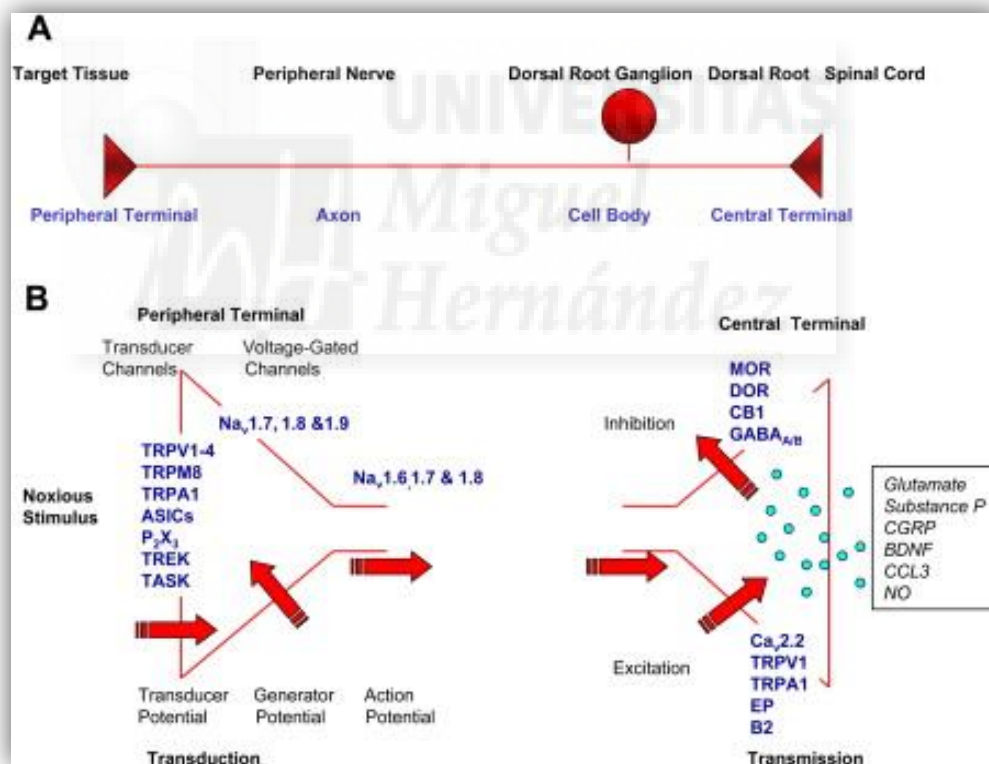


Figure 13. Nociceptor structure [10].

The first step of the pain pathway is the transduction of the noxious stimulus into electrical activity. This process is carried out by ion channels placed in the peripheral terminal (Fig. 13B) which induce the depolarization of the membrane once they are activated. If membrane depolarization is sufficiently large and intense, it evokes voltage-dependent sodium

channels activation and gives rise to an action potential which is conducted along the axon to the central terminal. After this action potential wave reaches the central terminal the nerve impulse is transmitted to the CNS through the first synapse in the sensory pathway (Fig. I3B).

Nociceptors may have an extensive range of thresholds from innocuous to noxious but stimulus-response relationship reaches the highest point in the noxious range [5]. This phenomenon differentiates nociceptors from other sensory neurons that respond to innocuous stimuli, and confers them a characteristic sensory specificity [10]. Furthermore, nociceptors are also remarkably characterized for being polymodal receptors. This property implies that they are able to detect different types of stimuli, including those of a physical and chemical nature. In addition, other important property of these primary afferent nociceptors is their plasticity since their receptive features can be modulated by other processes like sensitization [1].

As it has been described, nociceptors show specific features that distinguish them from other sensory neurons. These differentiating properties are mainly conferred by specific ion channels located in the membrane of nociceptors' peripheral terminals. These channels are in charge of transducing different stimuli into electrical signals, responding with a high threshold to particular characteristics of mechanical, thermal and chemical stimuli. These channels have been recently coined with the term **NOCISENSORS**, referring to as *molecules that detect noxious stimuli and transduce the stimulus to a cellular response* [5].

During the last decade a plethora of studies demonstrate a substantial contribution of different ion channels to nociceptive signaling. The first nocisensor described and characterized in 1997 was TRPV1 (Transient Receptor Potential Vanilloid-1) from the TRP (Transient Receptor Potential) channels family [11]. Thus far, many other channels have been included into the list of nocisensors (Fig. I3B) such as mechanotransducers and acid sensing ion channels (ASIC) ([4], [8]) potassium channels as TREK-1 and TRAAK, implicated in heat-, cold- and mechanical-noxious stimuli transduction ([12], [13], [14], [15]) and other members of TRP-channels. Particularly, this large family of channels is one of the most important groups implicated in noxious-stimulus detection in nociceptors ([1], [4], [7], [16], [17]).

TRPV1 STRUCTURE-FUNCTION STUDY: ROLE OF THE TRP DOMAIN IN TRPV1 ALLOSTERIC GATING

DOCTORAL THESIS

LUCIA GREGORIO TERUEL

1.2. TRP CHANNELS

TRP-channels (Transient Receptor Potential channels) were firstly identified in *Drosophila melanogaster* fly due to a mutation in a TRP-gene that evoked transient instead of sustained response when photoreceptors were exposed to continuous intense light [18]. This family of channels has been detected in a great variety of species in nature such as yeast, worms, zebrafish, fruit fly and, mainly, in mammals. Specifically in mammals, it has been widely demonstrated that these proteins play an important role in numerous somatosensorial transduction processes including thermosensation, pheromones reception, vascular tone regulation, nociception and pain.

The number of members of TRP-channels family has been increasing up to 28 members described in humans since they were discovered. Those channels are subdivided in 7 subfamilies named as follow TRPC1-7, TRPM1-8, TRPV1-6, TRPA1, TRPP1-3, γ TRPML1-3 and the TRPN subfamily which has been only found in invertebrates (Fig. I4). It also exist the TRPY family which is evolutionarily distinct from the other subfamilies and has only been detected in yeast ([19], [20], [21], [22]).

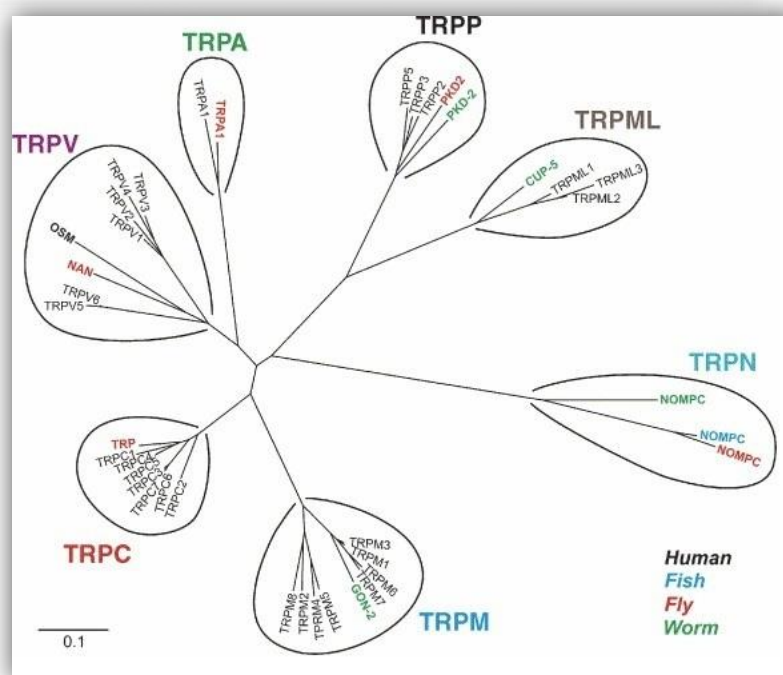


Figure I4. Phylogenetic tree of the TRP superfamily [21].

TRP channels possess a very wide distribution pattern in mammals and are ubiquitously expressed in several tissues. Particularly, they are located in central and peripheral nervous system where they play an essential role in sensory transduction ([22], [23]). All TRP members are selective cationic channels assembled as homo- or heterotetramers with a central aqueous pore (Fig. 15). The structure prediction of TRP channels is defined as a 6 transmembrane segments topology (S1 to S6) with a pore-forming loop region located between S5 and S6. The principal difference between the 7 subfamilies lies in the functional domains contained in the intracellular amino- and carboxi-terminals. They are variable in length and formed by different functional subdomains. Regarding amino termini region of many TRP channels the presence of ankyrin repeats domains (ARD) have been described. These motifs are formed by 33-residue motif consisting of pairs of antiparallel α -helices connected by β -hairpins loops. The number of ARD found in different TRP channels can be very disparate, since 3-4 in TRPCs to 29 in TRPNs. The function associated to those domains seems to be related with channels tetramerization and protein-protein or ligand-protein interaction [24].

Other important feature which characterizes some TRP subfamilies like TRPC, TRPM, TRPN and TRPV is the presence of the region called as TRP domain. This is a homologous sequence of ≈ 25 residues located in the proximal C-terminal domain following the sixth transmembrane segment ([25], [26]). The TRP domain contains a highly conserved 6-amino acids sequence termed TRP box which function is not completely characterized yet. But the fact that this region is highly conserved among TRP channels subfamilies indicates that this sequence plays an important role in channel assembly and/or function.

TRPV1 STRUCTURE-FUNCTION STUDY: ROLE OF THE TRP DOMAIN IN TRPV1 ALLOSTERIC GATING

DOCTORAL THESIS

LUCIA GREGORIO TERUEL

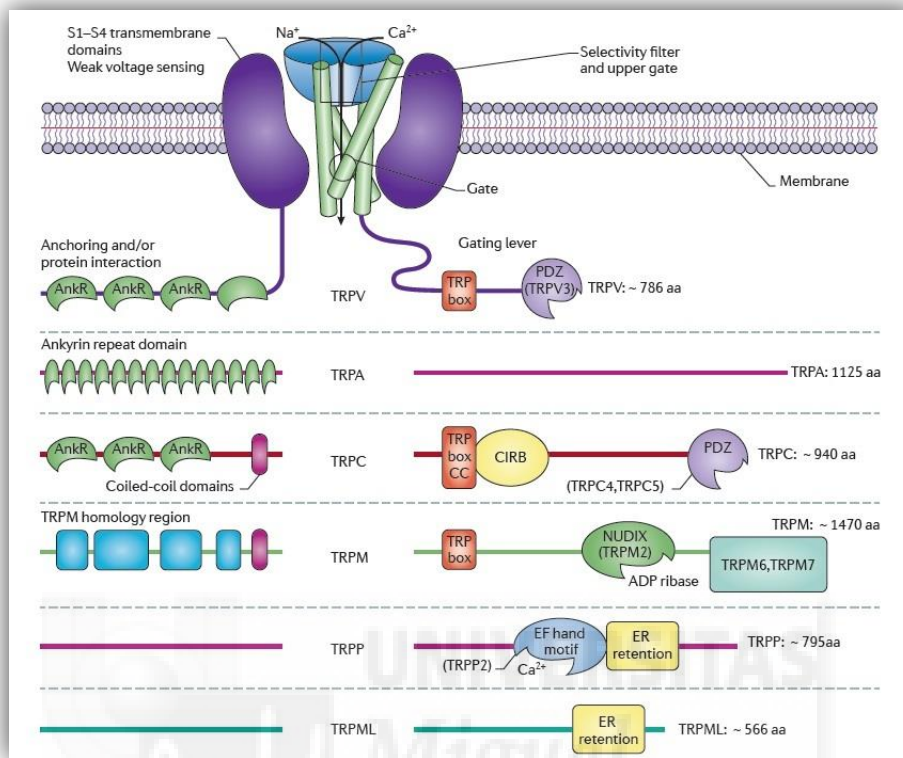


Figure 15. Structure in TRP channels family [20].

Several studies suggest that this region may be involved in activity regulation, tetramerization channel subunits and regulating the gating process, in particular the coupling between stimulus sensing and gate opening.

1.2.1. TRPC SUBFAMILY

TRPC (Canonical) subfamily consists in 7 (TRPC1-7) members which are broadly distributed in several tissues. They are non-selective cationic channels that are activated by the stimulation of G-protein-coupled receptors (GPCRs) or receptor-tyrosine kinases. Some channels of this subfamily can be co-expressed in the same cellular type and can assemble as heterotetramers giving rise to channels with different functional properties [20]. TRPC channels share an invariant sequence already described as TRP box (EWKFAR), as well as 3–4 NH₂-terminal ankyrin repeats [21].

1.2.2. TRPP SUBFAMILY

The **TRPP (Polycystin)** subfamily is constituted by PKD (Polycystic kidney disease) proteins; in turn, they are subdivided in two groups according to their structure. The first group includes the channel TRPP1 (PKD1) and other related proteins with a predicted topology of 11 transmembrane segments. Nevertheless, the last 6 of the 11 transmembrane segments (carboxy terminal region) seem to have a TRP-like domain. The other group is formed by 3 members named TRPP2, 3 and 5 corresponding to PKD2, PKD2L1 and PKD2L2 respectively. Their topology is predicted as a 6 transmembrane segments polypeptide with a large extracellular loop between S1 and S2. Some of these proteins seem to be implicated in mechanosensation in the primary cilium of kidney cells ([16], [27]).

1.2.3. TRPML SUBFAMILY

TRPML (Mucolipin) subfamily is comprised by three members (TRPML1, 2 and 3) which are characterized by their small size, less than 600 amino acids, and also by their low homology level with the rest of TRP subfamilies. These channels are mainly located intracellularly, specifically in the membrane of late endosomes and lysosomes although they also can be found in the endoplasmic reticulum. Structurally, TRPML channels are characterized by the presence of an extracellular loop between S1 and S2 including a lipase domain function. In addition, it has also been proposed that this subfamily of TRP-channels might be implicated in the aetiology of the mucopolipidosis disease ([22], [28]).

1.2.4. TRPN SUBFAMILY

The only member of **TRPN** subfamily is named after the 'NO-mechano-potential C' (**NOMP-C**) channel of *Caenorhabditis elegans*. TRPN channels have been only found in worms, flies and zebrafish, whereas mammals do not encode any homolog of this protein. This subfamily shows a large N-terminal region containing 29 of ankyrin repeats domains which was proposed as likely involved in the gating process of these channels. Afterwards, based on atomic force microscopy it was demonstrated that the ARDs act as a gating spring blocking the channel and that the protein is mechanically gated by pulling apart this blocking spring ([22], [29], [30]).

1.3. TRP NOCISENSORS

The rest of TRP subfamilies TRPV, TRPM and TRPA include the members which have been proposed as ion channel sensors of noxious stimuli or nociceptors. All those TRP channels involved in nociception are expressed in primary sensory neurons, or skin keratinocytes. Because they were activated by a different temperatures varying from noxious cold to noxious heat, it was proposed that each of these channels may confer the ability to respond selectively to innocuous or noxious temperatures across a wide thermal range [9]. For this reason, those channels are called **THERMOSENSORS** or **THERMOTRPS**.

1.3.1. TRPA SUBFAMILY

It only exist one member of the **TRPA (Ankyrin)** subfamily in mammals (TRPA1) which is expressed in dorsal root ganglia neurons, trigeminal ganglion and external ear ciliated cells. Topologically, it is important to highlight the presence of a large amino terminus which can be composed by more than a dozen of ankyrin repeats. Functionally, this channel is activated by many different agonists, mostly by environmental irritants and pungent chemicals like isothiocyanates (contained in mustard oil, wasabi and ginger), cinnamaldehyde (cinnamon) and allicin (garlic) [31]. Other substances such as acrolein (an irritant found in cigarette smoke), formaldehyde, and tetrahydrocannabinol (psychoactive component in cannabis) have been also demonstrated that directly activate TRPA1 ([31], [32], [33]). All these molecules have similar chemical properties suggesting an activation mechanism directly related with their chemical reactivity. The activation mechanism of TRPA1 by these compounds seems to be mediated by a reversible covalent modification of cysteine residues ([34], [35]). The cysteine residues implicated in this mechanism are situated in the N-terminal region of TRPA1 and together with some other residues in inner pore region participate in the gating process [36]. There are other endogenous molecules that act as TRPA1 activators like 4-hydroxynonenal (4-HNE) which is one of the most interesting activators as it mostly arises out of the process of lipid-peroxidation; and intracellular ions such as calcium and zinc ([37], [38]). Recent studies show other activators and functions where TRPA1 is involved in. For instance, it has been demonstrated that the oral pungency caused by oleocanthal, from an extract of extra-virgin olive oil, is mediated via de

activation of TRPA1 receptors selectively in the oral cavity [39]. Furthermore, this receptor has been detected in neurons that innervate the pit organ of snakes and it has been proposed to be implicated in the infrared image construction characteristic of these animals [40].

All of the above does not only demonstrate the involvement of TRPA1 in sensing noxious stimuli, but also emphasize its essential function as a significant sensor of chemical damage. Moreover, there are physical stimuli proposed to be TRPA1 activators like noxious cold ($\leq 17^{\circ}\text{C}$) or mechanical forces ([41], [42]). Nevertheless, it still exists some controversial arguments about the specific role of this channel in transducing these stimuli since different laboratories have reported apparently contradictory results about this property of TRPA1 functionality ([31], [32], [33]). Remarkably, it is important to mention that this channel shows voltage-dependent temperature activation as it was previously described for TRPM8 [43]. Interestingly, many authors suggest that TRPA1 is closely related to TRPV1 in functional aspects. Evidence that support this hypothesis is, for example, that TRPA1 is largely co-localized with TRPV1. Moreover, concerning the fact that bradykinin signaling can be related with TRPA1 through B2 receptors [31], just like TRPV1, some authors propose there is a functional coupling between these two receptors in response to bradykinin by nociceptors ([33], [41]).

1.3.2. TRPM SUBFAMILY

The **TRPM (Melastatin)** subfamily consists of 8 members (TRPM1-8) in mammals. Their structure is characterized for not containing ankyrin repeat domains in the N-terminal region. In addition, they show a large carboxy-terminal domain with a variable sequence and length ($\approx 1000\text{-}2000$ amino acids) in all the TRPM members [22]. Similar to other TRP channels, they also contain the aforementioned TRP domain in the C-terminal following the sixth transmembrane segment. According to similarities in their sequence four subsets have been proposed consisting of TRPM1/3, TRPM4/5, TRPM6/7 and TRPM2/8.

Members of TRPM channels exhibit characteristic properties such as calcium selectivity of TRPM4 and TRPM5, which is unusual among the TRP channels superfamily membrane ([44], [45]). TRPM6 and TRPM7 have an atypical protein kinase domain in their C-terminal region (referred to as chanzyme) ([46], [47]). TRPM2 is considered also a chanzyme with an ADP-ribose

TRPV1 STRUCTURE-FUNCTION STUDY: ROLE OF THE TRP DOMAIN IN TRPV1 ALLOSTERIC GATING

DOCTORAL THESIS

LUCIA GREGORIO TERUEL

pyrophosphatase domain (NUDT9 homology domain) included in its C-terminal region which binds and hydrolyzes ADP-ribose ([48], [49]). Likewise, TRPM2, TRPM4 and TRPM5 are modulated by warm temperatures; however, since they are not expressed in nociceptive neurons they are not considered thermosensors.

The last member of this subfamily is TRPM8 which has been identified as a candidate cold sensor (thermosensor); likewise it is also known it plays an important role in noxious cold nociception. TRPM8 is expressed in small and medium TG (trigeminal ganglion) and DRG (dorsal root ganglion). Interestingly, a large fraction of these neurons also express TRPV1 channels and also stains for CGRP, implying their nociceptive nature. This channel is activated by temperatures below 26°C and over the range of noxious and non-noxious cold temperatures. In turn, it is also activated by cooling chemical compounds such as menthol, eucalyptol or ilicin ([50], [51]). The channel is voltage dependent and its temperature activation leads to shifts toward more physiological potentials of its voltage activation threshold ([52], [53]). Regarding the regulatory mechanisms of TRPM8, acidic pH and PIP₂ (Phosphatidyl inositol 4,5-biphosphate) have differential effects on activation by menthol, icilin or temperature ([54], [55], [56]). PIP₂-mediated regulation of TRPM8 activity involves some basic residues of the TRP domain in the carboxy terminal region [56].

1.3.3. TRPV SUBFAMILY

The **TRPV (Vanilloid)** family owes its name to the first member described as TRPV1 since this channel was activated by vanilloid compounds such as capsaicin. This channel subfamily has six mammalian members (TRPV1-6) and other channels found in invertebrates, e.g. the *C. elegans* Osm-9 [57] and the *Drosophila* Nanchung (Nan) [58]. TRPV channels subunits have the typical topology described for other TRP channels members consisting in six transmembrane spanning segments (S1-S6) with a pore-forming loop between the S5 and S6. The two cytosolic domains in the amino- and carboxy-termini are variable in length and contain different number of functional subdomains. As common structural features in this subfamily, there is the presence of three to four ankyrin domains in the N-terminal region which are implicated in protein-protein interaction with cytoskeletal or other cytosolic proteins that modulate these channels

[26]. Moreover, all TRPV members also contain the highly conserved sequence described as TRP domain situated in the proximal region of C-terminal ([20], [59]) which has been suggested to participate in channel assembly and gating process in some members like e.g. TRPV1 ([60], [61], [62]). Other functional domains that may appear in the C-terminal region are phosphoinositide and calmodulin binding domains or PKC consensus sites, all of them important for modulation of channel activity [26].

Based on their structural and functional characteristics TRPV channels are classified in two subsets: one group is formed by the TRPV1-4 channels which are implicated in thermal sensation (also known as thermoreceptors) ([63], [64]). The other group includes TRPV5 and TRPV6 sharing $\approx 74\%$ identity but are much less similar (22-24% identity) to the rest of TRPVs ([20], [65]) giving rise to a separate group.

Calcium selective TRPV channels.

TRPV5 and TRPV6 form homomeric and heteromeric channels that are mainly expressed in transporting epithelia of the kidney and intestine, respectively. These channels show inwardly rectifying currents and they are the most Ca^{2+} -selective channels of the mammalian TRPs with a permeability ratio of $P_{\text{Ca}}:P_{\text{Na}} > 100$, although they conduct monovalent cations in absence of extracellular Ca^{2+} . This property has been attributed to the presence of an aspartic residue located in the pore region which confers structural properties to the selectivity filter ([26], [66], [67], [68]). Taking together, reported data suggests that TRPV5 and TRPV6 may be involved in vitamin-D stimulated calcium uptake via epithelial cells in expressing tissues. Experiments carried out in knockout mice for TRPV5 showed diminished renal Ca^{2+} reabsorption and hypercalciuria. Afterwards, TRPV6 knockout mice showed a decrease in intestinal Ca^{2+} reabsorption function ([69], [70]). There are other features which are important in this TRPV subset. Both channels are tightly regulated by Ca^{2+} and Mg^{2+} in a voltage-dependent manner. ([68], [71]). In addition, in heterologous systems, TRPV5 and TRPV6 channels form homo- and heterotetrameric channels and are constitutively active [67].

TRPV1 STRUCTURE-FUNCTION STUDY: ROLE OF THE TRP DOMAIN IN TRPV1 ALLOSTERIC GATING

DOCTORAL THESIS

LUCIA GREGORIO TERUEL

TRPV channels as thermoreceptors.

The development of the study on the molecular mechanisms implicated in heat sensation was thrust by the cloning and functional characterization of the capsaicin receptor (TRPV1). Physiologically, we are able to sense and distinguish an extensive range of temperatures from noxious cold to noxious heat. Temperatures over 43°C and lower than 15°C not only evoke a thermal sensation but also give rise to painful sensing [72]. Related to this, neurophysiological studies determined that the pain sensation in brain induced by heat was derived from the activation of mechano- and thermosensitive peripheral C-fibers. The triggering mechanism of pain sensation evoked by cold or heat temperatures involved the activation of ionic channels located in the cutaneous synaptic terminals of nociceptors. This hypothesis was confirmed when the capsaicin receptor TRPV1 was identified and characterized as an ion channel activated by a temperature threshold around 43°C [11]. This channel was the first of a group of channels that were lately discovered and proposed of being implicated in temperature sensing. Hence, TRPV2, TRPV3 and TRPV4 were cloned and characterized as thermoreceptors ([73], [74], [75], [76], [77]).

TRPV1, TRPV2, TRPV3 and TRPV4 are non-selective cationic channels, activated by diverse stimuli that include chemical compounds and physical stimuli like mechanical stress and temperature. The mechanism by which these channels are able to sense temperature and the fact that this physical stimulus may evoke channel opening is one of the main gaps of our knowledge regarding TRP channels studies and, therefore, actively pursued. Temperature dependence of a biological reaction can be quantified by using the 10°C temperature coefficient Q_{10} . All ion channels, are temperature-dependent because the flux of ions through the opened channels increases with rising temperatures with a Q_{10} range value between 1.2 and 1.4. However, it has been reported that this factor has values between 6 and 30 for TRP channels activated by heat temperatures, consistent with the strong dependence of these channels by temperature activation [20].

TRPV1 was the first cloned member of mammalian TRPV channels [11] from a rat genomic library of mRNA obtained from DRGs. To date, it is the most widely characterized member of the TRPV subfamily. TRPV1 is widely expressed in neuronal tissue, such as DRG, TG

and nodose ganglion (NG) neurons. Specifically, this channel is placed in spinal and peripheral nerve terminals of small- and medium-diameter peptidergic and non-peptidergic sensory neurons. Peptidergic neurons are implicated in the development of neuropathic pain and inflammation while non-peptidergic neurons play an important role in mediating chronic pain ([78], [79]). TRPV1 can be detected also in central neurons like hippocampus, hypothalamus, cerebellum and cerebral cortex. Furthermore, this channel is expressed in non-neuronal tissues such as keratinocytes, in the urothelium and smooth muscle cells of the bladder, in glial cells, liver, mast cells and macrophages ([21], [80]).

As reported, it is well known the activation of TRPV1 by capsaicin, the pungent molecule which gives the spicy food their characteristic hot taste. In addition, other vanilloid compounds have been described as activators of this channel such as resiniferatoxin (obtained from the cactus, *Euphorbia resinifera*) and different chemicals which include anandamide (an endocannabinoid), camphor and the pungent compounds present in black pepper (piperine) and garlic (allicin) ([21], [22]). The binding domain of TRPV1 for capsaicin and anandamide has been located to the intracellular domain adjacent to the transmembrane helix TM3 [81] but also between the inner half of the S3-S4 segments with the contribution of other domains [82]. Besides, endogenous lipids, so-called “endovanilloids”, which lack a vanilloid moiety, also activate this channel [83], e.g. N-acyldopamines and lipoxygenase products of arachidonic acid. Moreover, it has been shown that TRPV1 is also gated directly by protons [78]. In addition, TRPV1-mediated calcium influx initiated by the application of noxious chemicals or heat is further enhanced by low extracellular pH [22]. Thereby, the tissue acidosis that occurs in ischaemia or inflammation after tissue injury reduce the activation threshold of the channel giving rise to channel opening under normal conditions [84].

As mentioned, TRPV1 is activated also by physical stimuli like noxious heat ($\geq 43^{\circ}\text{C}$) with a Q_{10} value of more than 20. Nevertheless, the molecular basis for thermal sensitivity remains still unclear. Interestingly, heat sensing of TRPV1 it also occurs in cell-free patches suggesting that the temperature sensor should reside in the protein itself [59]. Another physical stimulus proposed as direct activator of TRPV1 is the transmembrane voltage. It has been shown that depolarizing voltages alone open the channel in absence of any other stimulus, albeit with a high threshold $\approx 150\text{mV}$ difficult to be experienced by a living cell [52]. However, heat or capsaicin can shift this relationship to less depolarized potentials such that the channel opens under more

TRPV1 STRUCTURE-FUNCTION STUDY: ROLE OF THE TRP DOMAIN IN TRPV1 ALLOSTERIC GATING

DOCTORAL THESIS

LUCIA GREGORIO TERUEL

physiological voltages. Further, depolarization reduces the threshold for activation by heat and capsaicin [85].

It is also important to highlight the desensitization process that TRPV1 experiences, predominantly via a Ca^{2+} -dependent process in view of the fact that is largely suppressed by buffering of intracellular $[\text{Ca}^{2+}]$ [80]. This phenomenon can occur rapidly during single application of an agonist or slowly following repeated agonist applications. According to the mechanism, it has been suggested that Ca^{2+} may be signaling via calmodulin since disruption of the proposed region for interacting with this protein in the C-terminal partially inhibits desensitization [86]. Likewise, PKA- and PKC- (Protein Kinase A and C, respectively) mediating phosphorylation of residues in N- or C-terminal may reverse the desensitization process [87], [88].

TRPV1 is involved in many different signaling pathways in the cell which are activated by pro-algesic compounds and evoke the potentiation of the channel activity. The modulators can directly affect the channel activity, by influencing the membrane expression of the protein, or by modulating the expression level of TRPV1 gene. Some of the compounds which directly act on the channel are N-araquidonoil-dopamine (NADA), N-oleoildopamine and acid 12-hidroperoxieicosatetraenoic (12-HPETE). These metabolites act as endovanilloids activating TRPV1 and increasing the calcium influx to the cytoplasm ([89], [90]). At the same time Ca^{2+} works as a second messenger by activating signaling pathways as e.g. PKC and Calmodulin kinase-dependent (CAMKII) which alter TRPV1 functionality by phosphorylating the channel. It is important to highlight that most of these compounds shift the temperature threshold ($\approx 43^\circ\text{C}$) to physiological values ($\approx 35^\circ\text{C}$) giving rise to the activation of the channel at body temperature producing hyperalgesia ([79], [91]). Pro-inflammatory agents also produce an increase in TRPV1 activity through an indirect mechanism. These compounds such as neurotrophic factors (NGF) interleukins, histamine, bradykinin, ATP, etc. bind to their receptors in the nociceptor membrane and activate intracellular signaling pathways which affect TRPV1 functionality. These alterations involve the PKC, PKA, Phosphoinositol kinase 3, (PI3K) and phospholipase C (PLC) that may increase channel activity ([22], [79], [91]). This increment may be due to a decreased in temperature threshold promoting channel opening under physiological conditions. In parallel, some of these routes like PKC-dependent pathway may also increase the protein amount by

inducing exocytosis of vesicles containing the channel and giving rise to insertion of functional TRPV1 into the cell membrane ([92], [93]).

The ion channel TRPV2 was first named as vanilloid receptor like protein (VRL-1) because of the homology sequence with TRPV1 sharing 50% of identity. TRPV2 is expressed prominently in medium- to large-diameter sensory neurons, as well as in other brain regions, and in some non-neuronal tissues including the heart, macrophages, gastrointestinal tract, and smooth muscle cells ([21], [59]). It has been reported that this channel can be activated by extreme high temperatures ($\geq 52^{\circ}\text{C}$) and the non-selective agonist 2-aminoethoxydiphenyl borate (2-APB). TRPV2 can also be activated by hypoosmolarity or cell stretch, suggesting potential roles in mechanotransduction. However, recent studies demonstrate that TRPV2 knockout mice showed unimpaired responses to heat and noxious mechanical stimuli. They observed normal responses both in behavioral assays, in the basal state and under hyperalgesic conditions, and electrophysiological recordings from skin afferents. Thus, according to their results they considered that TRPV2 is important for perinatal viability but is not essential for the sensing process of those physical stimuli or hypersensitivity in the adult mouse ([94], [95]). Other activation methods and regulation processes have been suggested for TRPV2. There are many compounds that seem to regulate TRPV2 by channel insertion into the plasma membrane from internal vesicles, e.g. Insulin growth factor-1 (IGF-1) and phosphatidylinositol-3-kinase (PI3-K) ([96], [97]).

TRPV3 was cloned by sequence homology to other heat-activated TRP channels, and shares 40% identity with TRPV1. TRPV3 is detected in DRG and TG neurons, brain, tongue, and testis. In addition, this channel has been also found highly expressed in keratinocytes and in cells surrounding hair follicles. This channel exhibits a temperature threshold for activation in the physiological temperature range of 32 to 39 $^{\circ}\text{C}$, and it is sensitized in response to repeated applications of heat. There are also some chemical compounds which have been described as activators of this channel, e.g. camphor (from *Cinnamomum camphora*), thymol (from thyme), eugenol (from clove oil) and 2-APB. Interestingly, all of those compounds also sensitize the heat response of TRPV3 ([59], [76]). To further understand the specific role of TRPV3 in thermosensation, TRPV3 knockout mice were performed [98], observing that responses to innocuous and noxious heat were dramatically diminished. This fact suggested that TRPV3 plays an important role in thermal sensing process. Other processes which TRPV3 may be implicated

are hair growth and atopic dermatitis (AD) [99]) since spontaneous hairless and, lately AD development were observed in two rodent strains which two different mutations in this channel.

TRPV4 was detected in high level in the epithelia of the kidney, specifically in the distal tubule. In addition, it is widely expressed in other tissues like the epithelial of the trachea, lung and oviduct. It is also found in respiratory smooth muscle cells, bladder, keratinocytes and neuronal tissue such as DRG, and brain [59]. TRPV4 is activated by increases in temperature with a moderate threshold ($\geq 24^{\circ}\text{C}$). Intriguingly, this channel lacks the sensitivity to heat after patch excision ([100], [101], [102]). Cell swelling and mechanical forces are also physical stimuli able to open TRPV4. Among chemical compounds we can find different agonist of this channel, for instance 4 α -PDD (4 α -Phorbol 12,13-didecanoate), endocannabinoids and arachidonic acid ([100], [103]). The TRPV4 null mice experiments suggest that this channel may have an important function in systemic osmotic regulation and thermosensing ([104], [105]). Those mice have no different body temperature with wild type mice, nor they react in a different manner to cold stress but they react differently to moderate heat around body temperature [104].

1.4. TRPV1 AND PAIN

The mechanism of nociception allows living organisms to identify and differentiate innocuous stimuli and harmful noxious stimuli to avoid dangers in the environment. Nevertheless, under pathological conditions this safety mechanism may become unnecessary or exaggerated giving rise to an unpleasant condition compromising the quality of life. In order to decrease or eliminate the pain sensation in these abnormal situations it is important to understand the nature of nociception and the mechanism by which it is produced.

Exposure to the vanilloid compound capsaicin evokes an intense burning sensation and pain by activating TRPV1. Thereby, this pungent compound has been extensively used as a tool for studying the mechanism of pain by inducing pain behaviours in experimental animal models. There were many aspects because of discovery of TRPV1 caused an impact in the research of pain field. Firstly, the fact that this channel was highly expressed in small to medium-size sensory ganglia neurons, which were the main candidates for acting as nociceptors. Besides, TRPV1 is a

non-selective cationic channel mediating the influx of cations which may affect membrane potential in these neurons and consequently, the action potential generation. Furthermore, this channel was also activated by noxious heat giving rise to the first described molecular mechanism of thermal sensation transduced into electrical signaling. Thus, all these findings pointed to TRPV1 as an important molecular integrator or nocisensor of the noxious stimuli in the pain sensation mechanism.

To better understand the role of this channel in the molecular mechanism of pain sensing, a TRPV1 knockout mouse was designed. The experiments performed with this TRPV1 knockout mouse showed lessened nocifensive responses to acute thermal stimuli. Furthermore, they also demonstrated an important requirement of this protein for thermal hyperalgesia under inflammatory conditions [106] suggesting its role in thermosensation. The response to capsaicin was completely abolished both in *in vivo* experiments and in cultured DRG neurons, indicating that the recognition of this compound is specific for this channel. On the contrary, the response to noxious mechanical stimuli was similar to the wild type mouse behavior even when inflammatory conditions were induced to the animals [106]. This finding suggested that TRPV1 is not directly involved in the response to noxious mechanical stimuli and, consequently, it should exist a different mechanism for mechanotransduction.

1.4.1. TRPV1 AS A THERAPEUTIC TARGET

The identification of TRPV1 and the description of its role in pain sensing mechanism make this channel a very attractive and potential target for novel therapeutic strategies. The main purpose of the research in this area is to suppress nociception by targeting this channel. However, we cannot forget that this protein is widely expressed in several neuronal and non-neuronal tissues. This fact confers to TRPV1 the property of being a double-edged sword. On the one hand, the extended location of TRPV1 may be used as a target for different drugs against many diseases. On the other hand, those drugs may generate undesired side effects in the organism [107].

The role of TRPV1 in the control of peripheral neurons excitability significantly contributes to treatments development for several diseases [79] such as atopic dermatitis, asthma, rheumatoid arthritis, intestine inflammation and neurogenic hyperreflexia bladder ([27],

TRPV1 STRUCTURE-FUNCTION STUDY: ROLE OF THE TRP DOMAIN IN TRPV1 ALLOSTERIC GATING

DOCTORAL THESIS

LUCIA GREGORIO TERUEL

[108], [109], [110]). Up to the moment, three main approaches have been used in drug development of pain relief by targeting TRPV1.

- The pungent compound capsaicin has been used for centuries to abolished pain sensing. The use of **TRPV1 agonists as pain-killer** treatments arises from the property of this channel for being desensitized, which corresponds to a non-active and transitional state of the receptor [111]. However, the therapeutic application of capsaicin is limited because this agonist evokes burning sensation and pain previous to pain relief by channel desensitization. Up to now, the main use of this treatment is to alleviate chronic painful conditions such as diabetic neuropathy and osteoarthritis [112]. Interestingly, other therapeutic approaches are being developed as a so-called 'molecular scalpel' consisting in intrathecal (sub-arachnoid space of spinal cord) injections of resiniferatoxin. This compound is a potent agonist of TRPV1 and could ablate cell bodies or central terminals of nociceptors expressing TRPV1 due to a large calcium influx in these neurons ([113], [114]). The possible use of this approach is to achieve long-term analgesia in patients who suffer chronic, intractable pain like that derived from cancer. The reason of that is because this technique is very aggressive and may cause potential problems inherent in any neuroablative strategy. Recently, new procedures are being studied for reducing the burning pain reaction at the application site. This strategy is based on an activity-dependent targeting of TRPV1 by using permanently charged agonists that only permeate through TRPV1 channel when it is open [115]. This type of agonist is expected to target hyperactive TRPV1 and restore normal nociception.

- The characterization of **TRPV1 antagonist** for inducing channel inhibition is also an aim in the design of new pain-killers targeting nociceptors. The first antagonist described was capsazepine, an analogous of the capsaicin molecule which acts as a competitive inhibitor of the channel ([89], [116]). Although this molecule is a potent inhibitor *in vitro*, some contradictory effects have been observed *in vivo*, showing non-analgesic or anti-inflammatory activity for the experiments performed in rats. Based on this action mechanism a large number of pharmaceutical companies have developed small molecules that inhibit TRPV1 with high specificity. Some of these compounds have already progressed into clinical trials showing a potential therapeutic efficacy as a TRPV1 antagonist drug ([17], [117], [118],). Another group of antagonists act as non-competitive inhibitors binding to a different site where capsaicin binds

([89], [90]). Some of these compounds are Ruthenium Red and several peptides with a high content of arginine residues which are strong channel blockers. However, there are some negative aspects related with the inhibition of TRPV1. Firstly, the suppression of TRPV1 by selective antagonism evoked hyperthermia in experimental animals and humans ([119],[120]). Since this phenomenon is not observed in TRPV1 knockout animals, authors suggest that it may exist a compensation mechanism in those TRPV1 null mice which regulates the body temperature. Secondly, clinical trials disclosed that the threshold for detecting painful heat was considerably raised in non-sensitized skin of healthy volunteers after the administration of a specific antagonist. This effect represents a risk of burn injury during common activities due to the increased heat pain threshold [118]. These facts are considered a significant barrier for the clinical application of TRPV1 antagonists. As suggested, it would be interesting to develop therapeutic agents that selectively inhibit the activated nociceptors under pathological conditions but not physiological activity of TRPV1. Uncompetitive antagonists can be adequate candidates because they are a class of activity-dependent inhibitors that specifically bind to the agonist-receptor complex or to the open state of the channel. Related to this, a TRPV1 blocker compound (triazine 8aA) [121], which acts by an activity-dependent mechanism, has been recently reported. This molecule has been described as an open channel blocker showing an inhibiting channel activity at negative membrane potential without altering the capsaicin IC_{50} . The identification and validation of uncompetitive antagonists acting as open channel blockers of TRPV1 receptors warrant exploration as a strategy to develop selective analgesic drugs with higher therapeutic index than currently discovered channel antagonists.

- A new strategy for drug design by using **TRPV1 as target for drug delivery** has been recently proposed. It has been demonstrated that TRPV1 pore has the property of being dilated in a time-dependent and agonist-dependent manner ([122], [123]). This feature of the channel can be utilized to deliver small membrane-impermeable cationic drugs into cells that only express TRPV1. For instance, lidocaine is broadly use as a local anesthetic that works by blocking the activation of voltage-gated sodium channels. The problem of this usage is that this agent acts on all nerve fibers, affecting innocuous sensation, motor and autonomic control, as well as nociception. Interestingly, it was reported that selective silencing of nociceptive nerve fibers can be achieved by using a hydrophilic polar derivative of lidocaine when this is administered together with capsaicin. Thus, TRPV1 pore dilation may be induced by capsaicin activation of the channel allowing the permeation of these large cationic molecules [124]. To minimize patient

discomfort a non-pungent activator of TRPV1 would be ideal for avoiding the painful sensation induced by capsaicin previous desensitization.

The fact that inflammatory mediators increase the surface expression of TRPV1 has been broadly reported ([92], [125]). Therefore, as a new approach for drug design, it would be interesting to eliminate the increase of channels surface density in membrane nociceptors under inflammatory conditions by blocking neuronal exocytosis. It has been shown that interactions between TRPV1 and SNARE (Soluble NSF Attachment protein Receptor) complex proteins are essential for the trafficking and surface expression of TRPV1 channels in response to activation of intracellular pathways by inflammatory mediators. Furthermore, it was found that a small peptide DDO4107, which blocks vesicular fusion by interfering with the SNARE complex, robustly abolished TRPV1 inflammatory potentiation [126]. Interestingly, compounds such as this peptide could represent a new family of anti-inflammatory and analgesic molecules acting in pathologically activated nociceptors and by avoiding the abrogation of the TRPV1 subpopulation involved in anti-inflammatory and protective roles [121]. Noticeably, all the followed strategies for drug design targeting TRPV1 entail the imperative necessity of elucidating the molecular mechanism of TRPV1 functionality.

1.5. STRUCTURE-FUNCTION RELATIONSHIP IN TRPV1

The cDNA molecule codifying for the rat (*Rattus norvegicus*) TRPV1 determines that each subunit consists in 838 amino acids and it has a molecular weight of 95 KDa. The subunit topology shows 6 transmembrane-spanning segments (S1-S6) with a pore region between S5 and S6 regions and two large cytosolic amino- and carboxy-terminal domains. This predicted topology was supported by structural approaches from Moissenkova-Bell et al. [127]. They showed a 19-Å structure of TRPV1 determined by using single-particle electron cryomicroscopy. This structure exhibited fourfold-symmetry and contained two different regions: a large open basket-like domain which would correspond to the cytoplasmic N- and C-terminal fragments, and a more compact domain, corresponding to the transmembrane segments. The assignment of these regions was guided by fitting a TRPV1 model obtained from crystal structures of the

1. INTRODUCTION

structurally homologous Kv1.2 channel and isolated TRPV1 ankyrin repeats into the TRPV1 cryo-electromicroscopy structure.

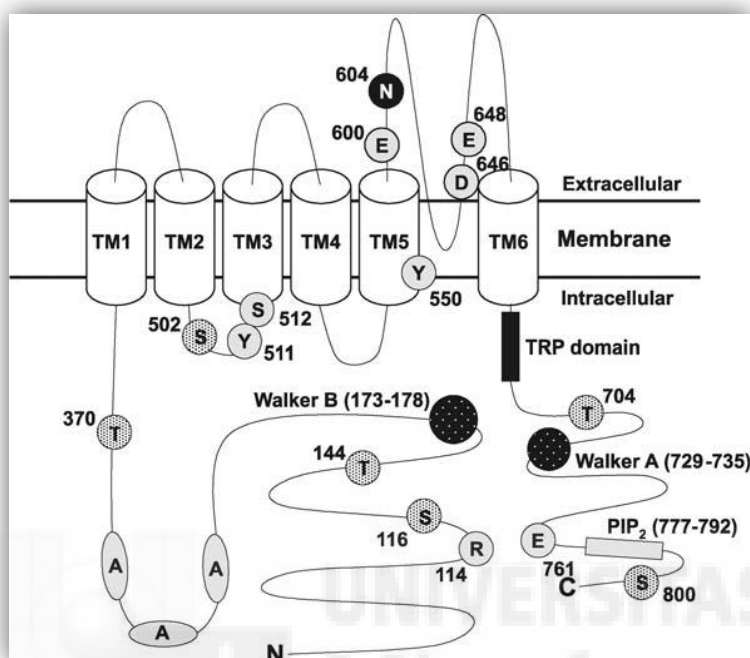


Figure 16. Regions and amino acids involved in *trpv1* function. [128]

1.5.1. PORE REGION

The pore region is formed by an amphipathic loop located between S5 and S6 transmembrane segments. Interestingly, the pore region sequence of TRPV channels shows high similarity to the equivalent sequence of the bacterial potassium channel KcsA and Shaker potassium channels. This region contains several acidic residues involved in the selectivity filter conferring specific permeation properties to the channel [129]. The substitution of some of these acidic residues by neutral amino acids alters the permeability of divalent cations and the sensitivity to Ruthenium Red blockage [130].

An asparagine residue in this region was found which appears glycosylated in rat TRPV1 when is heterologously expressed. Some experiments performed in transiently transfected HEK 293 and F-11 cells revealed that the glycosylated position corresponds to the residue N604 (Fig. 16) [131]. The mutation of this amino acid N604T considerably affected the channel response to

TRPV1 STRUCTURE-FUNCTION STUDY: ROLE OF THE TRP DOMAIN IN TRPV1 ALLOSTERIC GATING

DOCTORAL THESIS

LUCIA GREGORIO TERUEL

capsaicin and to the inhibitor capsazepine [132], as well as the desensitization process and its permeability properties. Up until recently, there were no evidences of the existence of a TRPV1 glycosylated form *in vivo*. But, lately, the N-glycosylated form of TRPV1 was reported in rat DRGs cultured neurons [133] suggesting that glycosylation properties *in vivo* may play a role in the protein functionality.

The detection mechanism of some TRPV1 activators has been also attributed to some residues in the pore region. The acidification of extracellular media was proposed as a chemical stimulus which directly activates TRPV1 at room temperature [78]. It has been reported that residues E648 and E600 (Fig. I6), located in the putative pore-forming region of the channel, are implicated in the direct activation of TRPV1 by protons as in the potentiation mechanisms that sets its sensitivity to other noxious stimuli in the presence of acidification [134].

Recently, it has been proposed that some residues of the pore region are implicated in temperature sensing ([135], [136]). Yang et al. reported that the replacement of 14 residues located between S5 segment and the pore helix generated non-sensitive channels to temperature but were normally responding to capsaicin. Additionally, they showed by using site-directed fluorescence approach that the channel opening triggered by temperature is initiated by a specific rearrangement of those amino acids. They also demonstrated that these movements are temperature-dependent since they did not observe this behavior during ligand- and voltage-dependent channel activation [135]. However, some controversial results were lately published by Yao et al [137] proposing that those amino acids were not as relevant for temperature activation as it was described. Yao et al. showed that the complete deletion of those residues in TRPV1 did not affect temperature sensitivity or capsaicin and low pH responses. In parallel, Grandl et al. suggested that amino acids located between the filter region and the S6 transmembrane segment are important for the thermal stimulus transduction. Mutation of these residues ablated long channel openings that are characteristic of the temperature-gating pathway. Interestingly, Grandl et al. also identified residues in the pore region of TRPV3 that were required for temperature activation [138].

1.5.2. CAPSAICIN BINDING SITE

The capsaicin molecule is formed by three well-differentiated regions. The A region is formed by an aromatic ring containing the homovanillic group (3-metoxi 4-hidroxibenzil). The B region corresponds to an amide bound, and the C region consists in an aliphatic portion which is the part of the molecule proposed for being potentially interacting with TRPV1 through hydrophobic interactions with an intracellular cavity (suggested by Humphrey H. Rang in the “Spring Pain Conference”, Grand Cayman, BWI, 1998; [139]). The identification of the region in charge of capsaicin interaction revealed that the intracellular loop placed between S2 and S3 transmembrane segments directly interacted with the agonist. Residue Y511 (Fig. 16) was proposed as the main candidate for capsaicin detection since its mutation completely abolished the capsaicin and resiniferatoxin activation but left heat and protons response intact. Supporting this idea, it was found that the region between S2 and S4 could structure a hydrophobic cavity where capsaicin molecule could bind [81].

1.5.3. TEMPERATURE SENSITIVITY

The specific role of TRPV1 in detecting heat stimuli still remains surprisingly elusive. As it is aforementioned, some authors proposed that some residues of the pore turret region in the P-loop are directly implicated in the temperature sensing process. However, other studies suggested that the C-terminal plays a role either in containing or strongly modulating the temperature sensor [140]. They performed a TRPM8 chimeric channel containing the equivalent section of C terminus from TRPV1. This small portion of the protein conferred to the chimera heat sensitivity. Despite of these findings, further studies and more conclusive results are needed to identify the molecular basis of temperature sensitivity.

It is difficult to explain how TRPV1, and other thermoTRPs, are exceptionally high temperature sensitivity and can be activated by small differences in temperature over a narrow range. Clapham and Miller [141] proposed that, according to the laws of thermodynamic, a strong temperature dependence of TRP channel gating is accompanied by large changes in molar heat capacity, (ΔC_p). Furthermore, this work leads to the conclusion that hot- and cold-sensing TRPs operate by identical conformational changes; although, it may not be experimentally

possible to cover a temperature range wide enough to actually observe both hot-sensing and cold-sensing in a unique channel. That means that TRP channels have apparently evolved to produce a large heat capacity change upon opening. They also suggest that the molecular origin of this phenomenon corresponds to the exposure of hydrophobic groups to water, as it has been described as the common molecular basis of heat- and cold-driven unfolded proteins. Considering these findings, the authors suggest that the opening process induced by temperature changes may be due to small rearrangements in multiple regions of the protein more than to the existence of localized temperature-sensing domains.

1.5.4. AMINO TERMINAL DOMAIN

The amino terminal region of TRPV1 is considered as an important fragment in the modulation of channel activity due to the implication of this region in protein-protein interaction processes. Furthermore, published works reported that some residues of this region are directly implicated in phosphorylation mechanisms. This region contains consensus sequences for several enzymes implicated in these phosphorylation processes such as PKA, PKC, calmodulin kinase II or Src kinase ([142], [143], [144], [145]). In TRPV1, the phosphorylation mechanism is mainly involved in channel sensitization/desensitization, strongly modulating its activity.

Ankyrin repeat domains located in the N-terminal of TRPV1 indicated that this region is probably interacting with cytosolic proteins, as it was described for other membrane proteins. Some of these cytosolic interacting proteins are calmodulin (CaM) [146] and vesicular proteins involved in regulated exocytosis such as Snapin and Synaptotagmin IX [92]. Another protein that has been proposed for interacting with the N-terminal region of TRPV1 is the gamma-aminobutyric acid receptor-associated protein (GABARAP) [147]. The interaction of both proteins was detected in DRG neurons and in heterologous expression system eukaryotic HEK 293 cells. Authors attributed an important role in the channel expression pattern to this interplay. The presence of GABARAP would increase the interaction between the carboxy-terminal domain of the channel and the cytoplasmic protein tubulin. This fact influences transport and recruitment of the channels to the plasma membrane.

1.5.5. CARBOXY TERMINAL DOMAIN

The cytoplasmic C-terminal domain of TRPV1 also shows structural motifs and specific sequences that seem to be involved in protein-protein interactions. For example, a small sequence of approximately 30 residues length, which is essential for calmodulin binding, was found in this domain [148]. It was reported that the deletion of this segment significantly reduced CaM binding and calcium-induced desensitization of the channel.

The membrane protein Pirt (phosphoinositide interacting regulator of TRP) has been identified for being interacting with the C-terminal of TRPV1. Pirt is expressed in the peripheral nervous system (DRGs and trigeminal ganglia) but not found in the central nervous system. It has been demonstrated the presence of Pirt in most of the nociceptive neurons in DRGs including those expressing TRPV1 [149]. Pirt knockout mice revealed impairment in capsaicin and noxious heat responsiveness. These stimuli induced significantly attenuated currents in Pirt deficient DRG neurons when compared with wild type DRGs. Besides, the heterologous expression of Pirt in TRPV1 HEK 293 stable cell line enhanced the current intensity evoked by capsaicin without altering the channel expression level. Authors also showed that Pirt directly interacted with TRPV1 and phosphatidylinositol-4,5-bisphosphate (PIP₂) through its C-terminus potentiating TRPV1 activity.

Regarding this aspect, it has been also described the direct interaction between the C-terminal domain of TRPV1 and PIP₂ molecule itself. As in other TRP channels, this interaction plays a very important role in the capsaicin sensitivity by the receptor [150]. Thereby, deletion of the potential binding region to PIP₂ in C-terminal TRPV1 lessened temperature and capsaicin gating [86]. It has been suggested that residue S800 (Fig. 16), in the PIP₂ recognizing sequence, is phosphorylated by PKC [143] and consequently, producing channel activation by avoidance of the inhibitory effect that PIP₂ binding causes to the channel. Noticeably, there are other residues that also participate in the modulation of the channel activity by phosphorylation. For instance, the amino acid T704, which is included in a phosphorylation consensus sequence for PKC and CaMKII, is involved in the interaction of vanilloids with the channel altering their affinity ([80], [151]).

TRPV1 STRUCTURE-FUNCTION STUDY: ROLE OF THE TRP DOMAIN IN TRPV1 ALLOSTERIC GATING

DOCTORAL THESIS

LUCIA GREGORIO TERUEL

Recently, a new molecule that could be modulating TRPV1 activity by direct has been reported by Nieto-Posadas et al. [152]. The authors suggest that the bioactive phospholipid lysophosphatidic acid (LPA) activates TRPV1 through a unique mechanism that is independent of G protein-coupled receptors. The amount of this phospholipid is increased upon tissue injury and it activates primary nociceptors giving rise to neuropathic pain. The presented results showed that LPA produces acute pain-like behaviors in wild type mice, albeit, this response is substantially reduced in TRPV1 knockout animals. They proposed that LPA regulates TRPV1 activity by direct interaction with the C terminal region of the channel.

The carboxy terminal domain of TRPV1 also contains a highly conserved sequence referred to as TRP domain [25]. Initially, the TRP domain was described as a 25 residues sequence, located in the C-terminal region adjacent to the receptor internal gate. This sequence has been found in other TRP subfamilies, such as TRPMs and TRPCs although in most of those cases its function is not well defined. TRP domain also includes a 6-mer conserved sequence termed TRP box ([25], [153], [151]). In TRPCs, this short sequence remains unaltered (EWKFAR) albeit its function on these channels is not fully understood. However, in TRPM and TRPV channels this sequence is less conserved than in TRPC subfamily, with a consensus sequence corresponding to :[VIYFL]WK[FAY][QN]R and [IL]W[KR][LA]Q[RWVI]), respectively [154]. The role of TRP domain in TRPV1 functionality has been proposed as implicated in intersubunit interaction that may contribute to the coupling of stimulus sensing to channel opening ([60], [61], [62]). Supporting this idea, they showed that the corresponding sequence with the TRP domain (⁶⁸⁴Glu-⁷²¹Arg) had a propensity to fold into an α -helix and to form coiled-coil structure. These facts are consistent with the idea that this region may be involved in channel tetramerization since these structures are two hallmarks of association domains of channel proteins [155]. Indeed, it was shown that when the corresponding TRP domain sequence was removed in full-length TRPV1 monomers the formation of stable heteromeric assemblies with wild-type subunits was blocked. Furthermore, purified recombinant C terminus of TRPV1 formed discrete and stable multimers *in vitro*. Besides, when the TRP domain sequence was ablated in a poreless TRPV1 subunit suppressed its robust dominant negative phenotype. All those findings suggested that TRP domain region is involved in subunit tetramerization to give rise functional channels [60].

Regarding the role of TRP domain in channel functionality different approaches were carried out for elucidating its function in TRPV1 activity. One of the strategies generated chimeric channels by the substitution of the TRP domain of TRPV1 with the cognate region of TRPV channels. These chimeras were not activated by depolarizing voltages as it is observed in TRPV1 and additionally, functional chimeras showed defective sensitivity to activating stimuli such as capsaicin and heat. Furthermore, biophysical properties of partially-activated chimeric channels revealed that the TRP domain act as a molecular determinant of the activation energy of channel gating [61].

The other strategy corresponded to an alanine scanning mutagenesis of the TRP box of TRPV1 (IWKLQR) to further characterize its role in TRPV1 activity [62]. The mutations introduced in this motif altered channel gating by increasing the free energy of channel activation. Interestingly, they observed that replacement of I696, W697 and R701 by alanine severely affected voltage- and heat-dependent activation and notably reduced the capsaicin responsiveness. In summary, these results suggested that the mutation of TRP box residues to alanine affected TRPV1 function by affecting events downstream of the initial stimuli-sensing step and imply that intersubunit interactions within the TRP box play an important role in TRPV1 gating. In the present work we will try to elucidate the specific function of the TRP domain in TRPV1 gating process.



2. OBJECTIVES

TRPV1 STRUCTURE-FUNCTION STUDY: ROLE OF THE TRP DOMAIN IN TRPV1 ALLOSTERIC GATING

DOCTORAL THESIS

LUCIA GREGORIO TERUEL



TRPV1 STRUCTURE-FUNCTION STUDY: ROLE OF THE TRP DOMAIN IN TRPV1 ALLOSTERIC GATING

DOCTORAL THESIS

LUCIA GREGORIO TERUEL

The main objective in this research project is to study the TRPV1 protein functionality in terms of its structural features. The aim of this work is focused on further characterizing the role of the TRP domain in the molecular mechanism of TRPV1 activation. This region is located in the C-terminal domain, and it has been widely reported that it is involved in oligomerization processes and activity modulation.

The main strategy is divided into two specific goals:

- i) To identify the physicochemical features of I696, W697 and R701 residues of TRP box, required to maintain functional TRPV1 channel properties.
- ii) To determine which amino acids are essential for reverting a non-functional TRPV1 chimeric channel containing the cognate TRP domain of TRPV2 to a functional state.

TRPV1 STRUCTURE-FUNCTION STUDY: ROLE OF THE TRP DOMAIN IN TRPV1 ALLOSTERIC GATING

DOCTORAL THESIS

LUCIA GREGORIO TERUEL





3. RESULTS



TRPV1 STRUCTURE-FUNCTION STUDY: ROLE OF THE TRP DOMAIN IN TRPV1 ALLOSTERIC GATING

DOCTORAL THESIS

LUCIA GREGORIO TERUEL

3.1. CHARACTERIZATION OF TRP BOX IN TRPV1

TRP box is a highly conserved 6-mer sequence (IWKLQR in TRPV1) located at the core of the TRP domain region. Some studies reported that this region is involved in inter- and intrasubunit interactions of TRPV1 channel [62] suggesting that the TRP box may be implicated in the functional coupling between stimulus sensing and pore opening. Valente et al, using an Ala-scanning of the TRP box sequence, found that residues I696, W697 and R701 (numbers corresponding to TRPV1 from *Rattus norvegicus*) were essential for the correct functionality of the channel. Concerning these results, we decided to further interrogate the role of these three amino acids in TRPV1 gating.

3.1.1. MUTAGENESIS STRATEGY

To further understand the role of these positions in channel gating, we evaluated the impact of introducing the rest of 18 natural amino acids in each of the three positions (Fig. R1). We decided to omit to cysteine since this amino acid could form disulfide bonds with other cysteine residues and, consequently, it could generate undesired secondary structures which may interfere in the interpretation of the results. We used a site directed mutagenesis approach where three pair of degenerate primers were designed, one pair for each position. Thereby, we obtained the 18 mutants from one unique PCR reaction.

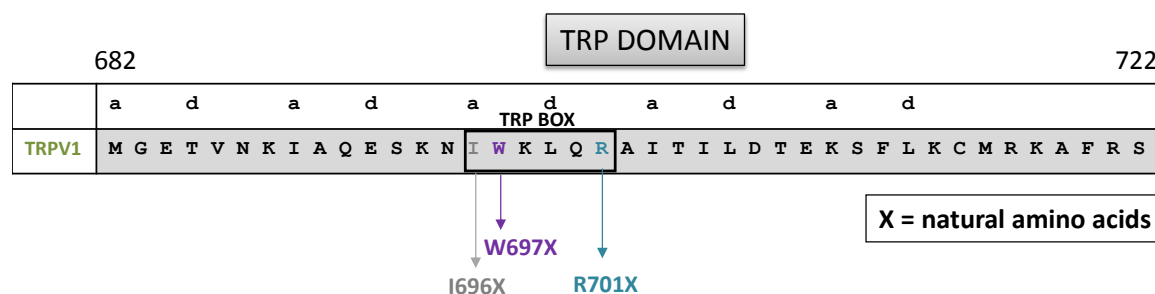


Figure R1. Schematic representation of TRP box sequence in TRPV1. TRP domain sequence of rat TRPV1. TRP box sequence is highlighted in an open rectangle. The three positions I696, W697 and R701 are individually substituted by 18 of the 20 natural amino acids generating 54 point mutations. The “a” and “d” positions of the predicted coiled coil are tagged. Numbers refer to the position of amino acids in rat TRPV1 cDNA.

The plasmid containing the cDNA encoding TRPV1 contains the insert and the pcDNA3 vector (Invitrogen). The mutations are performed by PCR technique using site directed mutagenesis with this plasmid as template for amplification. For this procedure we used PfuTurbo DNA polymerase (Stratagene) which showed lower error rates than other enzymes avoiding the insertion of undesired mutations. The DNA obtained as PCR product was transformed in the bacteria strain *XL1-Blue* to obtain a higher number of copies. Afterwards, the plasmidic DNA was extracted and purified using specific plasmidic DNA extraction kits, and thereafter sequenced to obtain and verify the mutation. Once we checked that the mutation was included we proceeded to perform the functional characterization.

3.1.2. FUNCTIONAL CHARACTERIZATION OF TRP BOX MUTANTS

We used patch clamp to study the biophysical properties of the TRP generated mutants. Specifically, we characterized the response of these channels to two activating stimuli: depolarizing voltage and the chemical agonist capsaicin. These experiments will define the characteristics determining the structural properties needed at positions I696, W697 and R701 of TRPV1 compatible with channel function. For the biophysical characterization of TRP box mutants, the receptors were heterologously expressed in HEK 293 cells. We performed patch clamp experiments in whole cell configuration. We used TRPV1 transfected cells as positive control and pcDNA3 as negative. We applied depolarizing voltages up to 240 mV to study the response of mutant channels to this activating stimulus. Furthermore, we characterized the response to the agonist by applying 100 μ M capsaicin at negative and positive potentials.

Figure R2 exhibits current density values for all the mutants obtained in the three positions. This parameter represents the current obtained divided by the cell capacitance. The normalization of current values respect to the cell surface is very important since we are working with transiently transfected cells and they can express different protein levels depending on the cell size. These data revealed the important role that I696, W697 and R701 residues play in TRPV1 functionality.

TRPV1 STRUCTURE-FUNCTION STUDY: ROLE OF THE TRP DOMAIN IN TRPV1 ALLOSTERIC GATING

DOCTORAL THESIS

LUCIA GREGORIO TERUEL

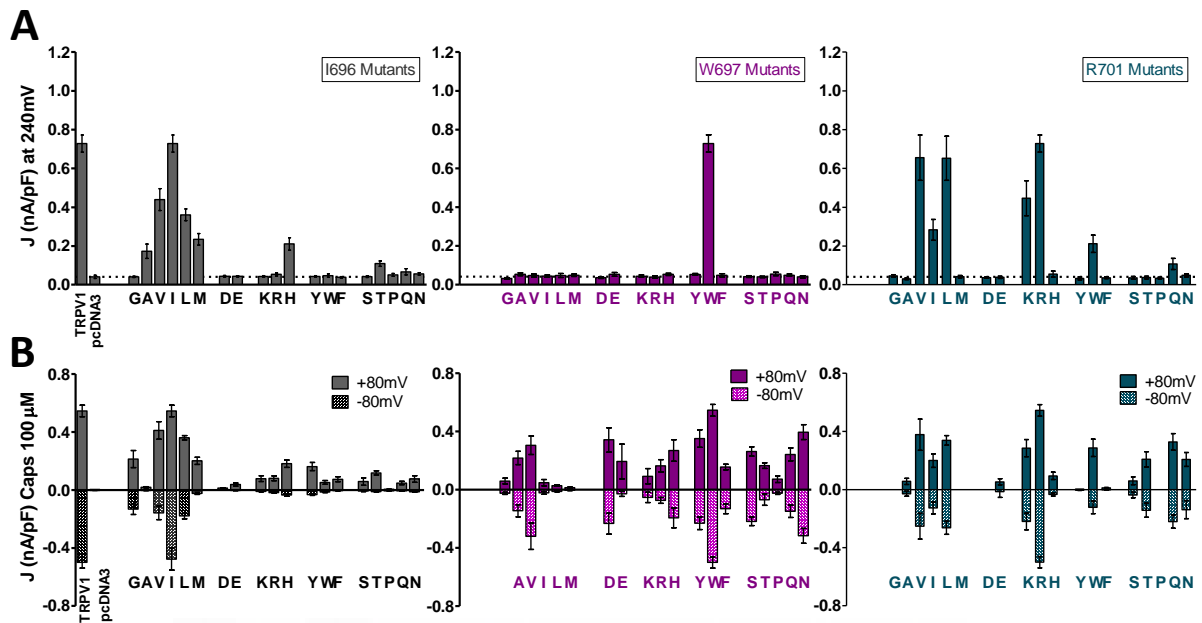


Figure R2. Current densities of TRPV1 and TRPbox mutants in I696, W697 and R701 positions. Current densities of TRPV1 and I696 (grey), W697 (purple) and R701 (blue) mutants evoked at 240 mV (A) and in presence of capsaicin (B) at -80 and +80 mV. Ionic currents from mutants were activated by 100 μ M capsaicin, whereas those of TRPV1 were evoked by 1 μ M. Higher concentrations of capsaicin was difficult to use for TRPV1 because the large currents evoked at positive potentials could not be clamped. Data are shown as mean \pm SEM, with number of cells \geq 4.

As depicted in Fig. R2, the mutations introduced in the three positions (I696, W697 and R701) showed disparate responses after the application of the activating stimuli. Regarding the activation by voltage, the pull of mutants for each position showed different behaviors when depolarization was applied (Fig. R2A). For I696 mutants we observed that only some of the mutants containing a hydrophobic residue in this position, similar to the original amino acid in TRPV1 wt, were partially activated when positive potentials were applied. It is important to highlight that the replacement of I696 by an alanine or glycine gave rise to less- and non-active channels, indicating that the amino acid size at this position seems to be also important for channel function. These results suggested that not only the non-polar surface area but also the amino acid size might be relevant in this position for the correct coupling of the channel. Noticeably, we also detected modest channel activation in cells expressing the mutant I696H. Deprotonated histidine has a non-polar surface area very similar to the aliphatic residues, and shows a comparable volume to valine and isoleucine. Thus, these results support the tenet that

3. RESULTS

residue with hydrophobic properties within a volume range is required at I696 for generating functional TRPV1 channels.

Analysis of the response to 100 μ M capsaicin was carried out at depolarizing (+80mV) and hyperpolarizing (-80mV) conditions. Interestingly, most of the active I696X mutants did not show any response to the agonist capsaicin at negative potentials (Fig. R2B). Only for I696L and I696V we detected ionic currents in both conditions induced by depolarizing voltages and by capsaicin at -80mV. In contrast, when capsaicin was applied at +80 mV, we observe that all active mutants responded well to the vanilloid at depolarizing potentials. Remarkably, as we observed from voltage activation, only the mutants with a hydrophobic amino acid included in I696 position were activated by capsaicin.

The same experiments were performed with W697X mutants. Figure R2A shows that none of the W697X mutants were voltage-sensitive channels. Even though we applied depolarizing voltages up to 240mV, we were not able to evoke the activation of any of the W697X mutants, not even the most conservative substitutions such as aromatic residues tyrosine and phenylalanine. However, this pattern was not found in W697X mutants when 100 μ M capsaicin was administered (Fig. R2B). In this case, high concentration of capsaicin induced detectable currents from most W697X mutants. Analysis of the responses did not reveal any apparent correlation between partially activated mutants and the physico-chemical properties of the incorporated amino acid in this position. Furthermore, most of the responsive mutants were activated by the vanilloid at both hyper- and depolarizing voltages.

Finally, we studied the response of the mutants obtained for R701 position to these activators. As seen in figure R2A, several mutants corresponding to different amino acid families, except negatively-charged amino acids, were partially activated by depolarizing voltages. The same activation pattern was observed when R701 mutants were stimulated with capsaicin (Fig. R2B). Because R701 is plausible located in a CaMKII phosphorylation consensus site (Hyd-**R**XXX(T/S)-Hyd), where **R** represents the residue R701 [144] its substitution can affect not only channel activation properties but also could be altering other processes such as phosphorylation and desensitization mechanisms.

TRPV1 STRUCTURE-FUNCTION STUDY: ROLE OF THE TRP DOMAIN IN TRPV1 ALLOSTERIC GATING

DOCTORAL THESIS

LUCIA GREGORIO TERUEL

Taking together, these results showed that I696 and W697 residues play an essential role in TRPV1 functionality. In general terms, the replacement of any of these two positions by any amino acid gave rise to less sensitive channels than the original protein to voltage and capsaicin. The fact that all mutant channels displayed altered responses to both activators suggests that the TRP box is implicated in a gating step common to both stimuli, most likely the coupling between their sensors and channel pore. Consequently, we decided to focus in I696X and W697X mutants. For I696 position we selected all the mutants that responded to both voltage and capsaicin stimuli. For W697, we chose one mutant representative of each amino acid family according to their physico-chemical properties, hydrophobic (valine and methionine), polar (asparagine), aromatic (tyrosine), positively-charged (histidine), negatively-charged (aspartic acid).



3.1.3. I696X MUTANTS CHARACTERIZATION

A preceding work revealed that the modification of I696 to alanine altered channel function by affecting events downstream of the initial stimuli-sensing step and implied that intersubunit interactions within the TRPbox play an important role in TRPV1 gating [62]. These findings supported the structural model proposed in this work, where I696 is placed at the “a” position of the putative coiled-coil motif and possibly interacting with the rest of subunits of the tetramer.

In our results we observe that the substitution of I696 residue of TRPV1 by any amino acid severely impaired voltage- (Figs. R2A and R4) and capsaicin-dependent activation (Fig. R2B and R6). We also detected a strong outward rectifying I-V relation with a barely detectable ionic current at hyperpolarized membrane voltages in the presence of high concentrations of capsaicin in most of the I696X mutants studied. The same behavior was previously reported by Valente et al. for I696A mutant. We next disclose a detailed study about the changes induced by I696 mutations in TRPV1 gating processes.

PROTEIN EXPRESSION LEVEL

It has been widely demonstrated that the TRP domain sequence in TRPV1 acts as a molecular determinant of subunit multimerization. Thus, mutations in this sequence could alter the structure of this region and consequently, the tetrameric assembly needed for a functional channel. In turn, perturbations of the protein assembling may give rise to an improper folding of the protein inducing its own degradation process. Since we are introducing mutations in the TRP box, which is located in the center of TRP domain, we considered relevant to check the mutant's protein expression level. Furthermore, these results would determine whether there was a relation between the absences of receptor function in some mutants with abrogation of the protein expression.

TRPV1 STRUCTURE-FUNCTION STUDY: ROLE OF THE TRP DOMAIN IN TRPV1 ALLOSTERIC GATING

DOCTORAL THESIS

LUCIA GREGORIO TERUEL

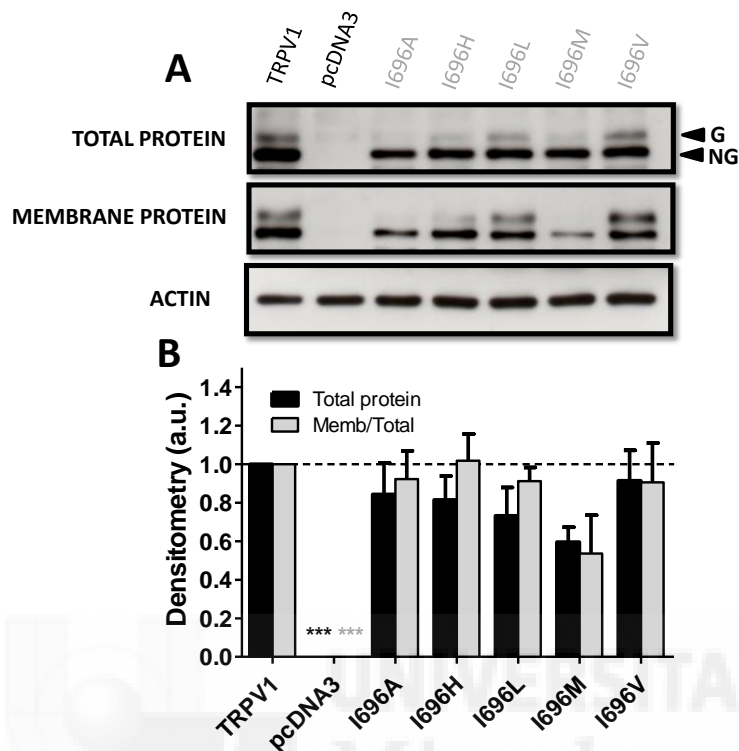


Figure R3. I696 mutant's expression level and membrane detection. *A*, Representative Western blot showing the total protein extracts and membrane fraction of transiently transfected HEK cells with TRPV1, pcDNA3 and a group of selected I696 mutants. Separate fractions were obtained by surface biotinylation. G and NG indicate glycosylated and non-glycosylated form. For the detection of bands were used antibodies against TRPV1 and actin as a loading control protein (α -TRPV1, 1:30000 and α -actin, 1:10000). Bands detection was performed by using ECL-select. *B*, Normalized values of densitometry obtained from the western blot bands by using TOTAL LAB software. Measurements represent mean \pm SEM, number of experiments = 3.

As depicted in Fig. R3, TRPV1 was detected as a double band corresponding to different glycosylated forms of the protein (referred as G for glycosylated and NG for non-glycosylated form) [131] (Since not all the mutants have the glycosylated form, we used the NG band for protein quantification.). Mock transfected cells did not show immunoreactivity against the anti-TRPV1 antibody, which demonstrate the antibody was specific for the channel. Regarding the protein expression of I696X mutants, I696M showed the lowest expression level when compared with TRPV1. The rest of mutants did not exhibit significant changes in their expression level when compared with the wild type protein (Fig. R3B). By using biotinylation protocol for membrane protein detection we found that all mutants reached the plasma membrane in a similar way to TRPV1 (Fig. R3A). And also the ration between the amount of protein found in

membrane and the total amount of protein was comparable to wild type. Furthermore, we observed that only mutants I696V, I696L and slightly I696H showed the glycosylated forms (G) characteristic of wild type channels. However, this phenomenon should not interfere in channels' functionality because it has been reported that defective glycosylation mutant of TRPV1 (N604T) exhibited normal plasma membrane expression and showed detectable currents values when activated by all agonist ([132], [133]). This finding suggests that the absence of this band in TRPV1 mutants could be due to modulation of protein folding which prevents the glycosylation of the protein either by altering the tertiary or quaternary structure of the protein.

VOLTAGE RESPONSE

We next studied the effect of mutating I696 position to valine (V), leucine (L), methionine (M), histidine (H), asparagine (N) and aspartic acid (D) on voltage-dependent channel gating. For this purpose, we performed patch clamp experiments of mutant channels heterologously expressed in HEK 293 cells by using whole-cell configuration. The protocol used for voltage-activation corresponded to 100 ms depolarizing pulses from -120 to 240 mV in steps of 20 mV. The next figure displays representative ionic currents evoked by the voltage step protocol (Fig. R4).

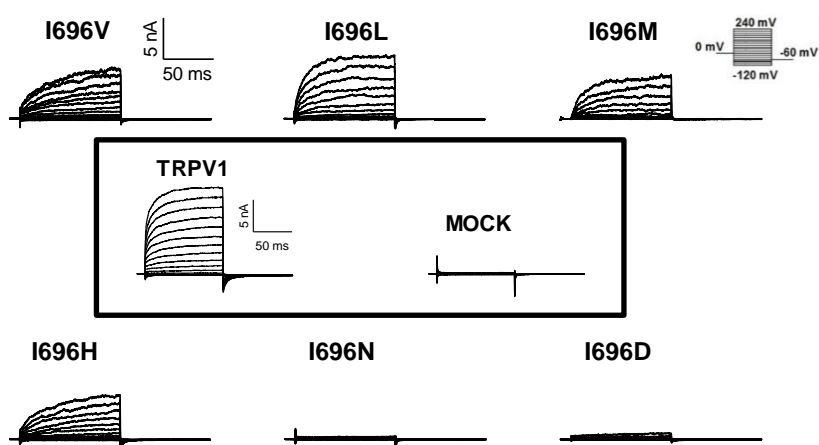


Figure R4. Voltage response of I696 mutants. Representative families of ionic currents evoked with a voltage step protocol consisting of 100 ms depolarizing pulses from -120 to 240 mV in steps of 20 mV. Holding potential = 0 mV; time between pulses 5 s.

TRPV1 STRUCTURE-FUNCTION STUDY: ROLE OF THE TRP DOMAIN IN TRPV1 ALLOSTERIC GATING

DOCTORAL THESIS

LUCIA GREGORIO TERUEL

Application of depolarizing pulses up to 240 mV evoked noninactivating ionic currents from TRPV1, I696V, I696L, I696M and I696H mutants. However, all active mutants displayed lower currents than those of wild-type channels. Mutants I696N and I696D did not elicit any response to this activating stimulus. Analysis of the conductance-voltage curves (G-V) of active mutants revealed that voltage sensitivity was altered in all I696X mutants studied (Fig. R5).

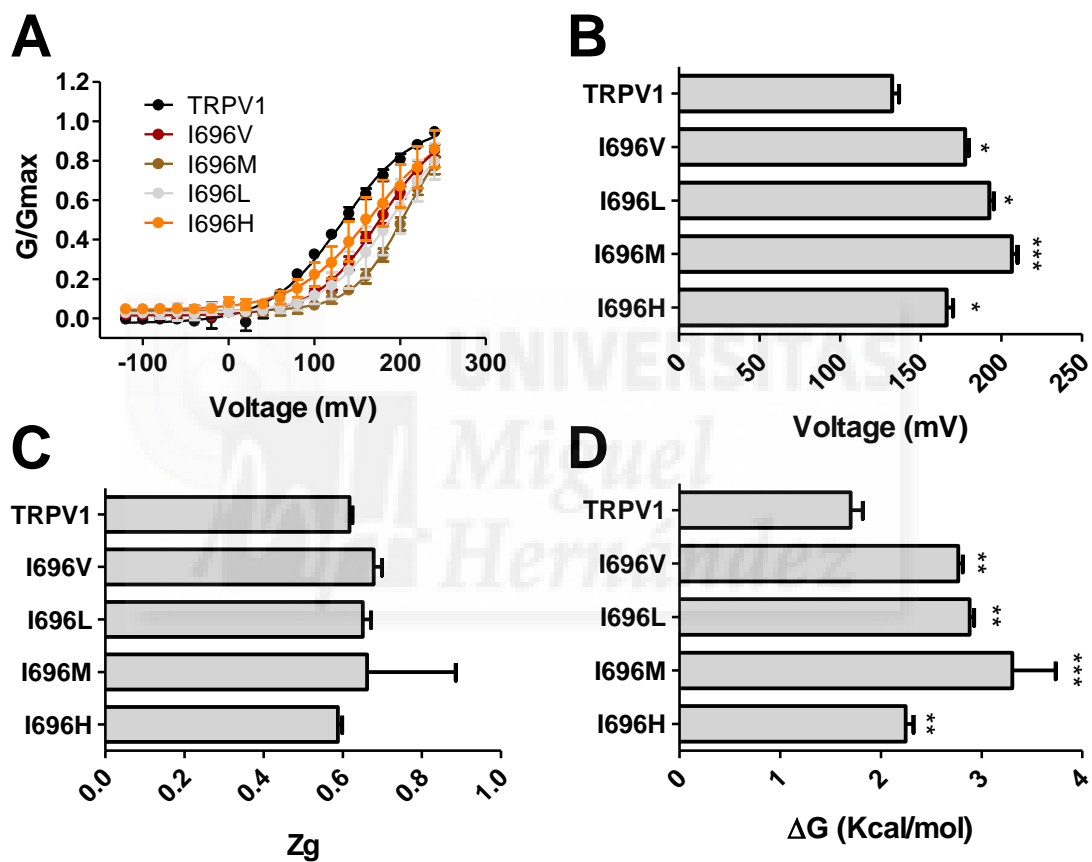


Figure R5. Normalized conductance and biophysical parameters of TRPV1 and I696X mutants. **A**, G-V relation is plotted for TRPV1 and mutants constructions. Conductance curves were obtained from the ionic currents shown in Fig. R4 using $G=I/(V-V_R)$, where V is the stimulation potential value and V_R is the reversal potential. Conductance values for each cell were fitted to the Boltzmann equation: $G=G_{max}/\{1+\exp[(V-V_{0.5})/a_n]\}$. Solid lines depict the best fit to a Boltzmann distribution. **B**, $V_{0.5}$ values for the different I696 mutants obtained from the Boltzmann distribution G-V relations. **C**, Apparent gating valence of the activation process: $z_g=25.69 \text{ mV}/a_n$. **D**, Free energy values at 0mV and 25°C (ΔG_0) for TRPV1 and mutants assuming a two-state model. $\Delta G_0 = Z_g F V_{0.5}$, where F is the Faraday constant (0.023 kcal/mol mV). All values are means \pm SEM; number of cells ≥ 5 ; one-way ANOVA, * $p \leq 0.05$.

The G-V curves for TRPV1 and active mutants calculated from the steady-state ionic currents evoked with the step protocol (Fig. R4) were suitably fitted to a Boltzmann distribution. This distribution is characterized by two parameters: $V_{0.5}$, the voltage at which the conductance was half-maximal, and a_n , the slope of the conductance-voltage relationship. Alteration of a_n by mutation can reflect changes in the apparent gating valence of activation (z_g). As seen, all I696X mutants exhibited an altered voltage-dependent activation when compared with TRPV1 currents. Normalized conductance-to-voltage ($G/G_{\max} - V$) curves gave rise to a $V_{0.5}$ for TRPV1 of 138.8 ± 3.25 mV and a gating valence (z_g) of 0.63 ± 0.04 (Fig. R5B-C). Noticeably, $V_{0.5}$ values were significantly shifted to more depolarized potentials for the mutants up to 165.9 ± 4 mV for I696H, 177.4 ± 2.2 for I696V, 192.4 ± 2.7 for I696L and 206.3 ± 3.6 for I696M (Fig. R5B). However, none of these mutations appeared to alter the apparent gating valence associated to channel opening (Fig. R5C) when compared with TRPV1. Notice that I696M mutant exhibited the largest rightward change in all parameters, together with the highest variability. This may be due to the fact that G-V curve for I696M mutant data did not reach saturation and the Boltzmann distribution fit gave rise to higher error values. Taking together, these results suggest that mutation of I696 in the TRP box residue to Val, His, Leu and Met impaired the voltage-dependent gating, probably by raising the free energy of voltage activation. This idea was further supported by the analysis of the free energy difference between the closed and open states at 0 mV and 25°C (ΔG_0) calculated from the values of $V_{0.5}$ and z_g considering a two-state model. Although it has been extensively reported that TRPV1 gating may be formed by several conformational states ([53], [156]) this approach is a simple and valuable manner to compare the effect of mutations on the energetic of channel gating. As observed in figure R5D the four mutants showed increased values of ΔG_0 when compared with wild type protein. For TRPV1, the ΔG_0 was 1.95 ± 0.12 kcal/mol, and for I696V, I696L, I696M and I696H were 2.77 ± 0.05 , 2.88 ± 0.05 , 3.3 ± 0.43 and 2.2 ± 0.07 kcal/mol respectively.

In contrast to these results, mutants I696D and I696N completely lacked voltage-induced responses. Even when we applied voltage stimuli up to 240 mV, we could not elicit ionic currents from these mutants. The same behavior was observed for the rest of mutants containing other charged or polar residues in this position. Thus, these results indicate that mutation of I696 to polar or charged residues significantly affected the voltage sensitivity of TRPV1.

Summarizing, the results described above implied that I696 mutation to any amino acid raises the activation energy of voltage-dependent gating. Furthermore, our findings signal that I696 position in TRPV1 requires an amino acid with certain hydrophobicity and size characteristics to generate voltage-gated channels.

CAPSAICIN RESPONSE

To better determine the biophysical properties of I696 mutants we next evaluated the effect of increasing concentrations of the vanilloid on the voltage activation of these mutants (Figs. R6 and R7). We decided to use both stimuli simultaneously because it is well known that capsaicin potentiates voltage responses and displaces the G-V relation of TRPV1 toward more physiological potentials. The synergistic effect of both stimuli could help us to evoke currents in mutant channels which were non-responsive under more moderate conditions.

For studying the capsaicin response, we performed patch clamp experiments of mutant channels heterologously expressed in HEK 293 cells by using whole-cell configuration. The protocol used for these experiments corresponded to a ramp protocol of 300 ms from the holding potential of 0mV to -80 mV, followed by 350 ms linear ramp up to 160 mV, in the presence of capsaicin, 1 and 100 μ M. We used this saturating vanilloid concentration to ensure the response of all channels, taking into consideration our previous results showing that mutation of these receptor sites decreased the sensitivity to the agonist [62]. In figure R6, we show some representative current-voltage relation (I-V) corresponding to TRPV1 and I696 mutants. Furthermore, the conductance-to-voltage relation (G-V) are depicted in figure R7. Some biophysical parameters for the mutants were calculated to elucidate how these changes are affecting gating process in TRPV1. As discerned, all I696 mutants showed an altered capsaicin-evoked response as compared with TRPV1.

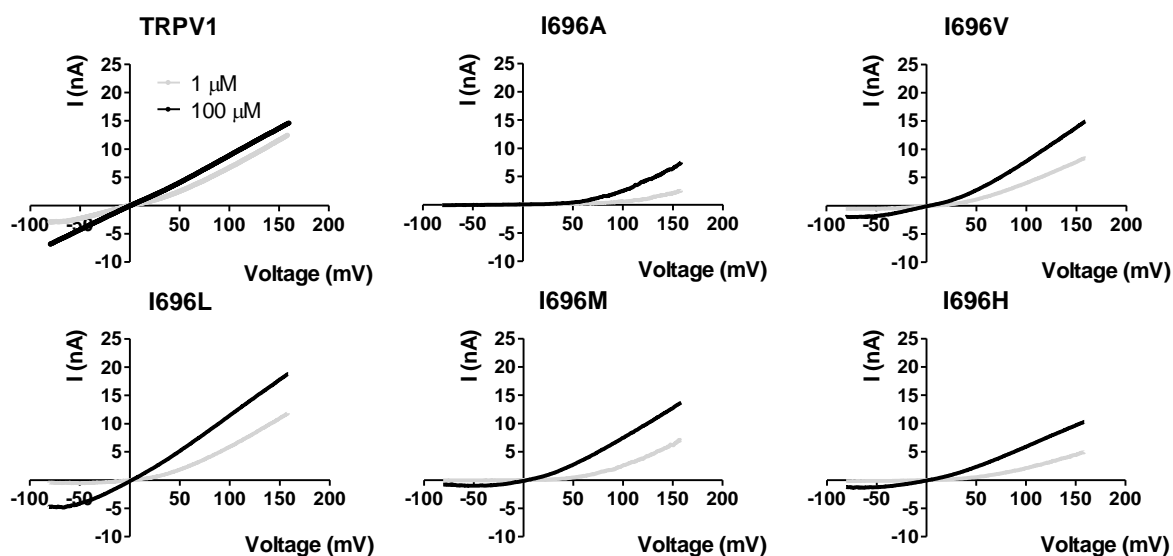


Figure R6. I-V relation of TRPV1 and I696X mutants in the presence of capsaicin. Some representative ionic currents evoked by increasing concentration of capsaicin from TRPV1 and some I696 mutants. I-V relations were recorded using a ramp protocol consisting of a voltage step of 300 ms from 0 to -80 mV, followed by a 350 ms linear ramp up to 160 mV. Cells were sequentially exposed to the increasing concentration of capsaicin 1 and 100 μM .

As illustrated in figure R6, the sequential addition of 1 and 100 μM capsaicin evoked similar current intensity for TRPV1. These results were consistent with the EC50 estimates previously obtained for TRPV1 which corresponded to values between 1 to 3 μM . Furthermore, in both cases the channel displayed ionic current at hyperpolarizing potentials induced by the presence of the agonist capsaicin. In 1 μM capsaicin, the evoked current at negative membrane potentials showed a non-linear response. Whereas, when 100 μM capsaicin was applied the inward current showed an ohmic behavior. Therefore, we considered this saturating vanilloid condition elicited maximum probability of channel opening in a voltage-independent manner.

TRPV1 STRUCTURE-FUNCTION STUDY: ROLE OF THE TRP DOMAIN IN TRPV1 ALLOSTERIC GATING

DOCTORAL THESIS

LUCIA GREGORIO TERUEL

Regarding I696 mutants, at 1 μM capsaicin all of them showed none or barely detectable ionic current at hyperpolarized membrane voltages. Noticeably, this phenomenon was also observed for I696H, I696M and I696A when 100 μM capsaicin was applied. The capsaicin energy contribution at this high concentration was still not enough stimulus for opening these mutant channels at hyperpolarizing potentials. However, mutants I696V and I696L displayed ionic currents at negative voltages in the presence of the maximum capsaicin concentration applied which are more similar to TRPV1. Analysis of conductance values shows the impact caused by substituting I696 residue by any amino acid in the biophysical properties of the channel.

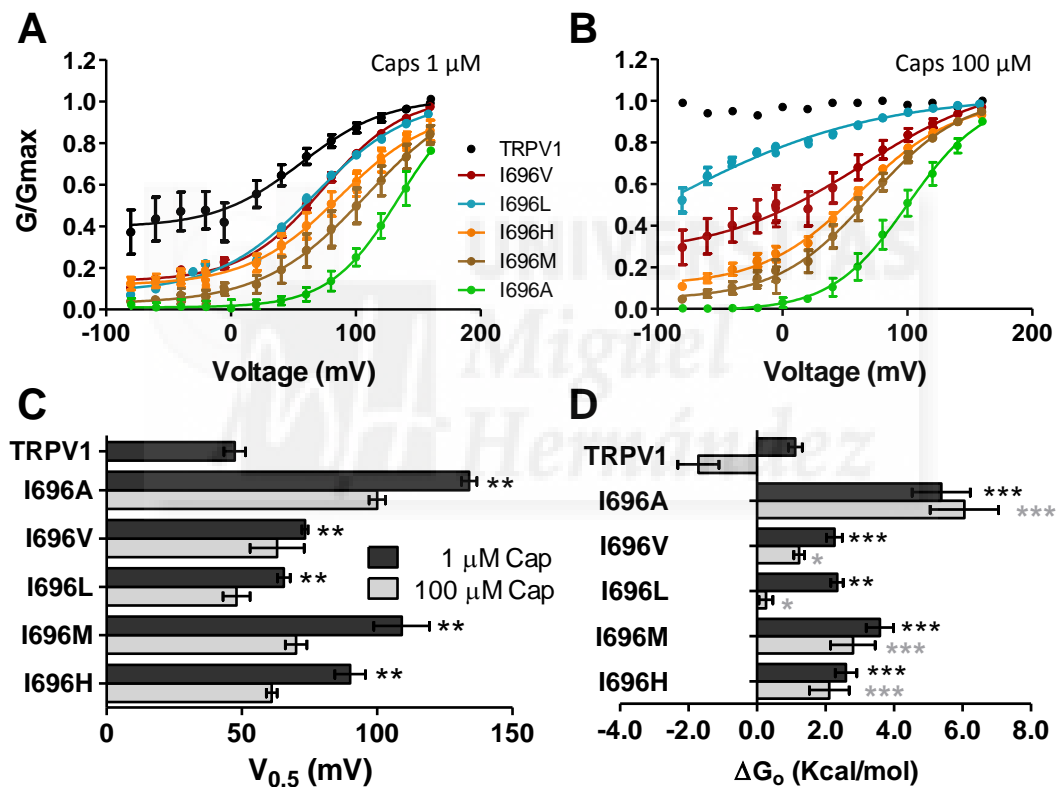


Figure R7. Normalized conductance and biophysical parameters of TRPV1 and I696X mutants in presence of capsaicin. **A and B**, G-V relation are plotted for TRPV1 and mutants constructions in presence of 1 (A) and 100 (B) μM capsaicin. Conductance curves were obtained as described in Fig. R5 from the ionic currents shown in Fig. R6. Solid lines depict the best fit to a Boltzmann distribution. **C**, $V_{0.5}$ values of the different I696X mutants obtained from the G-V curves. For TRPV1 we only calculated these parameters from the recordings at 1 μM capsaicin since data at 100 μM was not properly fitted as a Boltzmann distribution. **D**, Free energy values of the voltage-dependent and -independent components relations ($\Delta G_0 = \Delta G_0(V) + \Delta G_0(i)$), assuming a two-state model obtained from the Boltzmann distribution G-V. For TRPV1 at 100 μM , only capsaicin-dependent free energy is calculated. Data are given as mean \pm SEM, with number of cells ≥ 5 . * $p < 0.05$, as compared with wild type, using a one-way ANOVA statistical test.

The G-V curves were obtained from ionic currents evoked with the aforementioned ramp-depolarizing protocol. For TRPV1 only the conductance obtained in 1 μ M capsaicin (Fig. R7A) was suitable for fitting to a Boltzmann distribution. The G-V curve for TRPV1 at 100 μ M capsaicin resulted in a voltage-independent plot derived from the ohmic current described in figure R6. As observed, all I696 mutants showed voltage-dependent gating in the presence of capsaicin since they followed a Boltzmann distribution (Fig. R7 A-B). However, the normalized G-V relations showed that the vanilloid modulated differently the voltage-activated response of the different mutants. On the one hand, the agonist barely evoked any current at hyperpolarizing potentials for I696A, I696M and I696H, even when the concentration applied was 100 μ M. In contrast, mutants I696V and I696L displayed significant voltage-independent gating at hyperpolarized potentials which rose in a dose-dependent manner as it was detected for the wild type protein (Fig. R7A-B). Noticeably, mutant I696L exhibited the most similar phenotype to TRPV1 wild type channel in the presence of capsaicin.

Increasing the concentration of the vanilloid shifted the $V_{0.5}$ of all the studied mutants (I696A, I696V, I696L, I696M and I696H) toward more physiological potentials (Fig. R7C). However, they still are shifted to more positive potentials as TRPV1 in the presence of 1 μ M capsaicin (47.4 ± 4 mV). The statistically significant values were 134.04 ± 2.4 for I696A, 109.1 ± 10.3 for I696M, 90.01 ± 5.7 for I696M, 73.9 ± 1.7 for I696V and 65.5 ± 2.3 mV for I696L. Noteworthy, we detected that $V_{0.5}$ values for I696V and I696L were notably closer to TRPV1 than those exhibited by the other mutants studied. It is also important to mention that, despite of reducing $V_{0.5}$ toward more physiological voltages, the 100-fold higher concentration of capsaicin did not affect the $V_{0.5}$ parameter of I696 mutants as strongly as for wild type channels.

Analysis of the free energy of gating showed that capsaicin reduced the free-energy difference between the closed and the open states at 0 mV and 25°C of TRPV1 and all the mutants in a dose-dependent manner (Fig. R7D). These results yielded a free energy change, assuming a two-state model and considering voltage-dependent and -independent components, with a profile that closely resembled that of $V_{0.5}$. All mutants exhibited higher ΔG_0 values when compared with wild type protein, showing lower values for I696V and I696L than the other mutants. In addition, the highest concentration of capsaicin did not significantly reduced ΔG_0 values for most of the I696 mutants. Similarly, the presence of the vanilloid did not alter the gating valence of the voltage-dependent component ($z_g \approx 0.6-0.8$)

TRPV1 STRUCTURE-FUNCTION STUDY: ROLE OF THE TRP DOMAIN IN TRPV1 ALLOSTERIC GATING

DOCTORAL THESIS

LUCIA GREGORIO TERUEL

Taken together, these results imply a contribution of I696 position to the activation energy of channel gating. In general, the replacement of I696 residue by any of the natural amino acids gave rise to defective functional or non-functional channels. Only the mutation to valine, leucine, methionine and histidine showed a partial response to depolarizing voltages and the agonist capsaicin. As we can perceive from Table I, the amino acids allowed in the I696 position to generate functional channels were included in a strict range of volume and non-polar surface area.

amino acid	non-polar surface area(A ²)	amino acid	VOLUME (Å ³)
Asn	42	Gly	60.1
Asp	45	Ala	88.6
Gly	47	Ser	89
Cys	48	Cys	108.5
Ser	56	Asp	111.1
Gln	66	Pro	112.7
Glu	69	Asn	114.1
Ala	86	Thr	116.1
Arg	89	Glu	138.4
Thr	90	Val	140
Lys	122	Gln	143.8
Pro	124	His	153.2
His	129	Met	162.9
Val	135	Ile	166.7
Met	137	Leu	166.7
Tyr	154	Lys	168.6
Ile	155	Arg	173.4
Leu	164	Phe	189.9
Phe	194	Tyr	193.6
Trp	236	Trp	227.8

Table I. The numbers indicate the increasing values for non-polar surface area (Å²) and volume (Å³) of natural amino acid. I696 functional mutants are highlighted in grey.

In particular, the substitution of I696 residue to leucine showed the most similar functional properties to wild type protein in presence of capsaicin, followed by mutation to valine. Considering that both amino acid are chemically the most similar to isoleucine, these findings suggested that I696 position not only needs to maintain hydrophobic and size

properties, but also the chemical groups included in the side chain are also important for generating functional channels. These results may indicate that I696 position in TRPV1 must be located in a hydrophobic environment, shielded from the aqueous surroundings.

ALLOSTERIC MODEL

To further understand the results we have obtained from the functional characterization of I696 mutants, we considered whether they could be explained by an allosteric model. Thus far, we have been assuming a two-state gating model to simplify the calculus performed. This model implies a strict coupling between the sensor and the pore, in such a way that whenever the sensor is activated the channel will open and always by reaching the maximum opening probability. This two-state model has previously been used for describing the opening of TRPV1 induced by voltage [52]. On the contrary, other groups have shown results demonstrating that the process of TRPV1 channel gating induced by different activators corresponds to different open and closed states ([85], [157]).

Allosteric coupling has been proposed and demonstrated for several voltage-activated channels, for instance hyperpolarization- and cyclic nucleotide-gated (HCN) channels [158] and the high conductance voltage- and calcium-activated potassium (BK) channels [159]. A common feature of these channels, also found in some TRPs, is their polymodal activation, i.e. voltage and another stimulus. In fact, one of the main characteristics of the allosteric model is the existence of distinct structural domains known as sensors for these different stimuli. These different domains are independent of each other but all allosterically coupled to the channel's gate. According to this model, every stimulus drives a transition between resting and activating states of its own sensor. However, activation of any of these sensors may not necessarily lead directly to channel opening but preferably to an increase of the open state probability.

An allosteric gating scheme can be imagined as several unconnected state transitions whose rate (and equilibrium) constants are modified depending on the state or the other equilibria. For the analysis of this data is important to consider that the homotetrameric conformation of TRPV1 implies that every channel possess four identical voltage sensors and capsaicin binding sites. However, the location and molecular nature of voltage sensor and the number of molecules of capsaicin required to gate the channel are still unknown. In view of this

TRPV1 STRUCTURE-FUNCTION STUDY: ROLE OF THE TRP DOMAIN IN TRPV1 ALLOSTERIC GATING

DOCTORAL THESIS

LUCIA GREGORIO TERUEL

fact, akin to Brauchi et al 2004 and Matta and Ahern, 2007, we assumed that all voltage sensors in TRPV1 operate in unison and that all binding sites need to be occupied for the activation of the channel. In addition, we assumed that voltage and capsaicin sensors move simultaneously, giving rise to a simplified 8-state allosteric model (Fig. R8).

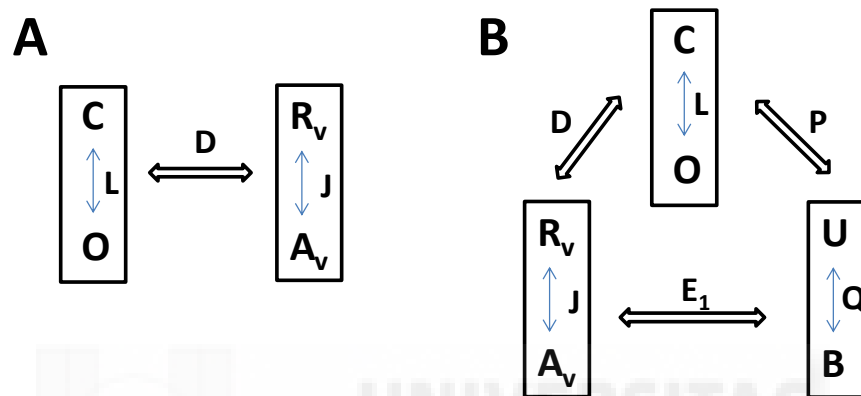


Figure R8. Allosteric model for channel activation. A, allosteric activation by voltage. Two independent equilibria that interact allosterically. **B**, allosteric activation by voltage and capsaicin. An additional equilibrium is included to the equation.

Figure R8A depicts an allosteric activation induced by voltage where two separate two-state equilibria interact allosterically with each other. In the first equilibrium *C* and *O* represented the closed and open states of the pore gate (respectively). This equilibrium was defined by a constant *L*, which would correspond to a very small value when no stimuli are being applied. The second equilibrium was defined by *R_v* and *A_v* which represented the resting and activated state of the voltage sensor. *J* defines the equilibrium constant for voltage sensor activation and is voltage dependent. *D* corresponds to an allosteric factor which determines the coupling between the voltage sensor and the pore of the channel. When the voltage sensor is activated, the equilibrium constant between *C* and *O* would be modified as *LD*. According to this model, the probability of being in any open state is:

$$P_o = \frac{1}{1 + \frac{1+J}{L(1+JD)}}$$

(Equation 1)

Where J is:

$$J = J_0 e^{\frac{zFV}{RT}}$$

(Equation 1.2)

Being J_0 the equilibrium constant at 0 mV.

Figure R8B shows a diagram of an allosteric activation by voltage and capsaicin. In this case, a third two-state equilibrium is added where U and B represent the unbound and bound conformation of the capsaicin site, respectively. The equilibrium constant of capsaicin binding corresponds to Q . With the third equilibrium two new allosteric factors are introduced: P which determines the coupling between capsaicin binding site and the pore of the channel and E , which defines the coupling between both sensors. When sensors act independently between them $E=1$. Whereas, when E differs from 1 we understand both sensor are allosterically coupled to each other. According to this model, the opening probability is given by:

$$P_o = \frac{1}{1 + \frac{1 + J + Q + JQE}{L(1 + JD + QP + JQDPE)}}$$

(Equation 2)

Where Q is:

$$Q = \frac{[caps]}{K_d}$$

(Equation 2.1)

Where K_d corresponds to the capsaicin dissociation constant and $[caps]$ is the concentration of capsaicin applied.

The free energy of channel activation can be estimated from the allosteric model by ([156], [160]):

$$\Delta G_o = -RT \ln(\pi_{i=1}^n K_i)$$

(Equation 3)

Where $RT = 0.58$ kcal/mol at 22°C, and K_i are the equilibrium constants considered in the model.

TRPV1 STRUCTURE-FUNCTION STUDY: ROLE OF THE TRP DOMAIN IN TRPV1 ALLOSTERIC GATING

DOCTORAL THESIS

LUCIA GREGORIO TERUEL

The next step was to fit our data obtained for TRPV1 and I696 mutants to the equations that describe the allosteric activation mechanism for voltage and both voltage and capsaicin together. This approach will assist in understanding how we are affecting the channel gating with the mutations introduced in the I696 position. We assumed G/Gmax values are equivalent to Po for whole cell currents.

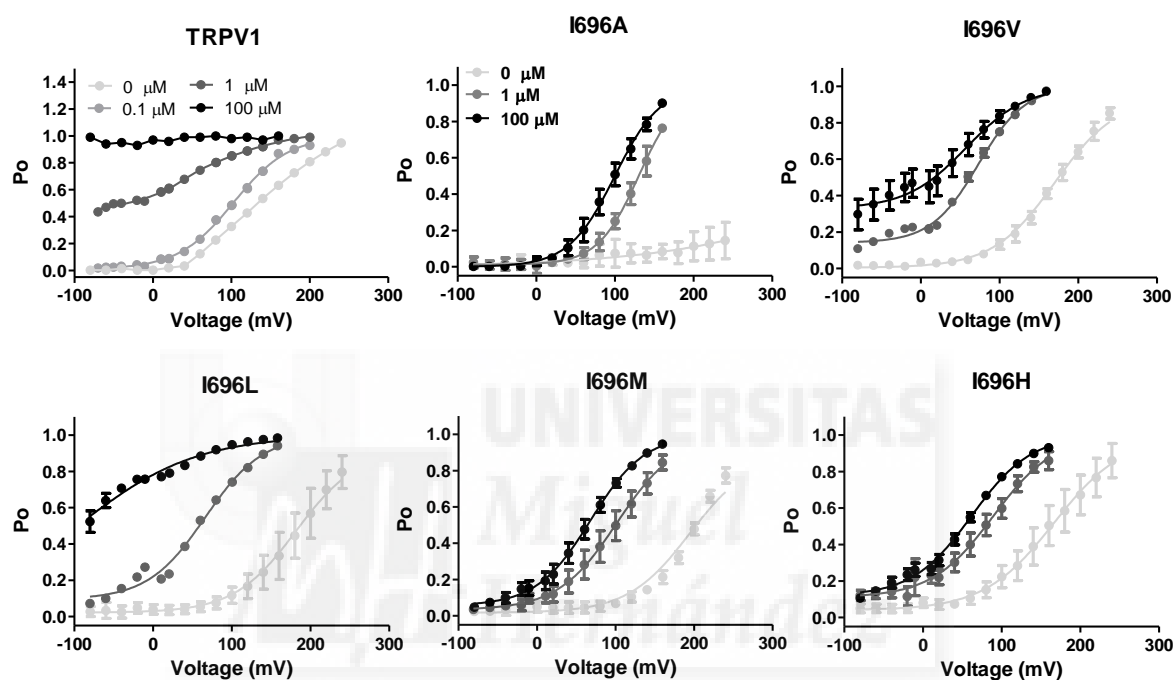


Figure R9. Fit of Po-V curves to an allosteric gating scheme. Normalized Po values are plotted against voltage for the indicated concentrations of capsaicin. Lines are the simultaneous best fit to Equation 1 or Equation 2, in absence or presence of capsaicin, respectively.

As observed in figure R9, Po values fitted properly to the proposed allosteric model for voltage in the absence (Equation 1) and the presence (Equation 2) of capsaicin. Po values are averaged and normalized from several experiments and continuous lines show the best fits for data at 0, 0.1, 1 and 100 μM of capsaicin for TRPV1 and I696 mutants. The parameters obtained are displayed in table II.

Voltage	TRPV1	I696V	I696L	I696M	I696H
Jo	0.0008	7.60E-06	6.40E-06	5.10E-06	9.51E-06
Z_g	0.65	0.67	0.66	0.68	0.6
L	2.00E-05	0.01	0.03	0.03	0.05
D	2.00E+06	84600	49000	35000	48000
ΔG_o (Kcal/mol)	2.0	2.9	2.7	3.05	2.2

Table II. Parameter values of allosteric model for voltage-gating activity of TRPV1 and I696X mutants. The energy was calculated from the allosteric model as $\Delta G_o = -RT \ln(J_oLD)$.

According to the fit, the values obtained for TRPV1 in all parameters are similar to the ones found in bibliography ([85], [161]), $L = 2E-05$, $D = 2E+06$ and $J_o = 8E-04$ (Table II). It is also important to mention that, for both TRPV1 and I696 mutants, z_g and ΔG_o had similar values as the obtained with the fitting to a Boltzmann from the experimental data. These findings may validate the allosteric model.

Regarding the values we obtained for I696 mutants, the most relevant alterations were noticed in parameters L and D . For all I696 mutants, L values were increased (0.01 for I696V, 0.03 for I696L, 0.03 for I696M and 0.05 for I696H) at least 500-2000 fold. According to this fit, the equilibrium between closed and open state, when all sensors are in their resting configuration, is shifted to the open state for these mutants. On the other hand, allosteric factor D was decreased in all cases ($8.46E+4$ for I696V, $4.9E+4$ for I696L, $3.5E+4$ for I696M and $4.7E+4$ for I696H) suggesting a defective coupling between their voltage sensors and the channel gate. Estimation of the ΔG_o values from the allosteric model reveals that mutation of I696 raises the free energy of activation by 0.2-1.0 kcal/mol (Table II). These results are consistent with the notion that the lower voltage sensitivity of I696X mutants arises primarily from an impact of these mutations on the equilibrium of the voltage sensor and its coupling to the pore.

We next fitted the data to the allosteric mechanism of gating in presence of different concentrations of capsaicin (Equation 2). For TRPV1 we used 0.1 and 1 μ M capsaicin since higher amount of capsaicin evoked ohmic currents which were not properly fitted to a sigmoidal shape. Whereas for I696X mutants we studied 1 and 100 μ M vanilloid concentrations. In contrast to

TRPV1 STRUCTURE-FUNCTION STUDY: ROLE OF THE TRP DOMAIN IN TRPV1 ALLOSTERIC GATING

DOCTORAL THESIS

LUCIA GREGORIO TERUEL

previous studies about allosteric model in TRPV1, we considered the possibility that both sensors might be allosterically coupled during the channel gating characterized by a coupling constant E . It is also important to highlight that none of the parameters were constrained for the fitting. Data obtained from this fitting is shown in Table III.

	TRPV1		I696A		I696V	
Capsaicin	0.1 μM	1 μM	1 μM	100 μM	1 μM	100 μM
J_0	2.70E-05	5.60E-05	9.50E-05	6.20E-06	9.00E-06	3.50E-05
Z_g	0.7	0.62	0.87	0.85	0.79	0.6
L	0.0044	0.024	0.0031	0.00037	0.01	0.007
D	9300	1500	64	1.50E+06	14000	19000
K_d	1.00E-05	8.00E-06	6.00E-06	5.00E-05	8.71E-06	2.00E-05
E	43	8.3	200	1.2	6.6	2.6
P	110	200	13	6	121	80
ΔG_0 (Kcal/mol)	1.76	0.50	2.8	1.74	1.22	-0.91
	I696L		I696M		I696H	
Capsaicin	1 μM	100 μM	1 μM	100 μM	1 μM	100 μM
J_0	4.00E-05	4.50E-05	5.20E-05	3.80E-05	1.60E-04	7.00E-05
Z_g	0.7	0.45	0.67	0.72	0.65	0.65
L	0.008	0.011	0.006	0.003	0.0094	0.005
D	5677	16000	4000	20100	651	6938
K_d	8.00E-06	6.00E-05	1.30E-05	7.00E-05	6.00E-06	1.7E-04
E	8	3.5	11	3.3	9.6	5
P	99	133	68	35	82	60
ΔG_0 (Kcal/mol)	1	-1.05	1.51	0.56	2.55	0.5

Table III. Parameter values of allosteric model for voltage-gating activity in the presence of capsaicin 0.1 and 1 μM capsaicin for TRPV1 and 1 and 100 μM for I696 mutants. The energy was calculated from the allosteric model as $\Delta G_0 = -RT \ln(J_0 LDEPQ)$.

Regarding the parameters derived from the action of capsaicin (P and K_d), we noticed that, for TRPV1, they showed reasonable values when compared with published data ([85], [161]). The application of capsaicin induced some changes in parameters L , D , P and E . We observed an increase in L (0.004 at 0.1 μM and 0.024 at 1 μM capsaicin) and P (110 at 0.1 μM and 200 for 1 μM) in a dose-dependent manner, whereas, parameters D (9300 at 0.1 μM and 1500 at 1 μM) and E (43 at 0.1 μM and 8.3 at 1 μM) were decreased. This finding is consistent with the decrease in voltage dependency that was observed under rising concentrations of capsaicin until getting an ohmic current at 100 μM , where channel gating will be driven by L , Q and P .

In contrast to these results, the values that best described the data of I696 mutants exhibited significant differences when compared with wild type data. The most disparate values were observed for I696A that showed an increase in values for E and D , and a decrease for P and L . This might be related with the significantly lower voltage-sensitivity of this mutant that prevented to reach near full opening at highly depolarized potentials. In agreement with this statement, when the vanilloid concentration was increased 100-fold, the values for all constants were in accordance with the other mutations.

In the presence of 1 μM capsaicin, the data revealed non-large changes in values for L , E , J_0 , K_d and z_g parameters for the remaining I696 mutants. However, these mutants mainly exhibited higher values for parameter D and lower for parameter P than wild type channels. Intriguingly, we detected a decrease in parameter D from the fitting of 1 μM capsaicin data, when compared with data obtained in the absence of the agonist. But we did not observe dose-dependent decrease values for this parameter in the presence of higher concentration of the agonist (100 μM) as it was detected for wild type channels. This means that an increase in the capsaicin concentration benefits the coupling between voltage sensor and channel pore. This might be in accordance with the barely voltage-independent conductance these mutants showed at hyperpolarized potentials.

In relation to the data obtained for capsaicin activation parameters for I696 mutants we observed that they showed similar K_d values to the ones obtained for wild type, around micromolar range ($\approx 10\text{E-}05 - 10\text{E-}06$). Nevertheless, these mutants showed lower values for parameter P which was decreased in the presence of higher vanilloid concentration unlike for TRPV1 channel. Mutant I696L displayed an increment in the values of L and P as the capsaicin

TRPV1 STRUCTURE-FUNCTION STUDY: ROLE OF THE TRP DOMAIN IN TRPV1 ALLOSTERIC GATING

DOCTORAL THESIS

LUCIA GREGORIO TERUEL

concentration was increased, akin to TRPV1. These findings may suggest that most I696 mutants showed an impaired coupling between capsaicin binding site and the pore of the channel. Since we detected values for parameter E different from 1, we assume that voltage sensor and capsaicin binding site are not totally independent from each other in the gating process. However, similar to wild type results, we observed that the allosteric factor E also diminished in a vanilloid dose-dependent manner. These results suggest that the binding of capsaicin molecules to their sensor influences the movement of voltage sensor. And, when the amount of capsaicin increases both sensors become less coupled to each other. In energetic terms, all mutants displayed higher ΔG_0 values than wild type channels. Overall, these data further support that mutation of amino acid I696 in the TRP domain has a significant impact in the allosteric mechanisms of activation, by affecting the equilibrium of pore opening and its coupling to the activating sensors.



3.1.4. W697 MUTANTS CHARACTERIZATION

Previous functional characterization of TRPV1 mutants in the W697 position showed that substitution by alanine strongly affected channel activation when it was stimulated with capsaicin, depolarizing voltages and heat [62]. According to the refined structural model they presented at this work, W697 is located at the position “*b*” of the putative coiled-coil motif, where it could mediate intersubunit interactions of the four helix bundle by TRPV1 subunits. As I696X mutants, we further studied the changes induced by mutations in the W697 position in TRPV1 gating. In our results we observe that all W697 mutants did not show a response to voltage (Fig. R2A and R11) but exhibited capsaicin-dependent activation (Fig. R2B and R12). We found that none of the W697 mutants was activated by the voltage applied (up to 240mV). However, they showed some voltage-dependent activation in presence of capsaicin. We next describe a more detailed study about the changes induced by W697 mutations in TRPV1 gating processes.

PROTEIN EXPRESSION LEVEL

Firstly, we checked the protein expression level and its presence in cell membrane by using biotinylation assay for some representative W697X mutants. This assay will unveil whether the absence of channel function could be related with impairment in protein expression.

TRPV1 STRUCTURE-FUNCTION STUDY: ROLE OF THE TRP DOMAIN IN TRPV1 ALLOSTERIC GATING

DOCTORAL THESIS

LUCIA GREGORIO TERUEL

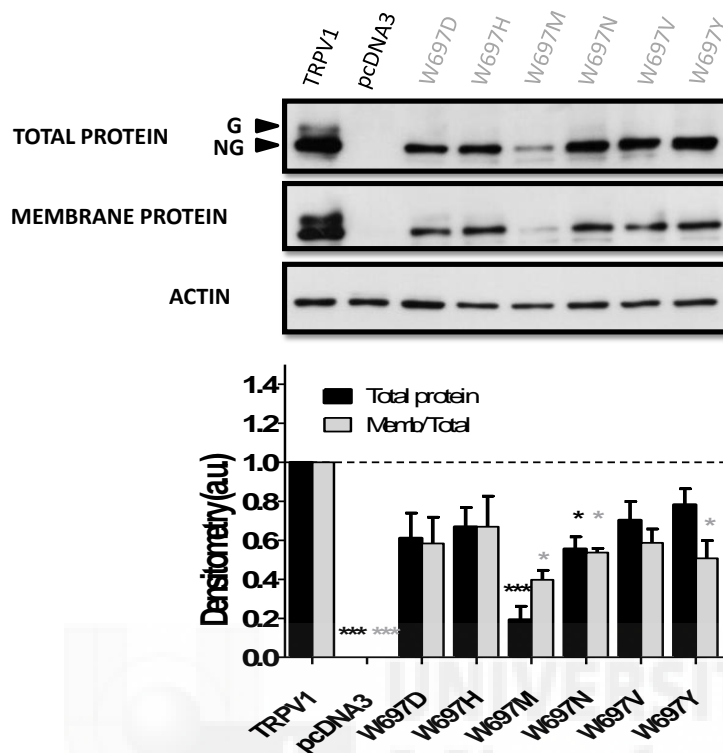


Figure R10. W697 mutant's expression level. *A*, Representative Western blot showing the total protein extracts and membrane fraction of transiently transfected HEK cells with TRPV1, pcDNA3 and a group of selected W697X mutants. Separate fractions were obtained by surface biotinylation. For the detection of bands were used antibodies against TRPV1 and actin as a loading control protein (α -TRPV1, 1:30000 and α -actin, 1:10000). Bands detection was performed by chemiluminescence using ECL-select. *B*, Normalized values of densitometry obtained from the western blot bands by using TOTAL LAB software. Ratio relates amount of protein from both samples membrane respect to total band. Measurements represent mean \pm SEM, number of experiments ≥ 3 . Statistical analysis one-way ANOVA (***) $p \leq 0.0001$.

As seen in figure R10, all W697 mutants tended to decrease their protein expression level when compared to TRPV1. W697M and W697N mutants showed significant changes in protein expression level when compared with the wild type protein (Fig. R10A-B) showing W697M the most dramatic decrease in protein expression (~80%) respect to the wild type protein. Interestingly, all mutants reached the cell membrane although in a lower rate than TRPV1, statistically significant for W697M, W697N and W697Y. Similar to I696X mutants, for W697X mutants we could discern some changes in the glycosylation pattern when compared with TRPV1 (Fig. R10A). None of the mutants showed the upper band over 100 KDa corresponding to the glycosylated form of the protein. This finding suggested that mutation of

W697 also produced a conformation change in the protein subunits that prevented their glycosylation.

VOLTAGE RESPONSE

Akin to I696 mutants, we further studied the voltage-dependent channel gating of some representative W697X mutants, selected from each group of amino acids (valine (V), methionine (M), histidine (H), tyrosin (Y), asparagine (N) and aspartic acid (D)). For this purpose, we performed patch clamp experiments of mutant channels heterologously expressed in HEK cells using whole-cell configuration. The protocol used for voltage-activation corresponded to 100 ms depolarizing pulses from -120 to 240 mV in steps of 20 mV. In figure R11, representative recordings evoked by the voltage step protocol are depicted.

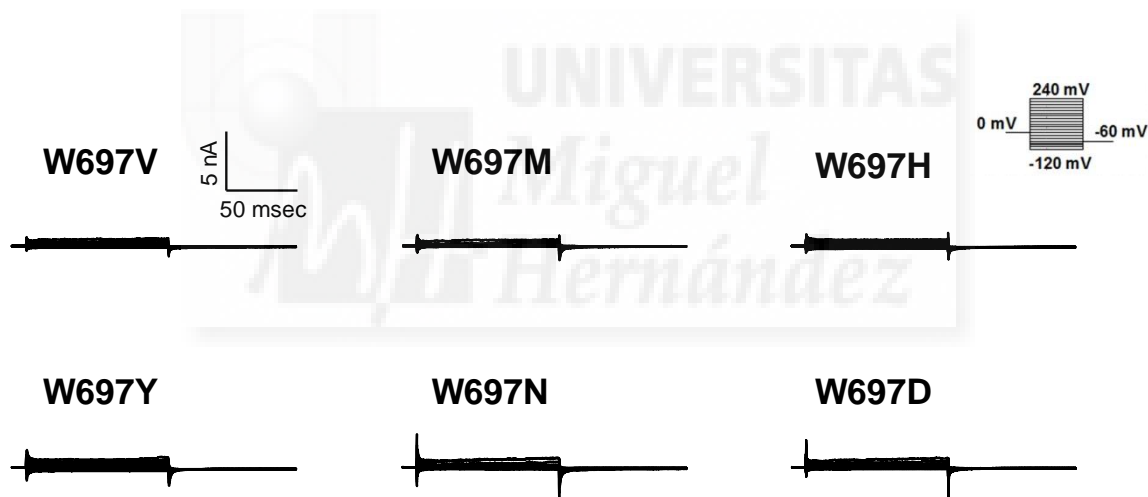


Figure R11. Mutation of the W697 residue produces non-responsive channels by voltage. Representative families of ionic currents evoked with a voltage step protocol consisting of 100 ms depolarizing pulses from -120 to 240 mV in steps of 20 mV. Holding potential 0 mV; time between pulses 5 s.

As observed, chosen W697X mutants did not show response to the depolarizing voltages (Fig. R11). This absence of protein functionality to voltage was also found in all of W697X mutants (Fig. R2A). The lack of response to depolarizing voltages as high as 240 mV suggests that W697X mutants lost their voltage dependency. This contribution of W697 to voltage sensing is intriguing since the TRP box is supposedly distant from the proposed voltage sensor. Nonetheless it is consistent with a contribution of this domain in the downstream events upon the activating stimulus that lead to gate opening.

CAPSAICIN RESPONSE

We next characterized the response of W697X mutants to capsaicin, at both negative and positive membrane potentials. The protocol used for these experiments corresponded to a ramp protocol of 300 ms from the holding potential of 0mV step to -80 mV, followed by 350 ms linear ramp up to 160 mV, in the presence of 100 μ M capsaicin.

In figure R12, we disclosed representative current-voltage relations (I-V) for W697X. We also tested 1 and 10 μ M capsaicin to activate the channels, but most of the mutants did not show fully activation in presence of the low agonist concentrations. In addition, we obtained the conductance-voltage relation (G-V) and calculated the biophysical parameters of gating for the selected mutants (Fig. R13). All tested W697X mutants displayed an altered capsaicin-evoked response in comparison with wild type channel currents.

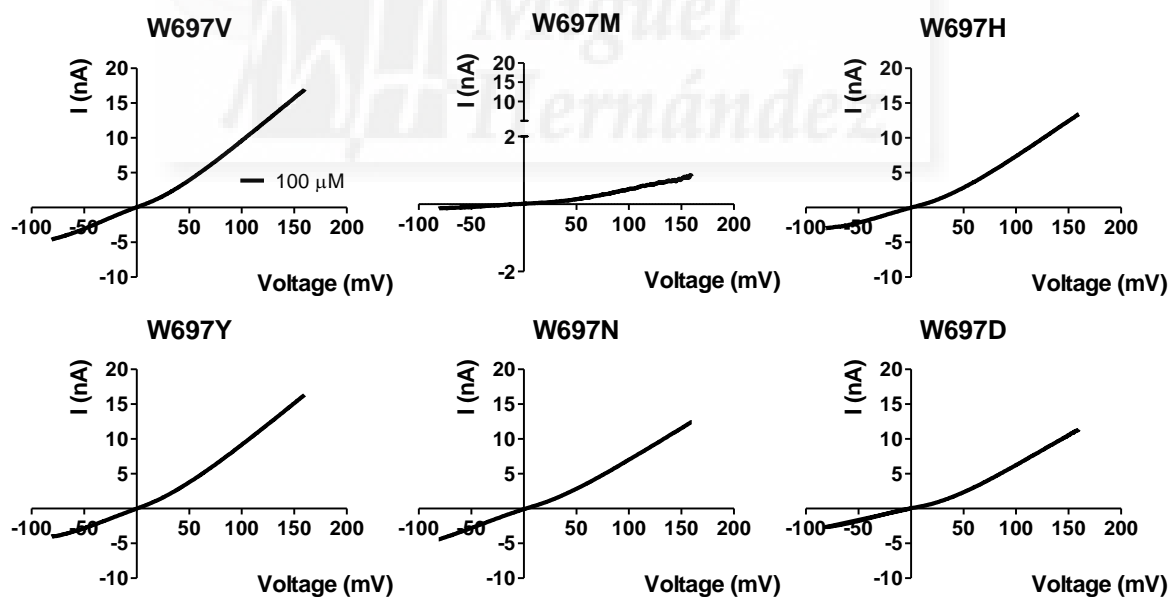


Figure R12. Capsaicin evoked current for W697X mutant channels. Representative ionic currents evoked by 100 μ M capsaicin from the mutants W697V, W697M, W697H, W697Y, W697N and W697D. For mutants I-V relations were recorded using a ramp protocol consisting of a voltage step of 300 ms from 0 to -80 mV, followed by a 350 ms linear ramp up to 160 mV.

3. RESULTS

As illustrated in figure R12, addition of 100 μM capsaicin resulted in large outward rectifying currents for all studied W697 mutants, even the W697M, that reversed around 0 mV. In contrast to mutants in I696 position, W697X mutants exhibited ionic current induced by capsaicin at hyperpolarizing membrane potentials. In general, these currents followed a similar nonlinear behavior as TRPV1 currents induced by 1 μM capsaicin. The I-V curve of W697M mutant displayed lower intensity than the rest of W697 mutants, likely due to the fact that this mutant expression is 80% lower than that of wild type and other mutants. However, we observed that this current showed voltage dependency induced by capsaicin as for the rest of functional mutants. Therefore, despite of the dramatic decreased of protein expression level, the mutant protein is expressed, reaches cell membrane current and is functional. We next evaluated the biophysical parameters obtained from the currents displayed in figure R12.

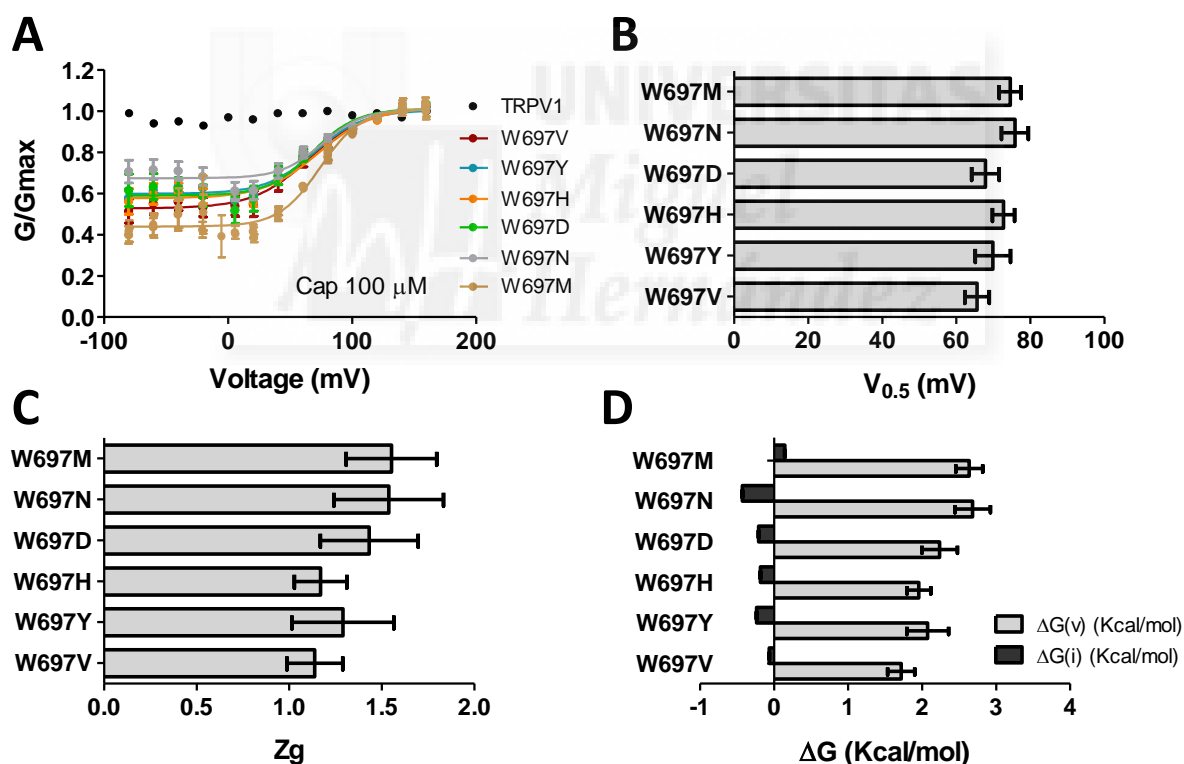


Figure R13. Voltage dependency and biophysical parameters of W697X mutants. **A**, G-V relation are plotted for TRPV1 and mutants constructions in presence of 100 μM capsaicin. Conductance curves were obtained as previously described in Fig. R5 from the ionic currents shown in Fig. 12. Solid lines depict the best fit to a Boltzmann distribution. TRPV1 data did not properly fit to a Boltzmann distribution. **B**, $V_{0.5}$ values for the different W697 mutants obtained from the Boltzmann distribution G-V relations. **C**, Apparent gating valence of the activation process: $Z_g = 25.69 \text{ mV} / a_n$. **D**, Free energy of the activation process from voltage ($\Delta G_o(v)$) or agonist ($\Delta G_o(i)$) activation, assuming a two-state model. All values are mean \pm SEM; number of cells ≥ 5 .

TRPV1 STRUCTURE-FUNCTION STUDY: ROLE OF THE TRP DOMAIN IN TRPV1 ALLOSTERIC GATING

DOCTORAL THESIS

LUCIA GREGORIO TERUEL

The G-V curves (Fig. R13A) were obtained from ionic currents evoked with the ramp-depolarizing protocol used in figure R12. At this capsaicin concentration we observed that, all W697 mutants exhibited voltage-dependent gating since they followed a Boltzmann distribution. As it corresponds with an ohmic current, the conductance obtained from TRPV1 currents followed a voltage-independent linear distribution. Despite of the impaired voltage-dependent activation of W697 mutants, these results imply that these channels were still able to sense voltage changes and operate in a voltage-dependent manner. Furthermore, we detected high conductance values (0.4 - 0.7) at hyperpolarized membrane potential indicating that capsaicin was able to induce channel opening in a voltage-independent manner.

Since W697 mutants exhibited voltage dependency in the presence of capsaicin, we were able to calculate the biophysical parameters of gating from the normalized G-V curves. The presence of capsaicin shifted the $V_{0.5}$ toward measurable potentials for these mutants (Fig. R13B). Interestingly, all the mutants showed very similar values for this parameter and non-significant differences were found between them ($V_{0.5}$ values in mV: 74.6 ± 2.9 for W697M; 75.8 ± 3.6 for W697N; 67.8 ± 3.7 for W697D; 72.7 ± 2.9 for W697H; 69.9 ± 4.7 for W697Y and 65.6 ± 3.3 for W697V).

We also calculated the apparent gating valence of the activation process for these mutants (Fig. R13C). This value was not significantly changed by the mutation included in each case. However, when we compare them with the values for wild type protein TRPV1 and I696X mutants, we detected a ≥ 2 -fold increase in W697 mutant's values (1.55 ± 0.24 for W697M; 1.53 ± 0.29 for W697N; 1.43 ± 0.26 for W697D; 1.17 ± 0.14 for W697H; 1.29 ± 0.27 for W697Y and 1.13 ± 0.15 for W697V), in accordance with the steeper G-V curves displayed in figure R13A. Even though these values were higher than the ones for wild type channels, they were still close to 1, which suggested that the movement of charges across the membrane due to the voltage sensing had not significantly changed in these mutants.

Finally, we studied the differences between the free energy of gating for the mutants studied. In figure R13D, we displayed the values of ΔG_0 between the closed and the open state for the voltage- and capsaicin-dependent components separately to better understand the contribution of each agonist to the gating process. The voltage-independent component

proceeded from the conductance required at negative membrane potentials in the presence of the vanilloid ($\Delta G_o(i)$). Voltage-dependent component ($\Delta G_o(v)$) elicited higher free energy of activation when compared with vanilloid values. This phenomenon arises primarily from the voltage insensitivity of these mutants (1.8-2.8 kcal/mol), since that form the voltage independent component is negative (-0.07 to -0.41 kcal/mol).

Summarizing, these data suggest that the replacement of W697 by other amino acids is not directly abrogating the ability of sensing the stimulus voltage. We conclude this from the result that these channels showed voltage-dependent activation in the presence of capsaicin, despite of their lack of activation by the physical stimulus alone. In fact, these mutants seemed to be affecting downstream processes in the gating mechanism, i.e. coupling between voltage sensor and the pore of the channel. Furthermore, although we observed differences in current density between these mutants (Fig. R2B), we did not find differences in the biophysical parameters of the selected mutants, independently of the physico-chemical nature of the amino acid inserted (Fig. R13). Collectively, this would mean that W697 position in TRPV1 could not be replaced by any other residue without dramatically affecting channel activity. These results might indicate that W697 position in TRPV1 must be located in a critical position for the correct coupling of channel sensors and gate.

ALLOSTERIC MODEL

Substitution of the W697 residue in TRPV1 by the natural amino acids gave rise to a critical impairment in channel functionality. Nevertheless, the process of channel gating being affected by these mutations is still not completely understood. To further investigate this issue, we evaluated our results obtained from electrophysiological experiments of W697X mutants by fitting them to the allosteric model of gating. In this case, since W697 mutants were non-activated by depolarizing voltages we could only study the allosteric activation mechanism in the presence of capsaicin at 100 μ M both hyperpolarizing and depolarizing membrane potentials (Equation 2). We decided to study this concentration of the agonist at which all channels showed detectable currents because most of the W697X mutants were not activated at lower concentration of capsaicin or they did not reach a G-V saturated curve. As described, we assumed G/G_{max} values are equivalent to P_o for whole cell currents.

TRPV1 STRUCTURE-FUNCTION STUDY: ROLE OF THE TRP DOMAIN IN TRPV1 ALLOSTERIC GATING

DOCTORAL THESIS

LUCIA GREGORIO TERUEL

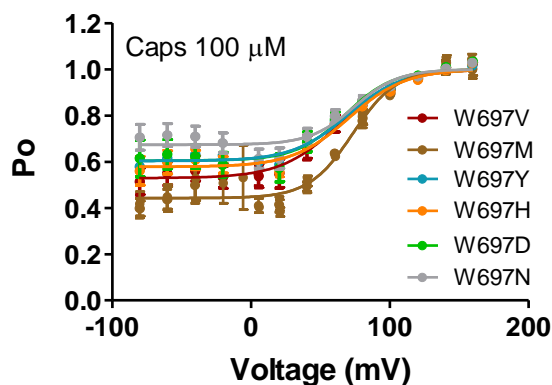


Figure R14. Fit of P_o -V curves of W697X mutants to an allosteric gating scheme. Normalized values of P_o plotted against voltage in presence of 100 μ M capsaicin. Lines are the simultaneous best fit to Equation 2.

As observed in Fig. R14, P_o values were fitted properly to the proposed allosteric model when considering activation by voltage and capsaicin (Equation 2). The fitting gave rise to the parameters reported in Table IV.

Capsaicin 100 μ M	W697Y	W697H	W697V	W697M	W697D	W697N
J_o	$3.3 \cdot 10^{-5}$	$5.0 \cdot 10^{-6}$	$7.5 \cdot 10^{-6}$	$1.0 \cdot 10^{-6}$	$1.0 \cdot 10^{-5}$	$1.0 \cdot 10^{-5}$
z_g	1.3	1.3	1.2	1.6	1.5	1.6
L	0.011	0.011	0.011	0.011	0.012	0.013
D	793	19484	13245	19343	3389	2084
K_d	$1.0 \cdot 10^{-5}$	$1.0 \cdot 10^{-5}$	$3.0 \cdot 10^{-5}$	$8.0 \cdot 10^{-6}$	$3.0 \cdot 10^{-5}$	$2.0 \cdot 10^{-6}$
E	1.77	0.52	0.92	0.83	1.1	0.61
P	140	133	133	131	151	159
ΔG_o (kcal/mol)	0.19	0.17	0.47	1.72	0.86	0.15

Table IV. Parameter values of allosteric model for voltage-gating activity in the presence of 100 μ M of capsaicin for W697X mutants. The energy was calculated from the allosteric model as $\Delta G_o = -RT \ln(J_o L D E P Q)$.

As discerned from Table IV, all studied W697X mutants showed similar values for most of the parameters calculated in this fitting, correlating the pattern of values for biophysical

parameters obtained from the electrophysiological studies. We only identified a significant change in voltage sensor parameters for mutants W697H, W697V and W697M which showed higher D and lower J_o values for these factors when compared to W697Y, W697D and W697N in presence of the same amount of capsaicin (100 μ M). This result suggests that W697X mutants incorporating an amino acid with hydrophobic characteristics exhibited better coupling between their voltage sensor and the channel pore at that high vanilloid concentration than mutants including polar residues. Furthermore, z_g values obtained from the fitting were very similar to the values calculated from the Boltzmann fitting to experimental data. This finding would support the accuracy of the allosteric model results.

We also noticed that capsaicin activation-derived parameters obtained for W697X mutants were more similar to the values obtained for TRPV1 than the values obtained from the I696X mutants. For W697X mutants Kd was estimated around micromolar range (10E-05, 10E-06) and P gave values between 130 and 160. Interestingly, the lowest values that were detected for parameter P corresponded to the mutants W697H, W697V and W697M, indicating a weaker coupling between capsaicin binding and channel gate than the rest of mutants studied. These results suggest that mutants substituting W697 by hydrophobic amino acids showed better coupling between the voltage sensor and the pore than between capsaicin binding site and the channel gate.

Other intriguing finding from the allosteric model fitting was that, for all W697X mutants studied, the value proposed for parameter E was very close to 1, which means that voltage sensor and capsaicin binding site acted independently in the gating process of these mutants. Summarizing, we observed that mutation of W697 position mostly affected the allosteric processes, but mainly the coupling between voltage sensor and channel pore and the coupling between sensors were being impaired. Furthermore, the free energy of channel gating in the presence of 100 μ M, revealed a values close to 0 kcal/mol, consistent with the notion that channel gating of these channels is largely driven by capsaicin in a voltage-independent manner. Noticeably, lower free energy values were found for mutants substituted by a polar amino acid, indicating a preference for this type of residue.

To further characterize the behavior observed in W697 mutants, we studied the action of increasing concentrations of capsaicin for W697Y mutant. This mutant, despite of being one

TRPV1 STRUCTURE-FUNCTION STUDY: ROLE OF THE TRP DOMAIN IN TRPV1 ALLOSTERIC GATING

DOCTORAL THESIS

LUCIA GREGORIO TERUEL

of the most similar amino acid to tryptophan, still showed significant alterations in protein functionality when compared with wild type channel.

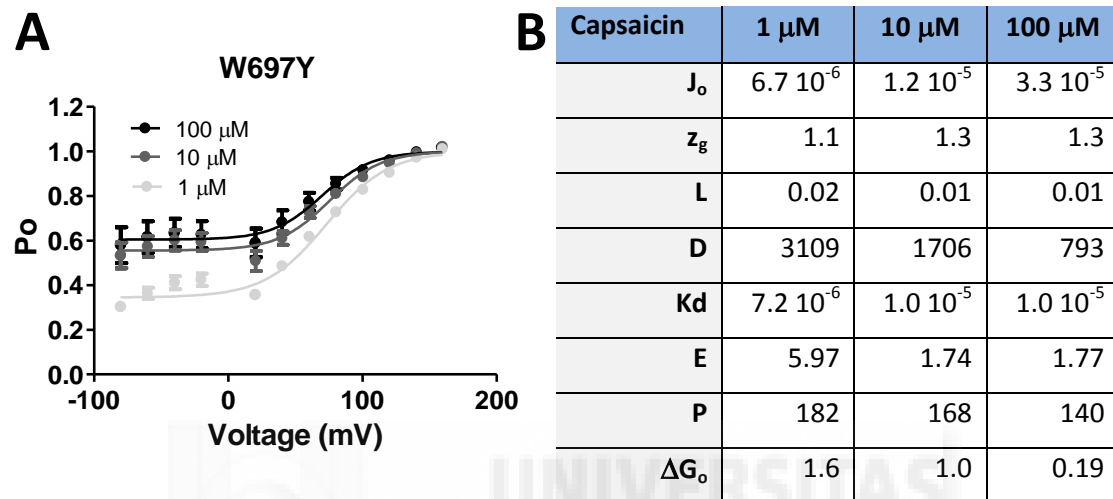


Figure R15. Fitting of an allosteric model for W697Y in presence of increasing concentration of capsaicin. **A**, Fit of P_o -V for W697Y curves to an allosteric gating scheme. Normalized values of P_o plotted against voltage for the indicated concentrations of capsaicin. Lines are the simultaneous best fit to Equation 2 in presence of 1, 10 and 100 μM capsaicin. **B (Table V)**. Parameter values obtained from allosteric model fitting.

The fit performed in figure R15A yielded parameters shown in figure R15B (table V). As it was found in the graph above, the model was properly fitted to P_o normalized values for the three conditions. As depicted in Table V, an increment in the vanilloid from 1 to 100 μM mostly reduced the value of the coupling E and D constants, and had minor effects on P, J_o and L, consistent with the tenet that mutation of this position primarily affected the allosteric coupling. As for wild type and I696X mutants, the free energy of activation, obtained from the allosteric model, decreased as the vanilloid was augmented.

3.1.5. STRUCTURAL FEATURES OF TRP BOX

The TRP box of TRPV1 is located a few amino acids after the putative channel gate, at the core of the predicted coiled-coil structure of the TRP domain which has been proposed to fold in a 4-strand, parallel coiled-coil structure in the homomeric channel ([60], [61], [62]). Nevertheless, the folding of this putative structure may show an assembling that diverge from a typical left-handed coiled-coil, as suggested by the occupancy of the e and g positions by non-charged residues. Considering these sequence variations and the functional data obtained from the alanine scanning mutagenesis of TRP box sequence, they suggested that I696 and W697 residues were located at the a and b positions of the putative coiled-coil motif, where they could mediate inter- or intrasubunit interactions of the four helix bundle assembled by TRPV1 subunits. Furthermore, our results about these two positions entirely support this model and, in turn, the provide news aspects to consider in this putative structure (Fig. R16).

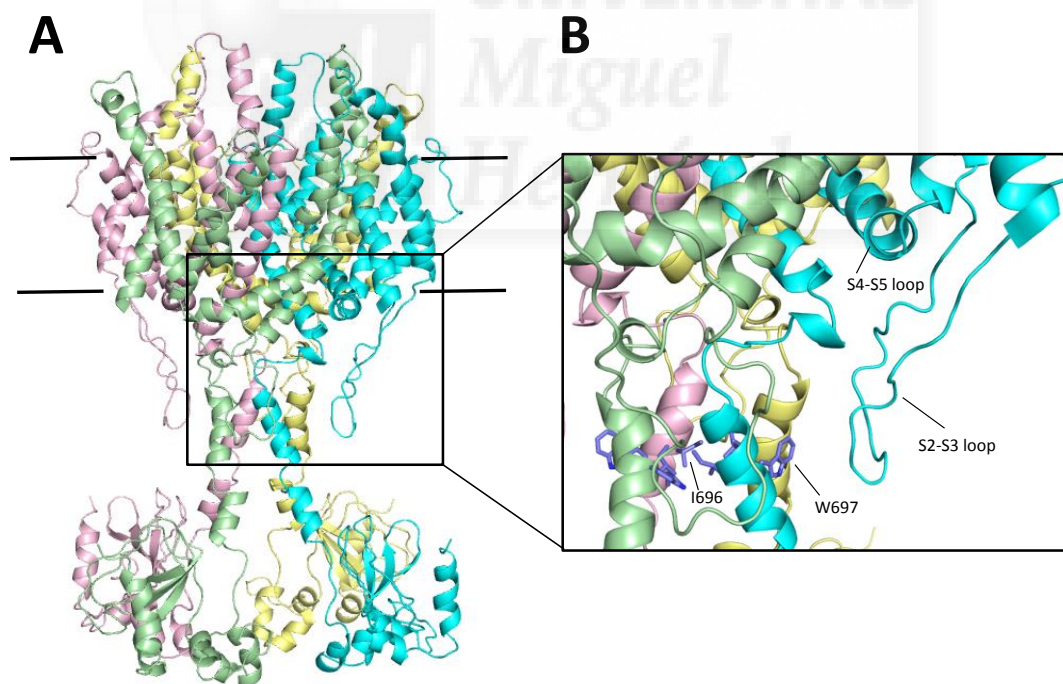


Figure R16. Putative model for full-length TRPV1 and the proposed coiled-coil structure of the TRP box. **A**, Global view of the tetrameric arrangement of TRPV1 in the closed state, inserted into the lipid bilayer. The N terminus domain of the channel is not displayed. **B**, Putative model proposed for TRP domain. Positions I696 in the bundle core and W697 in a more external position are marked. The model was performed as described (Fernandez-Ballester and Ferrer-Montiel, 2008). The molecular graphic representations were created using PyMOL v1.6.0 (<http://www.pymol.org/>).

TRPV1 STRUCTURE-FUNCTION STUDY: ROLE OF THE TRP DOMAIN IN TRPV1 ALLOSTERIC GATING

DOCTORAL THESIS

LUCIA GREGORIO TERUEL

Substitution of I696 residue by any of the natural amino acids caused a significant impairment in mutant channels functionality. Only a hydrophobic residue was allowed in the I696 position for generating functional channels. Furthermore, the volume of the amino acid placed in this position was also relevant for the correct coupling of the channel. These results might indicate that the I696 position in TRPV1 must be located in a hydrophobic environment, shielded from the aqueous surroundings and with delimited space where the residue can be embedded. Therefore, these findings supported the aforementioned model, which placed the I696 residue in the central position of the four subunits.

Replacement of W697 in TRPV1 also evoked a profound impact in channel activation. Mutation of this position fully abrogated the ability of voltage to act as a partial activator of channel gating. Notwithstanding, at variance with the lack of voltage sensitivity, several W697X mutants displayed partial activation by capsaicin, independent of their physico-chemical properties. Our data proposed that residue W697 must play an essential role in channel gating since none of the mutants were able to respond to depolarizing voltages. According to the model described above, the W697 residue could be interacting with the TRP domain of the adjacent subunit. Alternatively, it could be more externally oriented for interacting with other subunit domains such as the S4-S5 linker or the S2-S3 loop.

To learn more about the impact that mutations may cause in I696 and W697 positions in the structural model proposed, we studied the effect of these changes on the interaction energy values. This parameter measures the contribution to the tetramer binding energy that is caused by the interaction between a specific residue in one subunit and the other three. In each case, energy values have been obtained from the model explained above and normalized respect to the amino acid that is contained in TRPV1 wild type protein for each position. Thus, the replacement of this residue by any amino acid which evoked energy values higher than 0 kcal/mol implied that the interaction between one subunit and the others was negatively affected by this particular mutation.

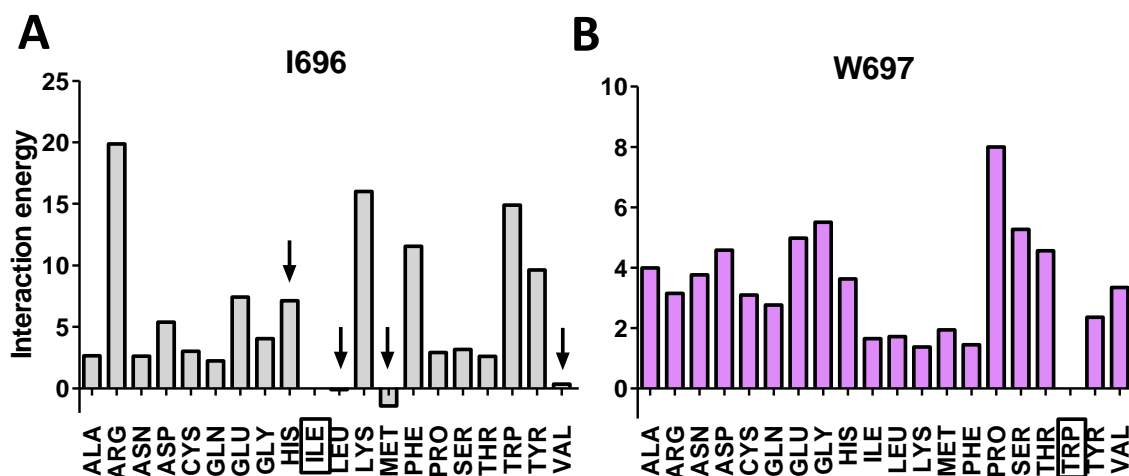


Figure R17. Interaction energy values for all mutants in I696 (A) and W697 (B) positions. Energy values represent the difference between the interaction energy obtained for each mutant and wild type protein. The original amino acid contained in TRPV1 (open rectangle) is normalized as 0 kcal/mol. Mutants responding to both depolarizing voltage and capsaicin are indicated in the graph (black arrow).

As depicted in figure R17, interaction energy values in both positions were significantly affected by most of the mutations included. Noticeably, we observed that mutations in I696 position showing the lowest energy values (I696L, I696M and I696V) were also partially activated by both stimuli applied. However, the mutant to histidine, which was also responsive to both stimuli, showed an unexpected high interaction energy value when compared when other non-functional mutants. This phenomenon could be due to the fact we are measuring energy values from a static image of the structural model. Therefore, this approach might not reveal possible rearrangements that may exist in the assembly of the four strands, suggested for this region as a coiled coil, to adapt different volumes and configurations of the side chain placed in this position. For this reason, the substitution of I696 residue by a histidine could generate functional channels in real conditions, as we detected in functional assays, despite of the high energy values obtained. Interestingly, all mutations included in W697 showed higher energy values than wild type protein. This data suggested that any amino acid placed in this position impaired the interaction between the four subunits. This pattern was also observed in the functional experiments performed where none of the mutants were activated by applying depolarizing voltages. Thus, these results confirm that W697 residue plays an essential role in channel gating since none of the natural amino acid placed in this position generate fully activated channels.

3.2. CHARACTERIZATION OF TRP DOMAIN IN TRPV1

The TRP domain plays a double role in TRPV1 functionality. As mentioned, the TRP domain has been described as an important region in subunit oligomerization; likewise, it has been suggested its involvement in the functional coupling necessary for channel gating ([60], [61], [62]). Considering these findings, we were interested in further understanding the implication of this region in channel functionality. For this purpose, we focused our research on identifying the amino acids from this region that are essential for preserving the intrinsic role of the TRP domain in TRPV1 functionality.

3.2.1. MUTAGENESIS STRATEGY

The main objective of this project is to recover the activity of a non-functional TRPV1 chimera where its TRP domain was replaced by that of the TRPV2 channel (TRPV1-AD2). We considered this chimera as interesting aim of study because, despite TRPV2 exhibits the most similar TRP domain sequence to TRPV1, this chimera did not show any response to capsaicin, voltage or heat. In contrast other chimeras like TRPV1-AD3, with the corresponding TRP domain of TRPV3 that shares lower percentage of identity with TRPV1, was partially gated by the activating stimuli [61]. In this approach, we proposed a site directed sequential and cumulative mutagenesis strategy of this region to restore the sequence of TRPV1. The aim of this strategy was to determine the minimum number of mutations in the AD2 context required to restore TRPV1 channel activity (Fig. R18). The design of the mutations was based on the importance from each residue in the original sequence attending to its structural features and identity. Thereby, we firstly inserted the corresponding amino acids in the positions we considered were deleted according to our alignment between the TRP domain sequences of TRPV1 and TRPV2. Afterwards, we recovered the amino acids which were placed in the corresponding positions “a” and “d” from the proposed coiled-coil structure. Finally, we restored the residues showing the most different physico-chemical properties. Following this stepwise we should be able to assign functional properties to specific residues or group of residues in the TRP domain sequence.

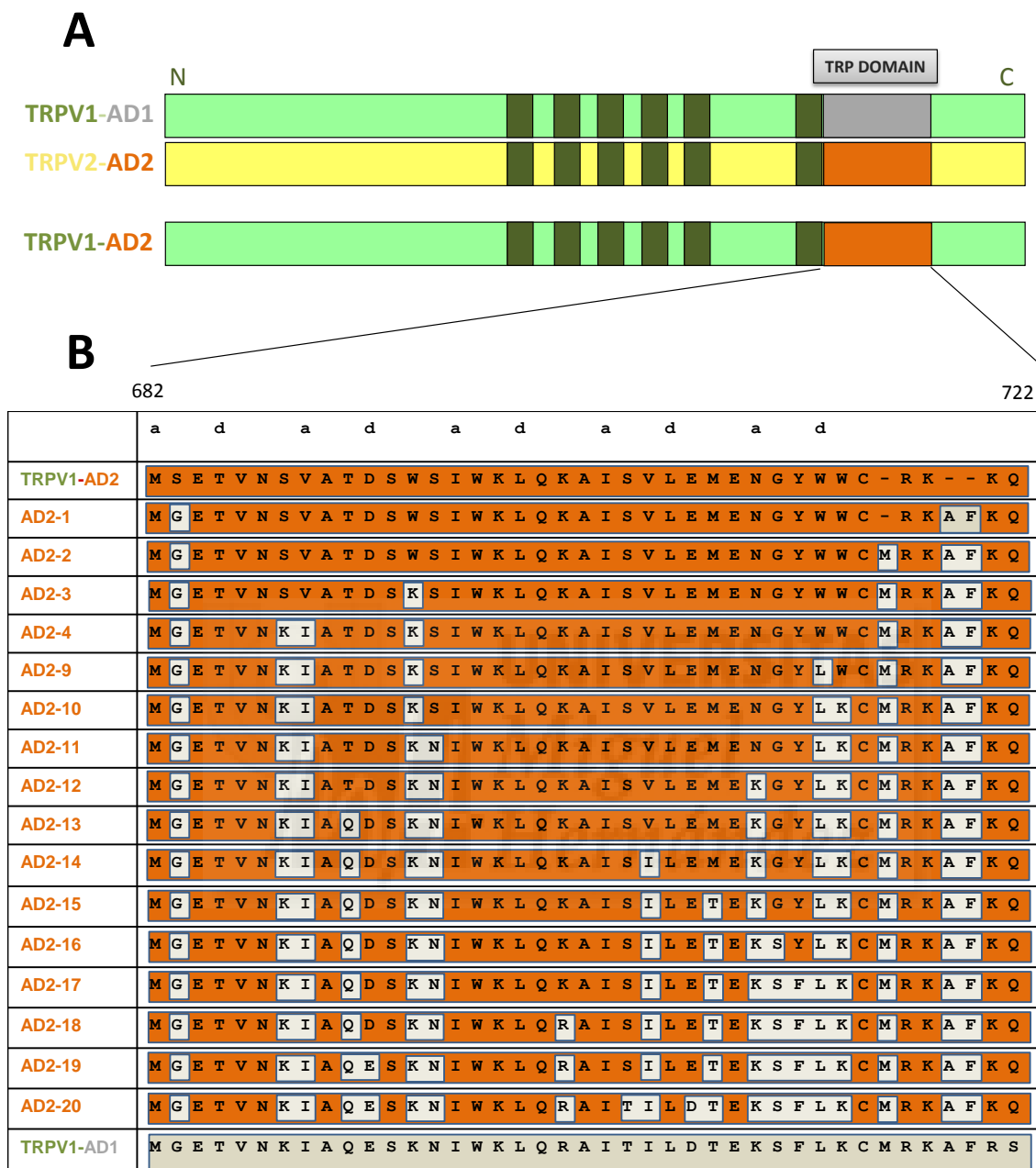


Figure R18. Schematic representation of step-reconstruction TRPV1-AD1 domain in the context of the TRPV1-AD2 chimera. **A**, The original chimera (TRPV1-AD2) corresponds to TRPV1 with its TRP domain (grey) replaced by the cognate part of TRPV2 (orange). **B**, The chimera TRPV1-AD2 is cumulative and sequentially mutated rescuing the TRP domain sequence from TRPV1 wt. In this process were generated 20 mutants AD2-1 to AD2-20. The mutated residues are highlighted with grey square. Residue numbers correspond to rat TRPV1. The “a” and “d” positions of the predicted coiled coil are boxed (http://www.ch.embnet.org/software/COILS_form.html).

TRPV1 STRUCTURE-FUNCTION STUDY: ROLE OF THE TRP DOMAIN IN TRPV1 ALLOSTERIC GATING

DOCTORAL THESIS

LUCIA GREGORIO TERUEL

The construct containing the cDNA encoding the chimeric channel TRPV1-AD2 was designed in the pcDNA3 vector (Invitrogen). The mutations are performed by PCR technique using site directed mutagenesis using this plasmid as template for amplification. For each mutant we designed a pair of primers which specifically included the mutation in the nucleotide sequence in each amplification cycle.

It is important to mention that, mutant AD2-20 contains two extra amino acids at the end of TRP domain corresponding to K721 and Q722. This is because of the insertion of amino acids A719 and F720 in the gaps detected in the alignment between both proteins.

3.2.2. FUNCTIONAL CHARACTERIZATION OF CHIMERIC CHANNELS

TRPV1 is a non-selective cationic channel showing high permeability to Ca^{2+} ions. Considering this property of the channel, we used two approaches to study chimeric channels functionality elicited by different activating stimuli. Firstly, we performed a calcium microfluorographic assay with the fluorescent dye Fluo4-NW to investigate the activation of the chimeric mutants with capsaicin. We used the vanilloid at 100 μM to ensure channel opening.

To study the biophysical properties of the functional chimeric channels, we characterized them with patch clamp using depolarizing voltages and heating temperature as stimuli. For all these experiments we used HEK 293 cells transfected with the cDNA encoding the different chimeric mutants after 48h expression.

AD2 CHIMERAS EXPRESSION LEVEL

The TRP domain has been proposed as a molecular determinant of channel multimerization. Since we are introducing critical changes in this region, we considered it was relevant to study the protein level of some representative chimeras in transiently transfected cells. In turn, differences in protein expression could be related with possible alterations in chimeras' functionality.

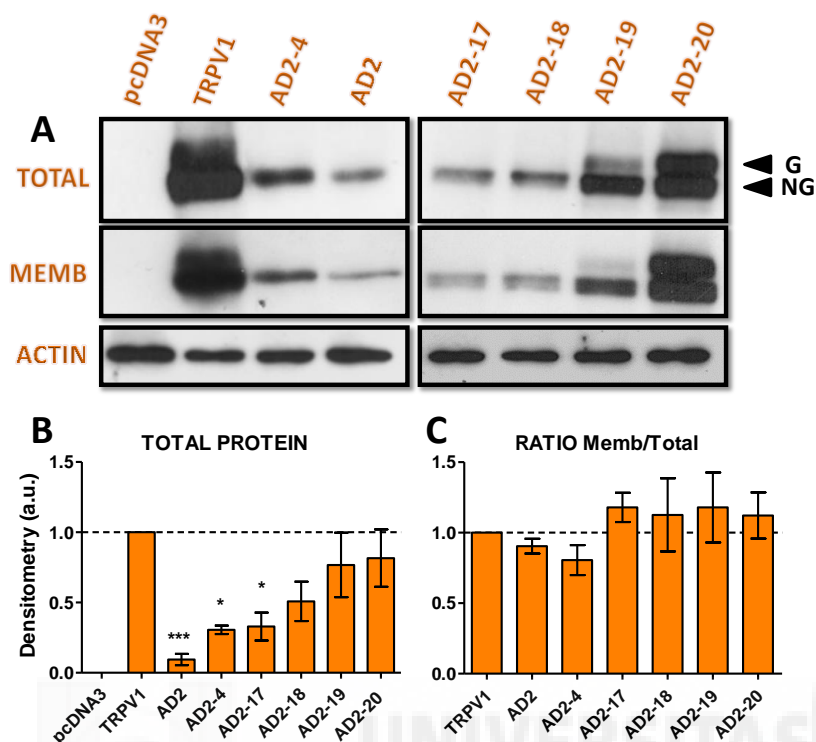


Figure R19. Expression level and membrane detection of TRPV1 and some representative chimeras. A, Total protein extracts and surface protein of transiently transfected HEK 293 cells with some representative chimeric channels, TRPV1, and pcDNA3. Separate fractions were obtained by surface biotinylation. Actin bands in total lysate fractions were used to normalize loading. The same amount of protein is loaded for every sample. For the detection of bands were used antibodies against TRPV1 and actin (α -TRPV1, 1:30000 and α -actin, 1:10000). Bands detection was performed by using ECL-select. **B,** Normalized values of densitometry obtained from the western blot bands by using TOTAL LAB software. **C,** Ratio relating amount of protein from both samples membrane respect to total band. Measurements represent mean \pm SEM, number of experiments \geq 3. One-way ANOVA, *** $p \leq 0.0001$.

Since not all samples showed the glycosylated band we used the lower non-glycosylated band to compare the protein expression pattern. As seen in figure R19A, all chimeric channels were detected in both total protein extracts and the cell surface while no bands were detected for mock transfected cells. However, the protein expression level was severely impaired in some chimeras, i.e. AD2, AD2-4 and AD2-17 as compared with wild type (Fig. R19B). Furthermore, these mutants lacked the upper band of the characteristic doublet corresponding to the glycosylated form described for TRPV1. Interestingly, the expression level of these chimeric channels was sequentially increased reaching approximate TRPV1 while the original sequence was recovered. Simultaneously, the glycosylated form of the protein was also recovered. First, it was slightly detected in AD2-18 and lately increasing its expression level until getting wild type values in AD2-19 and AD2-20. Thereby, AD2-19 and AD2-20 showed the most similar expression

TRPV1 STRUCTURE-FUNCTION STUDY: ROLE OF THE TRP DOMAIN IN TRPV1 ALLOSTERIC GATING

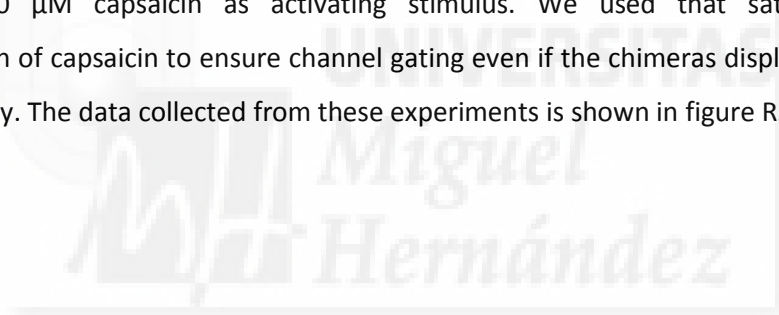
DOCTORAL THESIS

LUCIA GREGORIO TERUEL

pattern to TRPV1 channel. These results indicate that small changes in the TRP domain dramatically affect protein expression level. This phenomenon could be due to an impairment of protein folding causing the degradation of an improper conformation of the channel.

CALCIUM ASSAY SCREENING METHOD.

We screened the response of chimeric channels to capsaicin by Ca^{2+} microfluorography. HEK cells were transiently transfected with the mutated chimeras (AD2-1 – AD2-20). For this experiment we used the calcium-sensitive fluorescent dye Fluo4-NW (Molecular Probes) which increases its fluorescence upon calcium binding. This procedure allowed us to detect cells expressing functional chimeras by measuring the fluorescence increase in cytosolic Ca^{2+} after applying 100 μM capsaicin as activating stimulus. We used that saturating capsaicin concentration of capsaicin to ensure channel gating even if the chimeras display an alteration in ligand efficacy. The data collected from these experiments is shown in figure R20.



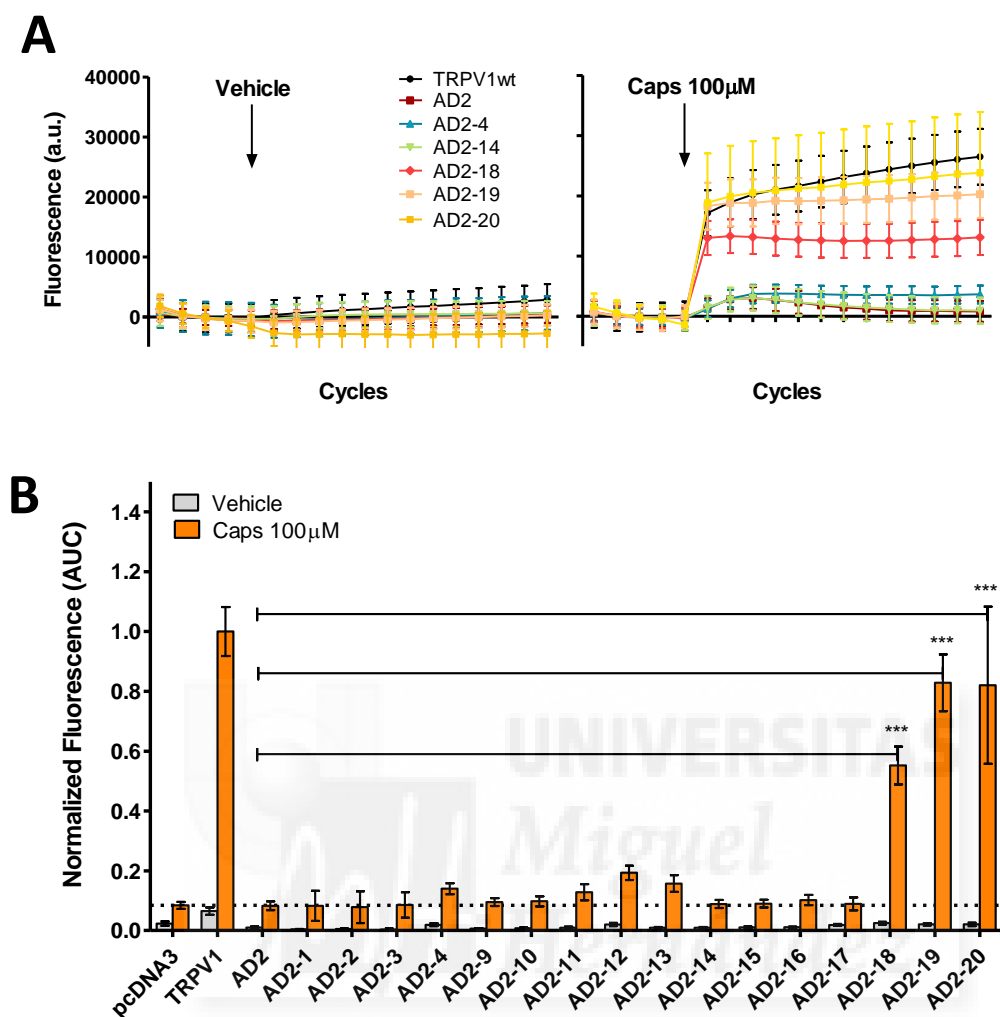


Figure R20. TRPV1 activity recovery from the non-active chimera TRPV1-AD2. **A**, Change in Ca^{2+} -dependent fluorescence of transfected HEK cells as a function of time, before and after the exposure to vehicle (0.1%DMSO) (left graph) or 100 μM capsaicin (right graph) at 25°C. Traces represent the average in fluorescence changes of all the experiments performed for TRPV1 wt and some representative AD2 mutants. The arrows indicate the onset vehicle and capsaicin exposure. **B**, Normalized values of fluorescence from Area under the Curve (AUC between the fifth and the last point) data for TRPV1 wt, AD2 mutants and mock transfected cells were used for quantification of the relative capsaicin-evoked fluorescence change. Data are shown as mean \pm SEM, with number of experiments ≥ 4 . Statistical analysis corresponds to one-way ANOVA, *** $p \leq 0.0001$

Figure R20 showed capsaicin-evoked Ca^{2+} -influx in TRPV1 transfected cells after the agonist was applied in the fifth cycle (Fig. R20A). In contrast, TRPV1-AD2 did not exhibit vanilloid evoked Ca^{2+} -influx. Analysis of the generated mutants revealed that only cells transfected with the mutants AD2-18, AD2-19 and AD2-20 showed capsaicin-induced responses, although AD2-18 displayed significant lower Ca^{2+} -signal. None of the other mutants (AD2-1 \rightarrow AD2-17) produced

TRPV1 STRUCTURE-FUNCTION STUDY: ROLE OF THE TRP DOMAIN IN TRPV1 ALLOSTERIC GATING

DOCTORAL THESIS

LUCIA GREGORIO TERUEL

responses to 100 μM capsaicin (Fig. R20B) significantly different from these recorded in mock transfected cells.

These observations can be explained by two main reasons; on the one hand, the lack of response to the agonist in some of the mutants could be due to a drastic decrease in capsaicin sensitivity of these channels. Although HEK cells transfected with other TRPV1 mutants expressing very low protein levels evoked detectable currents when the agonist capsaicin was applied at that high concentration (i.e. TRPV1-W697M in previous section). Alternatively, it could be possible that these non-functional channels exhibited altered gating properties that abrogated channel opening under normal conditions. To better characterize the behavior of these functionally impaired chimeric proteins we next performed electrophysiological experiments to define the biophysical properties of these channels.

We next studied which possible role may play in the recovery of functionality the point mutations performed in chimeras AD2-18, AD2-19 and AD2-20, namely K701R, D692E and S704T. For this purpose, we replaced these three positions in the initial chimera AD2 by the corresponding residues in TRPV1. Furthermore, we also characterized these three positions in TRPV1 wild type channel substituting the original residue by the equivalent in AD2. The data obtained from Ca^{2+} microfluorography experiments in presence of 100 μM capsaicin is shown in figure R21.

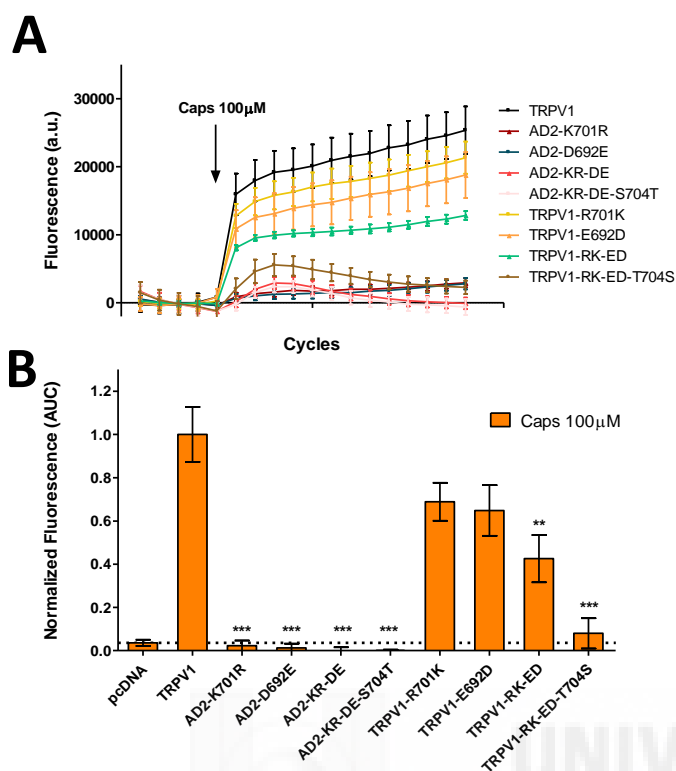


Figure R21. Role of residues R701, D692 and S704 in TRPV1 functionality. **A**, Change in Ca^{2+} -dependent fluorescence of transfected HEK cells as a function of time, before and after the exposure to 100 μ M capsaicin at 25°C. Traces represent the average in fluorescence changes of all the experiments performed. The arrows indicate the onset capsaicin exposure. **B**, Normalized values of fluorescence from the Area under the Curve (AUC between the fifth and the last point). Data are shown as mean \pm SEM, with number of experiments ≥ 4 . Statistical analysis corresponds to one-way ANOVA, *** $p \leq 0.0001$.

As discerned from figure R21, neither single nor combined mutations of K701R, D692E and S704T residues in chimera AD2 gave rise to capsaicin-sensitive channels when compared with mock-transfected cells response. However, the equivalent mutations in TRPV1 (R701K, E692D and T704S) revealed a detectable decrease in capsaicin-induced response in these mutant channels. We found the most significant decrease in fluorescence signal when the three mutations were combined. These results suggested that these amino acids need a cooperative environment provided by the rest of positions of the TRP domain, recovered in AD2-18, AD2-19 and AD2-20, to generate functional channels. Taking together these findings demonstrate that residues R701, E692 and T704 are important for the correct gating of TRPV1. Despite of introducing conservative changes in these positions their activity was dramatically reduced. However, the single restoration of these three residues in the context of AD2-TRP domain was not enough for recovering the original phenotype of the channel.

TRPV1 STRUCTURE-FUNCTION STUDY: ROLE OF THE TRP DOMAIN IN TRPV1 ALLOSTERIC GATING

DOCTORAL THESIS

LUCIA GREGORIO TERUEL

VOLTAGE RESPONSE

We next studied the response to voltage stimuli of chimeric mutants. For this purpose, we performed patch clamp experiments of mutant channels heterologously expressing in HEK cells by using whole-cell configuration. The protocol used for voltage-activation corresponded to 100 ms depolarizing pulses from -120 to 240 mV in steps of 20 mV. In figure R22 we show families of currents from representative chimeric mutants evoked by voltage.

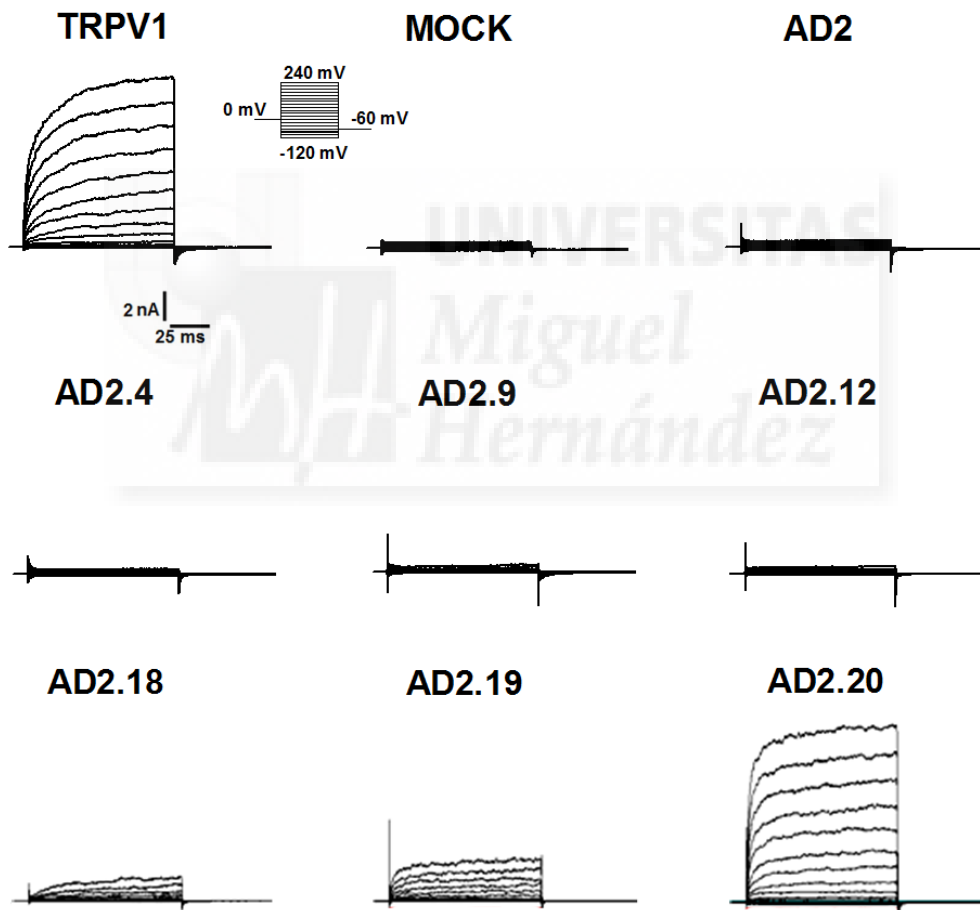


Figure R22. Reestablishment of voltage response of AD2-chimeric channels. Representative families of ionic currents evoked with a voltage step protocol consisting of 100 ms depolarizing pulses from -120 to 240 mV in steps of 20 mV. Holding potential 0 mV; time between pulses 5 s.

Application of depolarizing pulses up to 240 mV evoked detectable noninactivating ionic currents from TRPV1, AD2-18, AD2-19 and AD2-20. The rest of mutants did not elicit any

3. RESULTS

response to this activating stimulus when compared to mock transfected cells. Mutants AD2-18 and AD2-19 displayed significant lower currents than those of wild-type channels. However, AD2-20 exhibited equivalent currents to TRPV1 transfected cells.

Analysis of the G-V curves yielded from steady-state currents evoked for partially activated mutants AD2-18, AD2-19 and AD2-20 performed.

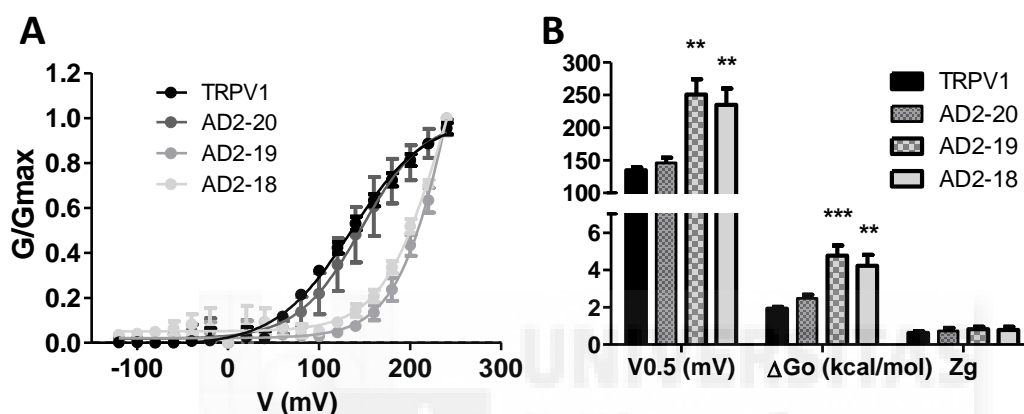
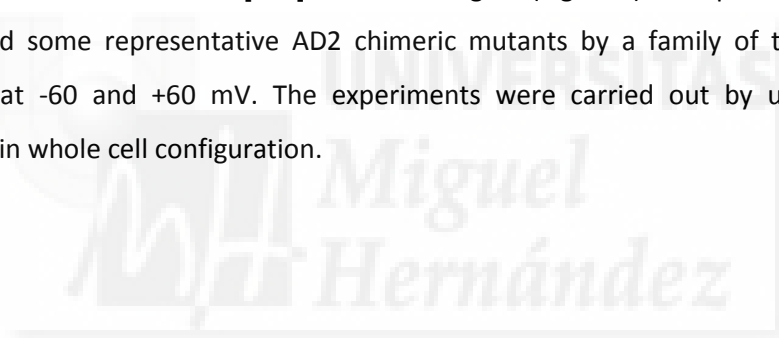


Figure R23. Normalized conductance and biophysical parameters of functional chimeric mutants. **A**, G-V relation for AD2-18, AD2-19, AD2-20 and TRPV1. Conductance curves were obtained from the ionic currents shown in Fig. R5 using $G=I/(V-V_r)$. Conductance values for each cell were fitted to the Boltzmann equation: $G=G_{max}/\{1+\exp[(V-V_{0.5})/a_n]\}$. Solid lines depict the best fit to a Boltzmann distribution. **B**, $V_{0.5}$ values, apparent gating valence of the activation process ($Z_g=25.69 \text{ mV}/a_n$) and free energy values at 0mV and 25°C (ΔG_o) assuming a two-state model. $\Delta G_o = Z_g F V_{0.5}$, for all species obtained from the Boltzmann distribution G-V relations. All values are means \pm SEM; number of cells ≥ 5 ; One-way ANOVA, *** $p \leq 0.0001$.

The G-V curves for TRPV1 and AD2-20 suitably fitted to a Boltzmann distribution (Fig. R23A) and AD2-20 Boltzmann resembling TRPV1 curve. Partially activated mutants AD2-18 and AD2-19 did not reach the saturated phase of the curve. Thus, these two chimeric mutants showed a significant increase of parameters $V_{0.5}$ and ΔG_o when compared with TRPV1 (Fig. R23B). Analysis of biophysical parameters obtained from these graphs revealed that non-significant changes were detected for $V_{0.5}$ and z_g when compared TRPV1 and AD2-20 (Fig. R23B) ($V_{0.5}$: 138.8 ± 3.25 and 147.5 ± 8.3 mV; z_g : 0.63 ± 0.04 and 0.75 ± 0.14 for TRPV1 and AD2-20, respectively). Furthermore, free energy difference between closed and open state of both channels did not show any significant difference when compared with each other (1.9 ± 0.11 for TRPV1 and 2.4 ± 0.24 for AD2-20). Therefore, our results indicate that we have fully recovered wild type phenotype in AD2-20 when activated by voltage.

TEMPERATURE RESPONSE AND THERMODYNAMIC ANALYSIS

The next step was to characterize thermodynamic parameters of temperature-dependent gating of these chimeric mutant channels. For this purpose, we performed direct, time-resolved measurements of heat activation by using patch clamp technique of some representative chimeric mutant channels over a full activation range ($\approx 36-60$ °C) at both hyperpolarizing (-60 mV) and depolarizing ($+60$ mV) potentials. From these experiments we determined transitions for entropy and enthalpy values from steady-state measurements and parameters which defined the energetics of heat activation. In this approach, we used an infrared laser diode as a heat source with light brought to the samples through an optical fiber. By restricting laser illumination to single cells, the system could promptly achieve a temperature jump > 60 °C under a millisecond [162]. In the next figure (Fig. R24) we represented the response of TRPV1 and some representative AD2 chimeric mutants by a family of temperature steps ($36^{\circ}\text{C}-60^{\circ}\text{C}$) at -60 and $+60$ mV. The experiments were carried out by using patch clamp experiments in whole cell configuration.



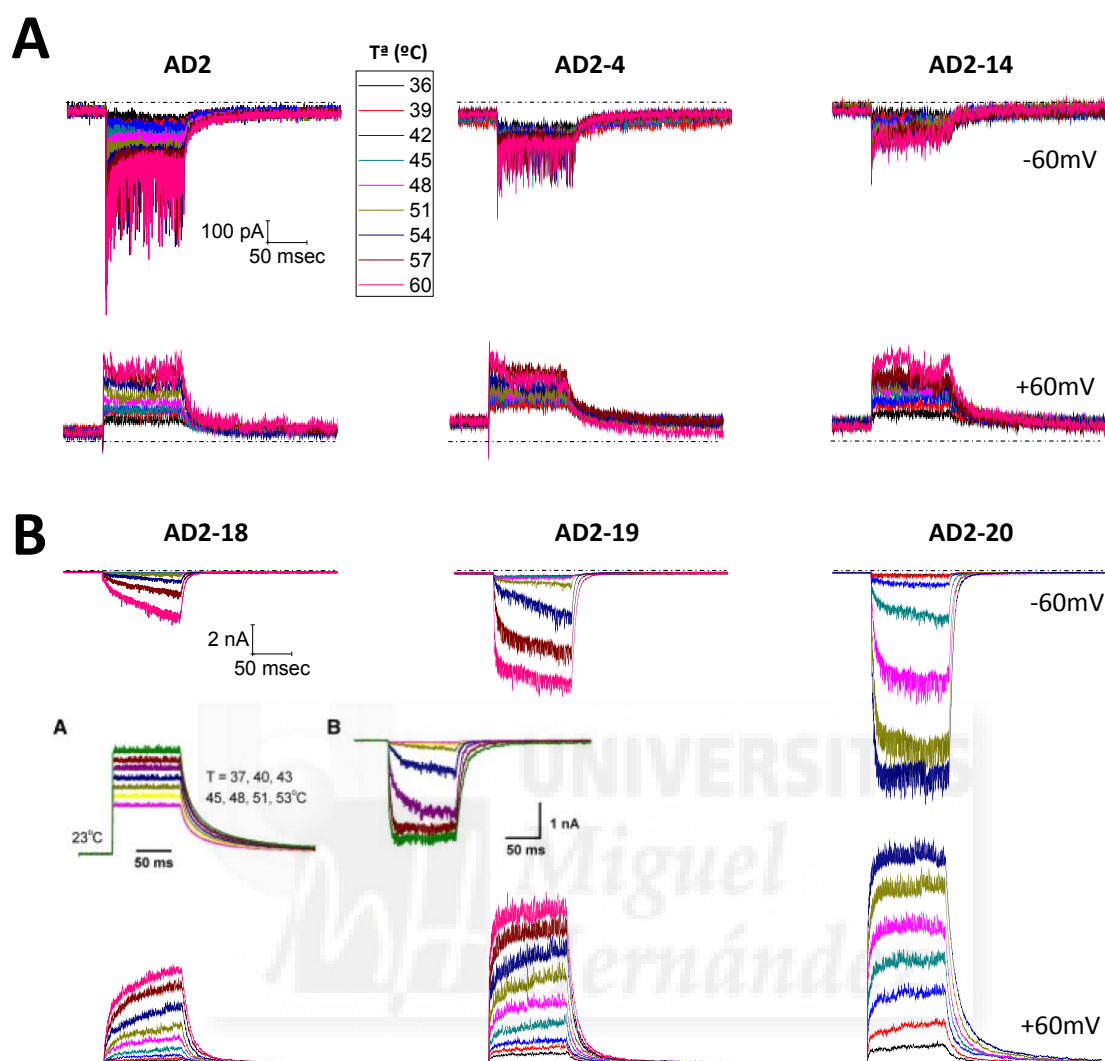


Figure R24. Rapid activation of TRPV1 and AD2 chimeric channels by heating temperature. Channel responses evoked by rapid temperature jumps at -60 and +60 mV as indicated for selected mutants (A) AD2, AD2-4, AD2-14 and (B) AD2-18, AD2-19 and AD2-20. **Inset A**, Temperature pulses generated by infrared diode laser irradiation. Each pulse had a duration of 100 ms and a rise time of 0.75 ms. Temperature jumped from 37-53 °C for TRPV1 recordings and 36-60°C for mutants. **Inset B**, TRPV1 responses evoked by the protocol described in A. Data were recorded in whole-cell configuration patch clamp.

As observed in figure R24 (inset B), significant activity for TRPV1 began above $\approx 40^{\circ}\text{C}$, in accord with the threshold of steady-state measurements described in the bibliography. Once above the threshold, temperature steps generated an exponential rise of the current. After this point, a small rise of temperature-induced large increases in both activation rates and steady-state currents. The response reached saturation at temperatures above 50°C since we observed activation with higher temperature did not evoke larger currents levels.

TRPV1 STRUCTURE-FUNCTION STUDY: ROLE OF THE TRP DOMAIN IN TRPV1 ALLOSTERIC GATING

DOCTORAL THESIS

LUCIA GREGORIO TERUEL

Regarding AD2 mutants we observed that most of the mutants showed an impaired response to heat activation. In particular, mutants AD2, AD-4 and AD2-14 (Fig. R24A) were totally insensitive to the range of heating temperatures applied at both negative and positive potentials. For the rest of mutants studied AD2-18, AD2-19 and AD2-20 (Fig. R24B), we detected partial activation starting in AD2-18 mutant around 50 °C, at hyperpolarizing potentials, that sequentially increased reaching wild type current levels when we recovered the full sequence of the TRP domain in AD2-20. In fact, we were not able to apply higher temperatures than $\approx 54^{\circ}\text{C}$ for the mutant AD2-20 since the seal became unstable and difficult to clamp. Moreover, the response of this chimeric channel had reached saturation at this temperature as we detected for TRPV1 channels. This gradual increase of activity in chimeras AD2-18, AD2-19 and AD2-20 was also detected in previous sections where we activated the channels with stimuli like depolarizing voltages or capsaicin.

In contrast, significant activity was detected at temperatures around 40°C for the functional chimeric mutants at +60 mV, indicating that these channels had a lower threshold of activation at depolarizing potentials. In turn, the current elicited at these conditions seemed less temperature-dependent showing smaller and more uniform increments between consecutive temperature steps.

From these experiments we next extracted thermodynamic parameters from steady-state measurements and activation rates. We could only calculate these parameters from AD2-19 (Fig. R25) and AD2-20 (Fig. R26) since these were the only mutants which reached steady-state currents.

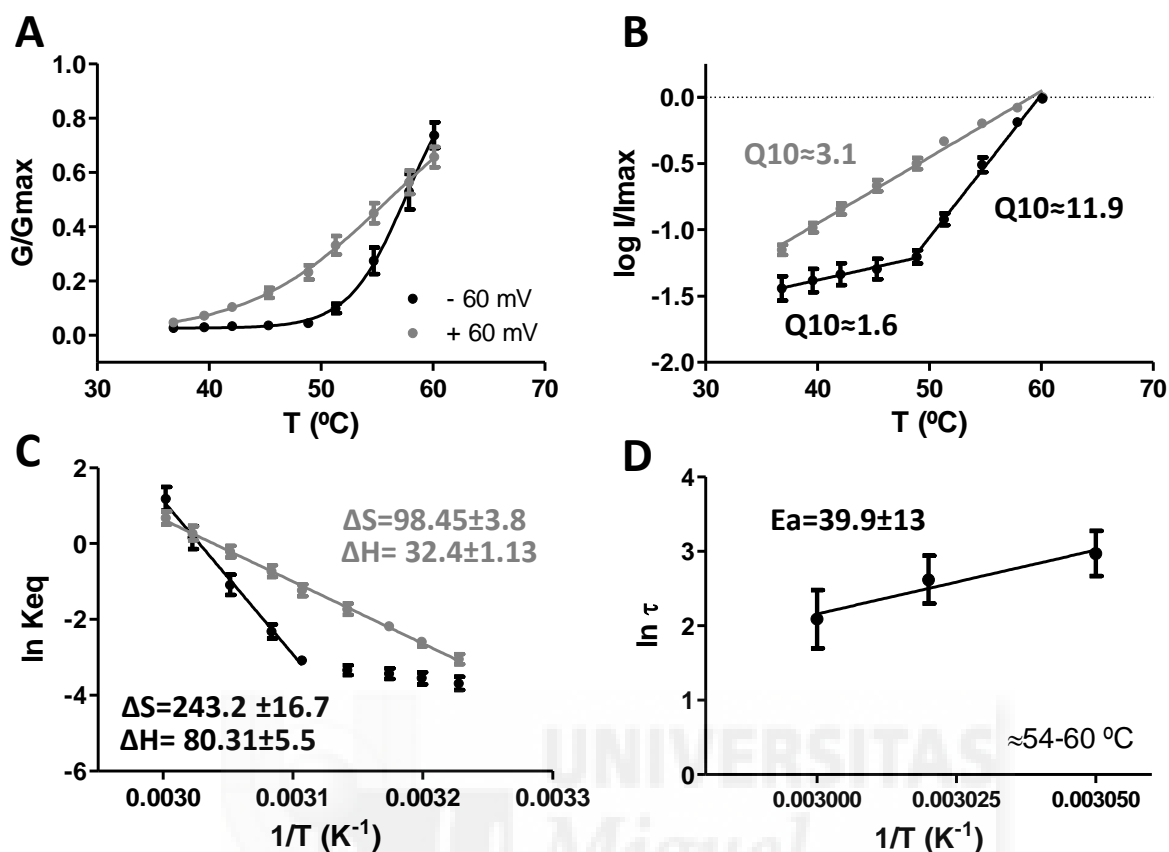


Figure R25. Thermodynamic analysis of AD2-19 mutant at -60 and +60 mV. **A**, G - T curve with normalized conductance values obtained from steady-state current values showed in Fig. R24B at -60 (black) and +60 mV (grey). Solid lines depicted the fitting to a Boltzmann distribution $G/G_{max}=1/\{1+\exp[-(\Delta H/R)*((1/T)-(1/T_{0.5}))]\}$. **B**, Plot of $\log I/I_{max}$ vs temperature of the data shown in Fig.23B. Q_{10} values are shown in the graph. The relationship is determined by $Q_{10}=\{(I_2/I_1)\exp(10/(T_2-T_1))\}$. **C**, Van't Hoff plot of the equilibrium constant, Keq , determined by $\ln Keq=\{(-\Delta H/RT)+(\Delta S/R)\}$, where $Keq=\{G/G_{max}/(1-G/G_{max})\}$. Solid lines depicted the fitting to a straight line. ΔH values are shown in kcal/mol and ΔS in $\text{cal}\cdot\text{mol}^{-1}\cdot\text{K}^{-1}$. **D**, Arrhenius plot for activation process. Activation rates were calculated from the activation time constants (τ) of current traces elicited at -60 mV. $\ln(K)=\ln(A)-[E_a/(RT)]$ where $\ln(K)=\ln(\tau)$. E_a value is shown in kcal/mol. Solid lines depicted the fitting to a straight line. Data showed an average value for number of cells ≥ 6 .

First, we represented an averaged normalized conductance versus temperature for all the experiments of AD2-19 mutant at -60 and +60 mV holding potential (Fig. R25A). As discerned from this graph, none of the plots reached the saturation level with the temperatures applied up to 60°C. However, we were able to estimate an accurate fitting to the Boltzmann equation in both plots. From this fitting we obtained $T_{0.5}$, the temperature at which the conductance was half-maximal. The values obtained for this parameter were 56.38 ± 0.866 °C at -60 mV and 55.85 ± 4.36 °C at +60 mV which were around 10°C shifted to higher temperatures when compare with wild type channel values (≈ 49 °C, [161]). Interestingly, we observed that the simultaneous application of depolarizing voltages (+60 mV) did not affect this parameter even though higher

TRPV1 STRUCTURE-FUNCTION STUDY: ROLE OF THE TRP DOMAIN IN TRPV1 ALLOSTERIC GATING

DOCTORAL THESIS

LUCIA GREGORIO TERUEL

conductance levels were detected for temperatures below 50°C. Furthermore, we detected that sigmoidal shape became shallower respect to the data obtained under hyperpolarizing membrane potentials. Therefore, depolarizing voltages contributed to a decrease in temperature-dependency of currents whereas $T_{0.5}$ values were not affected by this phenomenon.

We next analyzed steady-state data following two thermodynamical approaches. First, we used the 10-degree temperature coefficient (Q_{10}) to quantify the temperature sensitivity of the AD2-19 chimeric mutant (Fig. R25B). The Q_{10} value was obtained from the slope of a $\log(I)$ versus temperature according to the equation described in figure R25. In this equation I_2 represented the maximum current obtained for each cell measured at temperature T_2 , and I_1 represented the current value obtained for each pulse of temperature T_1 . In this graph we could appreciate two phases at hyperpolarizing voltages. The first phase was found between 36 and 50 °C considered almost temperature-independent with Q_{10} about 1.6. This phase corresponded to the initial plateau of the Boltzmann where the conductance was barely detectable and open probability was close to 0. The second phase, detected between 50 °C and 60 °C, exhibited higher temperature dependency showing a Q_{10} around 11.9, almost one order of magnitude higher than the first phase. However, this value was still distant from values which have been obtained for TRPV1 ($Q_{10}\approx 20$) and significantly shifted to higher temperatures. In contrast to these results, currents evoked by temperature pulses at depolarizing voltages did not show these two phases aforementioned. Moreover, depolarization elicited lower temperature-dependent activation processes giving rise to Q_{10} values around 3.1.

The second thermodynamical analysis we could extract from steady-state measurements was defined by assumption of a two-state gating model of TRPV1. Defining the equilibrium constant as $K_{eq} = O/C$, where O was the open state and C closed, the open probability (P_o) would correspond to:

$$P_o = \frac{1}{1 + K_{eq}^{-1}}$$

(Equation 4)

Therefore, $K_{eq} = (P_o)/(1-P_o)$. Since P_o parameter may be taken as G/G_{max} for whole cell currents, we used the data showed in Fig. R25A to obtain the equilibrium constant at both

potentials -60 and +60 mV. Afterwards, we represented $\ln(K_{eq})$ versus inverse of temperature following Van't Hoff plot with their corresponding ΔH and ΔS values, shown in figure R25C. The same as the Q_{10} graph, this plot showed again two phases for temperature dependency for experiments performed at hyperpolarizing voltages (-60 mV). The activation process observed between 50 °C and 60 °C exhibited large transition changes with an enthalpy change of ≈ 80 kcal/mol and entropy change of ≈ 240 cal.mol⁻¹.K⁻¹. These values were significantly lower than the ones obtained for TRPV1 in bibliography ($\Delta H=101 \pm 4$ kcal/mol and $\Delta S=315 \pm 12$ cal.mol⁻¹.K⁻¹), [161]. These results suggested that the impairment detected in AD2-19 functionality lied in altering the temperature sensitivity of the channel gating. Regarding the plot obtained at +60 mV we obtained an enthalpy change around ≈ 32.4 kcal/mol and an entropy change around ≈ 99 cal.mol⁻¹.K⁻¹. These findings confirmed the previous data supporting the lack of temperature dependency in AD2-19 channel activation under depolarizing conditions. Thus, for these conditions temperature did not drive the opening process as it did under hyperpolarizing potentials, mainly because the channels were already partially open by the positive voltage.

Next, we analyzed the time course of the AD2-19 activation process by fitting current traces of temperature response to a single exponential defined by,

$$f(t) = \sum_{i=1}^n A_i \cdot e^{-t/\tau} + C$$

(Equation 5)

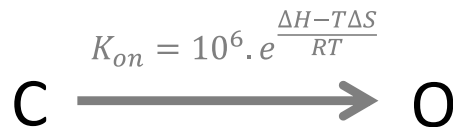
Where $f(t)$ represented the current at time t , A_i the current amplitude at time 0, τ corresponded to exponential time constant and C was the constant of integration. Then, we represented an Arrhenius plot of the time constants versus the inverse of the temperature (Fig. R24D). We only represented time constant values at high temperatures (54-60 °C) where the plot was approximately linear. At low temperature, the relationship did not follow a linear tendency and the slow rise times rendered the exponential fitting less accurate. This approach was only considered for temperature activation at hyperpolarizing voltages since the application of positive potentials evoked positive currents following a biexponential shape, as described by Yao et al, 2010.

TRPV1 STRUCTURE-FUNCTION STUDY: ROLE OF THE TRP DOMAIN IN TRPV1 ALLOSTERIC GATING

DOCTORAL THESIS

LUCIA GREGORIO TERUEL

In accordance with previous works, we assumed a simple two-state model to fit the responses at all temperatures and translate time constants into rate constants of the activation process ($\tau=K_{on}$). TRPV1 gating has been widely described to be multistate, therefore we assumed that the model describes only the major energetic changes of activation. The equation describing this model corresponded to:



(Equation 6)

Where ΔH and ΔS corresponded to thermodynamical parameters of the opening process and $10^6/s$ was the assumed value for the preexponential factor [161]. Consequently, we obtained activation enthalpy and entropy values from the rate constants (K_{on}) by fitting the Arrhenius plot (Fig. R25D) to the two-state model equation described above (Equation 6) in the form:

$$\ln(k_{on}) = -\frac{\Delta H}{RT} + \frac{\Delta S}{T} + \ln(v)$$

(Equation 7)

The activation enthalpy for the opening rate was $\Delta H = 39.9 \pm 13$ kcal/mol. This value was significantly distant (0.5-fold) from the equilibrium enthalpy change between the closed and open states. These findings indicated that the opening of the chimera AD2-19 alone could not totally account for the temperature dependence of the steady-state obtained response. The entropy transition of the activation process was $\Delta S = 130.5 \pm 50$ cal.mol⁻¹.k⁻¹, assuming a preexponential factor of $10^6/s$. This observation indicates that AD2-19, which only remains S704T and D707E mutations to recover TRPV1 sequence, shows a severe impairment in the coupling between temperature activation process and channel gate.

The same procedure was carried out with the chimeric mutant AD2-20.

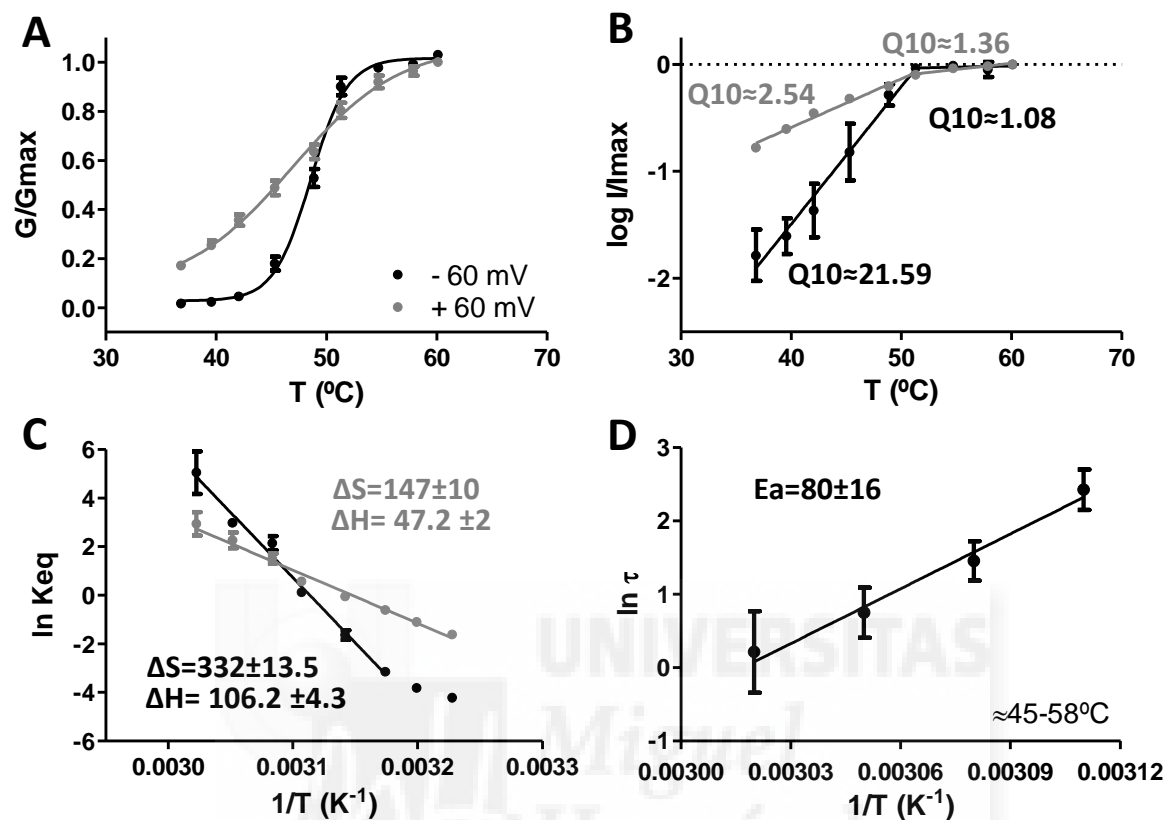


Figure R26. Thermodynamic analysis of AD2-20 mutant at -60 and +60 mV. **A**, G-T curve with normalized conductance values obtained from steady-state current values showed in Fig. R24B at -60 (black) and +60 mV (grey). Solid lines depicted the fitting to a Boltzmann distribution $G = G_{max} / \{1 + \exp[-(\Delta H/R) * ((1/T) - (1/T_{0.5}))]\}$. **B**, Plot of $\log I/I_{max}$ vs temperature of the data shown in Fig. 23B. Q_{10} values are shown in the graph. **C**, Van't Hoff plot of the equilibrium constant K_{eq} . Solid lines depicted the fitting to a straight line. ΔH values are shown in kcal/mol and ΔS in $\text{cal} \cdot \text{mol}^{-1} \cdot \text{K}^{-1}$. **D**, Arrhenius plot for activation process. Activation rates were calculated from the activation time constants of current traces elicited at -60 mV. E_a value is shown in kcal/mol. Solid lines depicted the fitting to a straight line. Data showed an average value for number of cells ≥ 6 .

We first represented an averaged normalized conductance versus temperature for all the experiments of AD2-20 mutant at -60 and +60 mV holding potential (Fig. R26A). From this fitting, the values obtained for $T_{0.5}$ parameter were 48.5 ± 0.58 °C at -60 mV and 46.8 ± 0.73 °C at +60 mV which were very similar to the values obtained for TRPV1 (≈ 49 °C). The application of depolarizing voltages evoked detectable conductance levels from the first temperature pulse applied at 36 °C, which were not detected at negative potentials. However, the simultaneous application of positive potentials did not affect $T_{0.5}$ values. Therefore, depolarizing voltages

TRPV1 STRUCTURE-FUNCTION STUDY: ROLE OF THE TRP DOMAIN IN TRPV1 ALLOSTERIC GATING

DOCTORAL THESIS

LUCIA GREGORIO TERUEL

contributed to a decrease in temperature-dependency of currents without affecting other parameters as $T_{0.5}$.

Thereafter, we estimated the temperature dependence of the gating process by calculating the Q_{10} factor. The Q_{10} value was obtained from the slope of a $\log(I)$ versus temperature according to the equation described in figure R25. In this graph (Fig. R26B) we could appreciate two temperature-dependent regimes at hyperpolarizing voltages. The first one was found between 36 °C and 50 °C showing a high Q_{10} about 21.6, which was very similar to the value obtained for TRPV1 ($Q_{10}\approx 20$) in this temperature range. The second phase, detected between 50 °C and 60 °C, showed much lower temperature dependency since we detected Q_{10} around 1.08. This phase corresponded to the top plateau of the Boltzmann where the maximum open probability was reached. However, when depolarizing voltages were applied, we barely differentiated the two-phases. In addition, the temperature-dependence of the gating process almost disappeared and we obtained Q_{10} values 2.54 between 36-50 °C and 1.36 between 50-60 °C.

We next estimated the thermodynamical parameters from the steady-state currents of AD2-20 mutant at negative (-60 mV) and positive (+60 mV) potentials. We represented $\ln(K_{eq})$ versus inverse of temperature following Van't Hoff plot with their corresponding ΔH and ΔS values, shown in figure R26C. This plot showed two phases for temperature dependency for experiments performed at hyperpolarizing voltages (-60 mV). The activation process observed between 36 °C and 50 °C exhibited large transition changes with an enthalpy change of ≈ 106 kcal/mol and entropy change of ≈ 330 cal.mol⁻¹.K⁻¹, as it was observed for TRPV1 ($\Delta H=101 \pm 4$ kcal/mol and $\Delta S=315 \pm 12$ cal.mol⁻¹.K⁻¹) [161]. The application of positive potentials drove to lower enthalpy and entropy values ($\Delta H=47.2 \pm 2$ kcal/mol and $\Delta S=147 \pm 10$ cal.mol⁻¹.K⁻¹) indicating a decrease of the involvement of temperature in channel gating under depolarizing conditions.

Finally, we calculated the activation enthalpy and entropy for the channel opening (Fig. R26D). The thermodynamic parameter values corresponded to $\Delta H = 80\pm 16$ kcal/mol and the entropy $\Delta S = 268.8 \pm 53$ cal.mol⁻¹.k⁻¹. These values were close to the equilibrium enthalpy and

3. RESULTS

entropy change between the closed and open states (≈ 0.8 -fold), indicating that the opening of the channel alone could justify the temperature dependence of the steady-state response.

Taking together, these results determined that the application of depolarizing voltages significantly affected the temperature-dependency of the gating process both in AD2-19 (Fig. R25) and AD2-20 (Fig. R26) mutants. As expected for high temperature dependent channels, the enthalpy changes for channel opening were high, although they were significantly decreased by the application of positive potentials. However, in all cases existed a precise coupling between enthalpy and entropy (Fig. R27A) where a variation in enthalpy causes a concomitant change in entropy so that they can cancel with each other. Consequently, the free energy difference between the open and closed states exhibited only small changes (Fig. R27B), allowing the channel to gate at high rates.

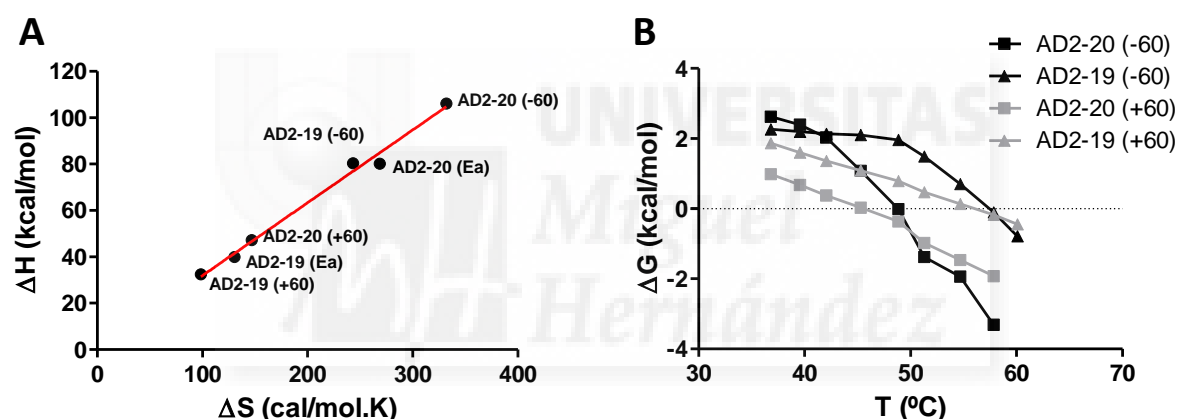


Figure R27. Energetics of temperature gating of AD2-19 and AD2-20 chimeric mutants. A, Enthalpy and entropy coupling. Each point represents the values obtained for these parameters from steady-state currents at depolarizing (+60) and hyperpolarizing (-60) potentials and from activation process (Ea) in all conditions. **B, ΔG (kcal/mol) vs temperature plot for AD2-19 and AD2-20 at -60 and +60 mV.** $\Delta G = RT \ln(K_{eq})$.

As discerned from figure R27A both mutants showed coupled enthalpy and entropy changes in all conditions. AD2-20 showed the highest values for both parameters at -60 mV holding potential by measuring at steady-state. In contrast, we obtained lower values for AD2-19 which implied that gating process of this mutant was less temperature dependent as compared with AD2-20. Furthermore, the activation enthalpy (Ea) for the opening rate was close to the equilibrium enthalpy change in AD2-20, whereas the activation energy value obtained for AD2-19 was distant from the values obtained for the equilibrium. These findings indicated that for

TRPV1 STRUCTURE-FUNCTION STUDY: ROLE OF THE TRP DOMAIN IN TRPV1 ALLOSTERIC GATING

DOCTORAL THESIS

LUCIA GREGORIO TERUEL

AD2-20 mutant the temperature dependence of the steady-state response could be driven by the opening of the channel alone evoked by heating temperatures.

The free energy changes are maintained at low levels due to the high entropic contribution which compensate that high enthalpy changes between closed and open state (Fig. 27B). The application of increasing temperatures induced a continuous decrease of this difference above 40°C for AD2-20 chimeric channel. However, AD2-19 data was rightward shifted around 10°C, showing a plateau between 36 and 50°C where the channel remained in the closed state. When compared AD2-19 and AD2-20, we observed that the mutant AD2-19 displayed higher energy differences than AD2-20 for the same temperature applied, indicating that the changes included in this mutant had an impact in protein activity by rising the activation energy of the channel. With the application of positive potentials both curves became shallower indicating a decrease in temperature dependency of the channel opening.

Under depolarizing voltages, ΔG_0 values were lower when compared with the ones obtained at negative potentials. These results suggest that voltage stimulus is partially driving channel opening and, consequently, energy contribution to channel gating derived from temperature is reduced in the whole range studied. Noticeably, AD2-20 chimeric mutant exhibited larger differences in ΔG_0 values between hyper- and depolarizing potentials than AD2-19. Thus, AD2-19 seems less sensitive to voltage since energy provided from this physical stimulus does not contribute to channel gating in the same manner as we detected for AD2-20. This may be due to a defective coupling between voltage sensor and channel pore which hindered the energy transfer between both modules.

ALLOSTERIC MODEL

As seen, small changes in the TRP domain of TRPV1 evoked dramatic alterations in protein functionality. To better understand how these mutations are affecting the gating process of this channel, we analyzed our results from electrophysiological experiments of functional AD2 mutants by fitting them to an allosteric model of gating. We studied the effect of these

mutations in channel gating induced by voltage and temperature at hyperpolarizing and depolarizing potentials.

First, we fitted the data obtained from voltage activation of AD2-20. It was the only mutant studied by this method since the rest of them did not reach saturating conditions hindering the fitting. According to functional studies, this mutant should display similar values to TRPV1 allosteric model parameters.

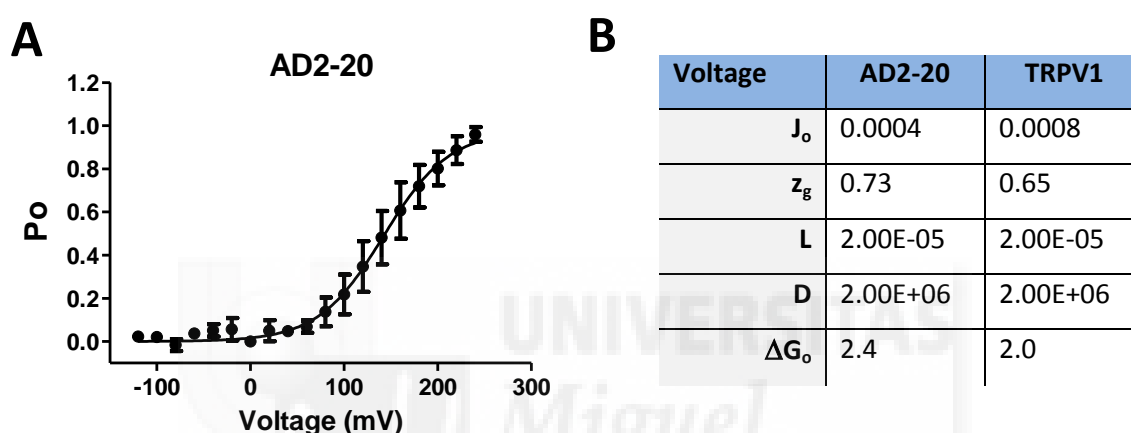


Figure R28. Fit of P_o -V curves of AD2-20 mutant to an allosteric gating scheme. **A**, Normalized values of P_o plotted against voltage. Line depicts the simultaneous best fit to Equation 1. **B** (Table VI). Parameter values obtained from allosteric model fitting.

As shown in figure R28A, the data obtained for AD2-20 mutant properly fitted to the allosteric gating model. The values obtained from this fitting are represented in table VI. Data obtained for AD2-20 indicated that this mutant behaved similarly to TRPV1. Allosteric constants L and D were not affected while we detected small changes in J_o and ΔG_o , in agreement with experimental data showing an increase in energetic of gating process. According to the allosteric model, this change in free energy may be due to a decrease in the equilibrium constant of voltage sensor which indicates a possible shift to the resting state. However, we did not find significant differences in $V_{0.5}$, z_g or ΔG_o values when obtained from experimental data and compared with wild type protein. Next, we studied the gating mechanism induced by temperature at negative and positive potentials.

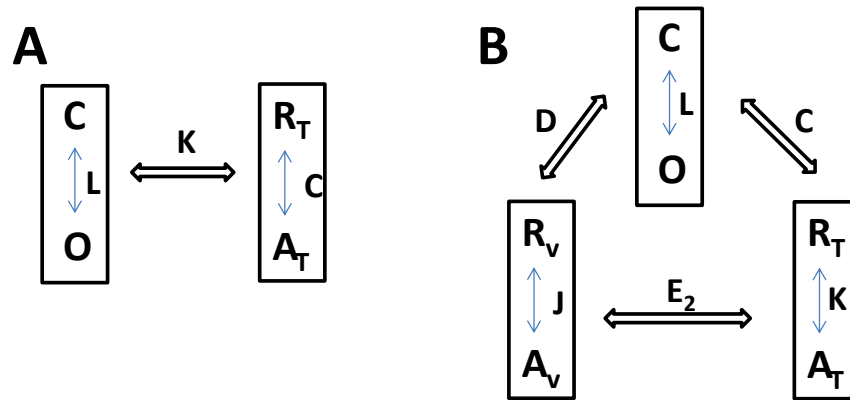


Figure R29. Allosteric model for channel activation. **A**, allosteric activation by temperature. Two independent equilibria that interact allosterically. **B**, allosteric activation by voltage and temperature where an additional equilibrium is included to the equation.

Figure R29A depicts an allosteric activation induced by temperature where two separate two-state equilibria interact allosterically with each other. The first equilibrium represented the closed and open states (*C* and *O*) of the pore gate. The second equilibrium was defined by *R_T* and *A_T* which represented the resting and activated state of the temperature sensor. *C* defined the equilibrium constant for temperature sensor. *K* corresponds to an allosteric factor which determines the coupling between the temperature sensor and the pore of the channel. When the temperature sensor is activated, the equilibrium constant between *C* and *O* would be modified as *LK*. According to this model, the probability of being in any open state is:

$$P_o = \frac{1}{1 + \frac{1+K}{L(1+KC)}} \quad (\text{Equation 8})$$

Where *K* is defined by:

$$K = e^{\frac{-(\Delta H - T\Delta S)}{RT}} \quad (\text{Equation 8.1})$$

Being ΔH and ΔS the changes in enthalpy and entropy between the open and the closed state.

Figure R29B shows a diagram of an allosteric activation by temperature and voltage. In this case, the voltage sensor two-state equilibrium is added to the diagram. We considered both sensors could be coupled by factor E . According to this model, the opening probability is given by:

$$P_o = \frac{1}{1 + \frac{1 + J + K + JKE}{L(1 + JD + KC + JKDCE)}}$$

(Equation 9)

Thereafter, we fitted our data obtained for AD2-19 and AD2-20 to the equations that describe the allosteric activation mechanism for temperature and both temperature and voltage together.

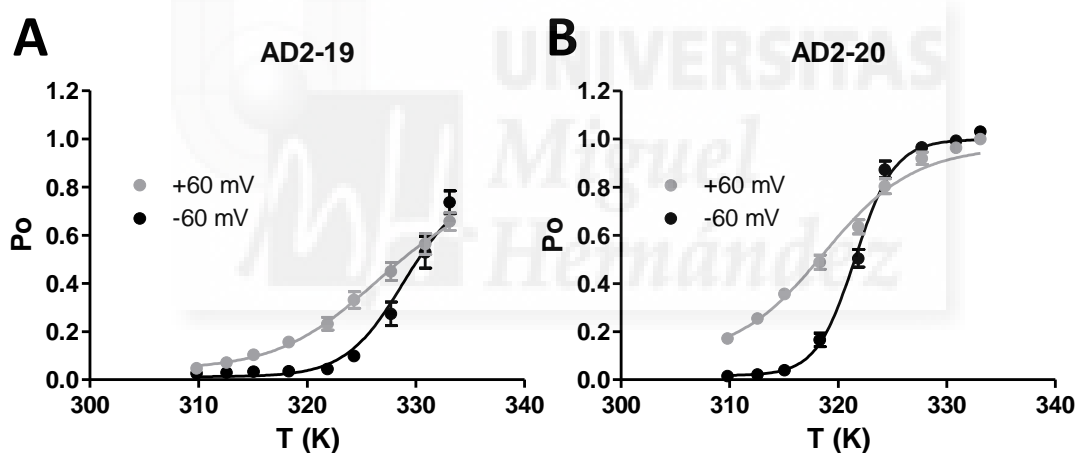


Figure R30. Fit of P_o - T curves to an allosteric gating scheme. Normalized P_o values are plotted against temperature for AD2-19 (A) and AD2-20 (B) the indicated voltages. Lines are the simultaneous best fit to Equation 8 (at -60 mV) or Equation 9 (at +60 mV).

Figure R30 showed P_o values fitted to the proposed allosteric model for temperature at negative (Equation 8) and positive potentials (Equation 9). We considered P_o parameter may be taken as G/G_{max} for whole cell current. Our data suitably fitted to the allosteric model proposed. We assumed that at -60 mV the voltage sensor remains in resting configuration and we considered the gating was only driven by temperature. P_o values are averaged and normalized from several experiments and solid lines show the best fits. The parameters obtained are displayed in table VII.

TRPV1 STRUCTURE-FUNCTION STUDY: ROLE OF THE TRP DOMAIN IN TRPV1 ALLOSTERIC GATING

DOCTORAL THESIS

LUCIA GREGORIO TERUEL

(mV)	AD2-19		AD2-20	
	-60	+60	-60	+60
Jo	---	5.774e-05	---	1.89e-06
H (kcal/mol)	80000	35000	110000	50000
S (cal.mol⁻¹.K⁻¹)	240	105	330	150
L	0.01235	0.2712	0.01283	0.107
E	---	1.319	---	15.61
C	328.7	127	33441	267
D	---	2727	---	985.6

Table VII. Parameter values of allosteric model for temperature and temperature-voltage-gating activity of AD2-19 and AD2-20.

According to the fit, the values obtained for enthalpy and entropy parameters were very similar to the ones experimentally calculated. Overall, the most relevant differences detected between both channels corresponded to parameters *C*, *D* and *E* while *L* and *J_o* were not significantly altered (Table VII), indicating an effect in allosteric coupling. The data revealed that AD2-19 exhibited conspicuously lower values for *C* than AD2-20, indicating impairment in the allosteric coupling between temperature sensor and channel pore. On the contrary, parameter *D* was higher pointing an improved voltage-coupling to the pore when compared with AD2-20. Noticeably, coupling between both sensors was also affected since parameter *E* showed values near 1 for AD2-19, indicating they act almost independently during channel gating in this chimera. Taking together, this data suggest that mutations included in AD2-19 (S704T and D707ED) have a significant impact in the allosteric coupling of temperature-dependent gating. These findings further support the experimental data where enthalpy, entropy, *Q₁₀* and activation energy values were severely reduced when compared with AD2-20 under the same conditions. In addition, allosteric model indicates that these mutations also disrupt the coupling between the voltage and temperature sensors.

On the other side, AD2-20 exhibited robust coupling of temperature sensor with channel gate according to values found for parameter *C*. Application of positive voltages dramatically reduced this allosteric constant, in agreement with an experimental data that decreased

temperature-dependency of channel gating when depolarizing voltages were applied. Furthermore, the voltage allosteric factor D also showed a significant decrease when the channel was activated by temperature at positive potentials. These results are consistent with a possible coupling between voltage and temperature sensors, showing high E values, akin to TRPV1. That would mean that the activation of one sensor significantly influences the other. This behavior is also consistent with experimental data where temperature dependent parameters enthalpy and entropy were significantly decreased in presence of positive potentials.

In general, these data further support that mutations S704T and D707E in the TRP domain of TRPV1 has a significant influence in the allosteric mechanism of temperature-induced activation. These changes primarily affected the temperature sensor coupling with the channel pore and voltage sensor.



TRPV1 STRUCTURE-FUNCTION STUDY: ROLE OF THE TRP DOMAIN IN TRPV1 ALLOSTERIC GATING

DOCTORAL THESIS

LUCIA GREGORIO TERUEL

3.2.3. STRUCTURAL FEATURES OF TRP DOMAIN

The TRP domain of TRPV1 is a segment adjacent to the inner pore helix that acts as a molecular determinant of subunit multimerization and necessary for the correct coupling of the channel. As mentioned, this region is predicted to fold in a 4-strand, parallel coiled-coil structure in the homomeric channel ([60], [61]). Considering the sequence modification performed in this work and the data obtained from functional experiments we further investigated the putative structure of this region of some of the mutants. For this purpose, we performed secondary structure studies using several online servers of structure prediction.

A

AD1	MGETV NKIAQESKNIWKLQRAITILDTEKSFLKCMRKAF ccccccchhhhhhhhhhhhhhhhhhhcchhhhhhhhhhee
AD2	MSETVNSVATDSWSIWKLQKAISVLEMENGYWWCRKKQ ccccceeecccchhhhhhhceeeeeeecccceeeec

B

SECONDARY STRUCTURE	AD1	AD2
Alpha helix (h)	68.29%	18.42%
3 ₁₀ helix (g)	0.00%	0.00%
Pi helix (i)	0.00%	0.00%
Beta bridge (b)	0.00%	0.00%
Extended strand (e)	7.32%	42.11%
Beta turn (t)	0.00%	0.00%
Bend region (s)	0.00%	0.00%
Random coil (c)	24.39%	39.47%

Figure R31. Secondary structure prediction of TRP domain of TRPV1 and TRPV2. **A**, Amino acid sequence of TRP domain of TRPV1 (AD1) and TRPV2 (AD2) with element of secondary structure predicted by using server GOR4 (http://npsa-pbil.ibcp.fr/cgi-bin/secpred_gor4.pl). **B**, The table indicates the percentage of each form of structure predicted for each sequence.

TRPV1 STRUCTURE-FUNCTION STUDY: ROLE OF THE TRP DOMAIN IN TRPV1 ALLOSTERIC GATING

DOCTORAL THESIS

LUCIA GREGORIO TERUEL

TRPV1 are highlighted in yellow in each chimeric mutant. Percentage of alpha helix according to the prediction is indicated.

As observed in figure R32, TRP domain sequence of AD2-20 showed the lowest percentage of alpha helix when compared with the chimeric mutants. This was due to the presence of two residues (D707 and T708) which slightly disrupted the secondary structure of this region. On the contrary, AD2-17, AD2-18 and AD2-19 exhibited higher percentage of alpha helix than the original sequence, showing an alpha helix prediction between I689 and K718 with no disruptions, except for AD2-18 which appeared altered in S693. These changes in secondary structure could affect channel activation and partially cause the dramatic differences we detected in functional assays between AD2-18, 19 and 20. The fact of introducing a more rigid structure in this region could affect intra- and intersubunit interactions in two different ways. On the one hand, this change on the side chains orientation of these residues could modify the interactions with other amino acids. On the other hand, an increase of alpha helix percentage in TRP domain could affect the strength and stability of coiled-coil arrangement. Stronger interactions between the four subunits could significantly affect channel gating by raising the energy needed for the channel to be open. In both cases, coupling between sensors and the pore would be affected by these changes. These assumptions are in agreement with experimental data which shows activation of chimeric channels AD2-18 and AD2-19 by different stimuli was severely impaired.





4. DISCUSSION

TRPV1 STRUCTURE-FUNCTION STUDY: ROLE OF THE TRP DOMAIN IN TRPV1 ALLOSTERIC GATING

DOCTORAL THESIS

LUCIA GREGORIO TERUEL



TRPV1 STRUCTURE-FUNCTION STUDY: ROLE OF THE TRP DOMAIN IN TRPV1 ALLOSTERIC GATING

DOCTORAL THESIS

LUCIA GREGORIO TERUEL

Extensive structure-function analysis of TRPV1 channels has been performed with the aim of identifying receptor domains involved in stimuli sensing and to understand their contribution to channel gating [82]. These studies have map down potential regions involved in voltage, capsaicin, pH and temperature sensing, along with domains that interact with proteins and phosphoinositides. In particular, the TRP domain, a 40-mer segment adjacent to the inner pore helix, has been reported as an essential region for the channel playing a dual role in protein functionality. On the one hand, It has been demonstrated its function in subunit oligomerization. Furthermore, this domain also appears to participate in the functional coupling of stimuli sensing and pore opening ([60], [61]). In the center of TRP domain was identified a 6-mer sequence, called TRP box, which was recognized as a molecular determinant in TRPV1 channel gating [62]. Interestingly, this sequence is highly conserved among other TRP channels suggesting an important role of the TRP box in these proteins.

In the present work, we focused our research on further characterizing the role of the TRP domain in the molecular mechanism of TRPV1 activation. We addressed the structural-function study of TRP domain by two complementary approaches. Firstly, we characterized the physico-chemical properties of two key residues in the TRP box, I696 and W697, needed to preserve protein functionality. Secondly, we determined which amino acids within TRP domain are necessary for the correct coupling of TRPV1 from the context of the cognate sequence of TRPV2. As detailed bellow, we will discuss separately the results obtained from these two complementary approaches.

4.1. CHARACTERIZATION OF TRP BOX IN TRPV1

Mutations within the highly conserved core of the TRP domain (referred to as the TRP box), abrogated all modes of TRPV1 channel gating, even though this region is located far from most of the putative regions acting as channel sensors [62]. These findings signaled the TRP box as a pivotal receptor domain in the allosteric mechanism of channel activation by coupling the energy of the activating stimuli to open the pore. To address this fundamental question, we mutated the most critical positions (I696, W697 and R701) in the TRP box to 18 L-amino acids, with the aim of further our understanding on the role of the TRP box in the allosteric linkage of sensors and the channel gate. We focused on studying voltage and capsaicin activation at a constant temperature (22°C).

The salient contribution of this study is that mutation of I696 and W697 primarily affects the allosteric coupling constants of the voltage and ligand sensors to the channel pore along with the equilibrium constant of pore opening, with minor alterations of the sensors equilibrium constants. Results showed for R701X mutants suggested that this position was also relevant for channel gating. The substitution of this residue generated functionally defective channels when activated by voltage and capsaicin. However, since this amino acid is plausibly located in a CaMKII phosphorylation consensus site, other molecular mechanism could be affected by these mutations. Therefore, we decided to focus the study on the effect of mutating the I696 and W697 positions.

Our results show that position I696 was only tolerant to substitutions by hydrophobic amino acids, and uncover an effect of the amino acid size at I696 in channel activation. All functional I696X mutants exhibited altered channel gating, characterized by a lower response to the activating stimuli. Smaller or larger amino acids than I696 negatively impacted channel activity resulting in lower current densities and higher free energy of activation. In marked contrast, position W697 tolerated virtually all substitutions since practically all mutants displayed channel activity in the presence of saturating concentrations of capsaicin. Intriguingly, none of the W697X mutants could be activated by depolarizing voltages as high as 240 mV in the absence of vanilloid, suggesting a complete uncoupling of voltage sensing and gate opening in these mutants. Taken together, these findings support the tenet that the TRP box in TRPV1, and probably in other TRP channels, is an important molecular determinant of

TRPV1 STRUCTURE-FUNCTION STUDY: ROLE OF THE TRP DOMAIN IN TRPV1 ALLOSTERIC GATING

DOCTORAL THESIS

LUCIA GREGORIO TERUEL

channel activation that pivotally contributes to the energetics of channel gating by modulating the allosteric coupling constants of channel sensors and the pore. It is interesting to note that all I696 and W697 mutants shown as representative, produced detectable levels of protein in HEK cells. Nonetheless, some of them significantly affected the recombinant protein expression. The most dramatic decrease was observed for W697M mutant, although this channel reached the membrane as the rest of correctly expressed mutants and was activated by the vanilloid. Thus, substitutions at these two positions generated TRPV1 channels with an altered gating. Noteworthy, all W697X mutants, as well as some of the I696X species (except I696H, I696V, I696L), analyzed by western immunoblot did not display the characteristic glycosylated TRPV1 band, suggesting that mutation of these two positions induced a conformational change in the receptor subunit that prevented TRPV1 glycosylation in the endoplasmic reticulum. The lack of glycosylated forms in most mutants is consistent with their lower capsaicin efficacy and smaller current densities as compared with wild type channels. This finding imply that mutation of these two positions in the TRP domain of TRPV1 modulates the protein conformation, presumably by perturbing interactions which are pivotal for preserving the quaternary structure of the channel, in agreement with the role of the TRP domain in subunit tetramerization [60]. This modulation of the protein conformation may underlie the effects observed in the allosteric coupling required for channel activation.

The data obtained in our work may help to elucidate the role of TRP box in functional coupling of TRPV1. In the absence of a three dimensional structure for the channel, it is rather unfeasible to provide a compelling mechanism. One can envision and hypothesize several possibilities that could account for the impact of mutating the TRP box in channel gating. In the 4-strand, parallel coiled-coil model proposed for the TRP domain ([60], [61], [163]), amino acids I696 and W697 are located at the **a** and **b** positions where they can mediate inter-subunit interactions important for the allosteric coupling of the activating stimuli to the opening of the channel gate. Our observation that I696 could only be replaced by hydrophobic amino acids, and the effect of the amino acid volume in channel gating evoked by voltage and capsaicin, are consistent with a location of I696 in the hydrophobic core of a coiled-coil fold. Incorporation of smaller and larger amino acids than Ile may strengthen the hydrophobic interactions at this level of the coiled-coil raising the energy of channel gating. The increase in the equilibrium constant of pore opening (L), along with the impact in the allosteric coupling constants (D , P

and E), exhibited by functional I696X mutants is consistent with this interpretation, thus giving support to the proposed helical organization of the TRP domain.

The location of W697 at the **b** position of the coiled-coil arrangement appears also compatible with the impact of its mutation on channel function. This amino acid could be located at the helical interface involved in intersubunit interactions. Alternatively, it could be more externally oriented for interacting with other subunit domains such as the S4-S5 linker or the S2-S3 loop or even a region in the N-terminus domain. Our result that W697 could be replaced by virtually all amino acids without losing channel function argues against a critical contribution to coiled-coil intersubunit interactions, and rather implies a more external spatial localization that would be more tolerant to substitutions. Noteworthy, although virtually all W697X mutants responded to a variable extent to capsaicin, none of them was activated by voltage indicating abrogation of voltage-dependent gating. However, capsaicin responses displayed some voltage dependency that, intriguingly, was not affected by the vanilloid concentration and exhibited a 2-fold increase in the gating valence associated to channel opening. A putative interaction of W697 with the S4-S5 linker during gating could explain the effect of the mutants. In this regard, the S4-S5 linker displays the presence of three positively-charged residues (K571, R575 and R579) that could create a positive surface potential for a π -cation-like interaction with W697. In support of this notion, substitution of W697 by negatively-charged and polar residues was better tolerated than by positively-charged and large hydrophobic amino acids. This interaction, optimal for a Trp residue because of its polarity and volume, could be essential for coupling the movement of the voltage sensor to the opening of the pore. A similar mechanism was proposed for Kv channels where gating required a compatible S4-S5 linker and the region adjacent to the channel gate ([164], [165]). However, the distance of the TRP box ($>10\text{\AA}$) from the pore gate argues against such mechanisms because it would require a large conformational change in the TRP domain to approach W697 to the S4-S5 linker. Nevertheless, the proposed interaction of amino acids near this region with PIP2 in the inner leaflet of the membrane may approximate this domain to the channel gate facilitating its interaction with protein domains located in the membrane interface such as parts of the S4-S5 linker ([164],[166],[167]).

It is tempting to propose an alternative hypothesis based on the potential interaction of W697 with the S2-S3 loop as suggested by the TRPV1 model [163], since both domains could lie near in the folded channel. In an extended configuration, this loop has the sufficient length to be close to the TRP domain and the S4-S5 helix. If so, the S2-S3 loop could act as a linker of the TRP box and the S4-S5 loop by interacting with both and, therefore, facilitating the coupling between the voltage and capsaicin sensors to the TRP domain and the channel's gate. Noteworthy, the S2-S3 loop displays positive charges that could interact with the W697 in a similar way as described for the S4-S5 linker. In this case, capsaicin binding to S2-S3 segment could induce structural changes improving the connection between the TRP domain and S4-S5 region, which was impaired by W697X mutations. This assumption would be in accordance with the results showing recovery of voltage sensitivity when capsaicin was simultaneously applied. Evidently, structural data are necessary to unequivocally unveil the structural layout and interactions of the W697 and I696 residues, which is essential to unambiguously disclose the role of the TRP domain in channel function.

4.2. CHARACTERIZATION OF TRP DOMAIN IN TRPV1

TRPV1 and TRPV2 channels have the highest percentage of identity in their TRP domain sequence from all TRPV channels. However, replacement of this domain in TRPV1 channel by the cognate TRPV2 (TRPV1-AD2) produced a severe impairment in protein functionality when activated by voltage, capsaicin, heat or acidic pH [61]. These results indicated that the TRP domain acts as an essential region for coupling the activating sensors and channel gate. To further investigate the role of this domain in channel gating, we performed a mutagenesis strategy for recovering the TRPV1 TRP domain sequence in the chimeric channel TRPV1-AD2. With this approach, we expected to assign a functional role in protein functionality to specific residues in the context of TRP domain. We focused in studying voltage and temperature response of these chimeric mutant channels.

The salient contribution of this study is that both sequence and structure of TRP domain determines gating properties of TRPV1. Modest changes in this sequence severely

affect coupling properties of channel gating between the voltage and temperature sensors and with the channel pore. Our results revealed that TRP domain had to recover around 93% of the original TRPV1 sequence from TRPV1-AD2 chimera for generating functional channels having detectable currents. All functional chimeric channels containing mutations in this region exhibited altered channel gating, characterized by a lower response to the activating stimuli. Conservative changes as contained in AD2-18 (E692D; T704S; D707E) and AD2-19 (T704S; D707E) negatively affect channel activation induced by voltage, capsaicin and temperature giving rise to lower current densities when compared with wild type. Furthermore, voltage and temperature threshold were rightward shifted to higher values since none of the channels reached saturating conditions as high as 240 mV or 60 °C. In contrast, mutations out of the TRP domain region present in AD2-20 (extended in two amino acids due to the insertion of K721 and Q722) did not significantly affect functional channel properties, as detected for biophysical and thermodynamic parameters of this channel.

The data obtained in this work may help us to understand the involvement of TRP domain in TRPV1 functionality in terms of molecular and structural mechanisms of channel gating. Our results indicated that changes affecting secondary structure, and consequently the coiled coil formation predicted for this region, completely prevented channel activation by any stimuli. It is evident that these mutations in TRP domain extremely affected protein stability. We detected a dramatic decrease in protein expression level for TRPV1-AD2 and other chimeric species such as AD2-4 and AD2-17, and likely the other non-functional chimeric mutants in between. This phenomenon was probably due to an incorrect protein folding and consequently, its degradation. These findings support the tenet that the preservation of the TRP domain in TRPV1 is required for correct protein folding and channel tetramerization [60]. However, we cannot discard the possibility of other regions are implicated in channel multimerization, since, despite the dramatic decrease of protein expression level, all chimeric channels reach cell membrane. Therefore, it is plausible that other channel domains may participate in subunit tetramerization such as N-terminus, transmembrane segments and distal regions of C-terminal domain ([168], [169]). Interestingly, protein expression level was sequentially recovered while TRP domain sequence, and secondary structure prediction, was restored. Nevertheless, all mutants between TRPV1-AD2 and AD2-18 analyzed by western immunoblot did not exhibit the glycosylated band described for TRPV1.

TRPV1 STRUCTURE-FUNCTION STUDY: ROLE OF THE TRP DOMAIN IN TRPV1 ALLOSTERIC GATING

DOCTORAL THESIS

LUCIA GREGORIO TERUEL

As seen in our results, mutants AD2-18, AD2-19 and AD2-20 were the only mutants exhibiting detectable currents evoked by voltage, capsaicin and temperature. In these mutants, activity was sequentially recovered from barely discernible currents in AD2-18, reaching wild type levels in AD2-20. Intriguingly, AD2-18 and AD2-19 channels contained conservative changes when compared with TRPV1 sequence, maintaining the physico-chemical properties of the mutated residue. One plausible explanation for these critical effects of mutations included in AD2-18 and AD2-19 is the alteration in protein structure. These conservative mutations had a modest effect on secondary structure prediction showing a slightly higher percentage of alpha-helix for those mutants. These channels exhibited a continuous alpha helix between I689 and K718, unlike TRPV1 and AD2-20 which showed a weak disruption of alpha helix in D707 and T708. These findings are in agreement with the presence of aspartic acid residues in secondary structure disruption sequences. Incorporation of a higher percentage of alpha-helix may strengthen the interaction between the 4-strand, parallel coiled-coil proposed for TRP domain, raising the energy of channel gating. Furthermore, secondary structure prediction revealed other differences in the proximal C-terminal domain between AD2-18 and AD2-19. Akin to TRPV1, AD2-19 exhibited random coil prediction for the 7-mer region adjacent to the pore, while AD2-18 showed extended strand disruption in V686 and N687 apparently induced by mutation E692D contained in this chimera. Extended strand arrangement allows the maximum space and freedom of movement for a side chain and may be involved in protein-protein interactions or parallel and/or anti-parallel β -sheet conformation. However, random coil structures do not form any secondary structure. These structural differences could interfere with the linkage between TRP domain downstream events and channel gate. All these structural changes in TRP domain may be affecting the energy transfer between sensing domains and channel pore hindering the gating process. This hypothesis is in accordance with the results obtained in the gating model where allosteric coupling parameters showed the highest variability with wild type channels.

Despite structural changes, we cannot discard that these mutations are affecting functional properties of these channels. One of the mutations present in these chimeric species is R701K (in AD2-18). Residue R701 has been reported as a participant in the interaction with PIP2 in the inner leaflet of the membrane ([166], [170]). In addition, this position is also included in a CaMKII recognition sequence, close to the phosphorylation site

T704 ([143], [144]) which is also mutated to a serine residue in AD2-18 and AD2-19 chimeras. Although these conservative changes maintain physico-chemical properties of amino acids, these chimeras exhibited severely impaired activation by all stimuli studied. This phenomenon correlates with the results obtained for mutants TRPV1-R701K and TRPV1-R701K-E692D-T704S which exhibited a significant impaired capsaicin response when compared with TRPV1 results in microfluorographic assay. Noteworthy, the replacement of nothing but these positions to TRPV1 original residue from the context of TRPV2 (AD2-K701R and AD2-K701R-D692E-S704T) gave rise to completely inactive channels. Taken together, these results indicate that R701 and T704 positions must be relevant for structural and/or functional properties of TRPV1 channel. Albeit, the replacement of these residues by wild type corresponding amino acids from the uncoupled chimera TRPV1-AD2 was not sufficient for reestablishing the coupling.

Regarding the preceding data, it is clear that this region participates in a common step of channel activation for all stimuli studied. This region located next to the pore can be important for the connection between different domains such as sensors and pore. Data obtained from allosteric model fitting of functional mutants revealed a possible coupling between temperature and voltage sensor in AD2-20 akin to TRPV1, in agreement with data obtained from patch clamp experiments. This coupling was disrupted in AD2-19 chimeric mutant displaying values for allosteric parameter E near 1, along with lower values in allosteric parameters C while allosteric factor D was augmented. Impairment of temperature coupling is reflected on defective temperature channel activation and improvement of voltage sensor coupling to the pore when both stimuli act together. The uncoupling between both sensors prevents the voltage sensor from being influenced by the temperature and allows a better coupling between voltage sensor and the pore when both stimuli are simultaneously applied.

4.3. STRUCTURAL FEATURES OF TRP DOMAIN AND IMPLICATION IN CHANNEL GATING.

The modular structure of TRP channels determines their modulation by agonists and their ion and selectivity properties. However, the mechanism by which sensing domains are coupled to channel gating and how these processes are connected to specific structural

TRPV1 STRUCTURE-FUNCTION STUDY: ROLE OF THE TRP DOMAIN IN TRPV1 ALLOSTERIC GATING

DOCTORAL THESIS

LUCIA GREGORIO TERUEL

regions in the channel are not completely understood. It is plausible that TRP domain plays an important role in this mechanism since it is adjacent to the pore and may act as a linker between channel gate and other domains in the protein. Our findings strongly substantiate the tenet that the TRP domain in TRPV1 is a pivotal structural determinant of allosteric channel gating. We demonstrate that the integrity of the TRP domain sequence is essential for correct channel functionality, since modest and conservative changes in several residues of this segment caused dramatic effects in channel coupling.

Here we provided evidence that mutations in two important sites of the TRP domain, located in the so called TRP box, primarily modulate the equilibrium constant of pore opening and the allosteric constants that couple stimuli sensing and gate activation. Notably, a critical contribution of W697 in coupling voltage-dependent gating was uncovered. Noteworthy, a critical contribution of W697 in coupling voltage-dependent gating was uncovered. Noteworthy, a Tryptophan residue is absolutely conserved in this position of the TRP box in all the TRP channels (TRPC, TRPM and TRPV) bearing a TRP domain, further supporting a central role in channel function. It is interesting to note that the mutation W692G in the TRP box of TRPV3, that alters the response of the channel to 2-ABP, has been linked as a cause of the Olmsted Syndrome, a rare congenital disorder characterized by diverse skin alterations and alopecia [171], further substantiating the relevant role of the TRP box in TRP channel function.

It has been demonstrated that the TRP domain in TRPV1 contains several important residues for the coupling of channel gating. This study revealed that conservative changes in this sequence such as D692E, R701K and T704S severely affected channel coupling when activated by voltage or temperature. However, our study unveiled that conservation of these positions is not enough for maintaining the channel biophysical properties but also required an appropriate context in TRP domain for correct channel functionality. Therefore, we were not able to assign a specific role to any residue in this region. It is important to mention that palmitoylated peptides patterned after the TRP domain of TRPV1 were found to selectively inhibit channel gating by physical and chemical stimuli, strictly dependent on its amino acid sequence [172]. These results also denote the relevance of the sequence in this region for channel gating and represent a novel strategy to modulate channel gating in this family of ion channels.

Summarizing, data obtained from both approaches contribute to define the role of the TRP domain in polymodal activation of TRPV1 channels. Our results lend support to data showing that conservation of TRP domain sequence is important for the correct channel coupling. It is suggested that changes modifying secondary and/or tertiary structure of this region are incompatible with functional channels. Since TRP domain region in TRPV1 is adjacent to the inner pore it is plausible that it could be mediating the transfer of energy derived from stimuli between the sensors and channel gate. Discrete changes in the structure of this region may alter inter- and intrasubunit interactions, and consequently, disrupt coupling between sensors and pore. However, structural information is required for a full understanding of the molecular details involved in channel gating.



TRPV1 STRUCTURE-FUNCTION STUDY: ROLE OF THE TRP DOMAIN IN TRPV1 ALLOSTERIC GATING

DOCTORAL THESIS

LUCIA GREGORIO TERUEL



5. CONCLUSIONS

TRPV1 STRUCTURE-FUNCTION STUDY: ROLE OF THE TRP DOMAIN IN TRPV1 ALLOSTERIC GATING

DOCTORAL THESIS

LUCIA GREGORIO TERUEL



TRPV1 STRUCTURE-FUNCTION STUDY: ROLE OF THE TRP DOMAIN IN TRPV1 ALLOSTERIC GATING

DOCTORAL THESIS

LUCIA GREGORIO TERUEL

1. Positions I696 and W697 in TRP box are key residues transducing stimulus sensing to pore gating through the allosteric coupling mechanism between voltage and capsaicin activating sensor and channel gate.
2. I696 residue only can be substituted by hydrophobic amino acids for channel function. The study also revealed an effect of the amino acid size at I696 in channel activation since the replacement of I696 by smaller or larger amino acids result in higher activation energy for activation.
3. Mutations of W697 position to any of the natural amino acids evoked a complete uncoupling of voltage sensing and gate opening. However, this position tolerated virtually all substitutions since practically all mutants displayed channel activity in the presence of saturating concentrations of capsaicin.
4. I696 and W697 residues are essential in TRPV1 channel folding since discrete changes in these position evoked relevant changes in the protein expression pattern and glycosylation process.
5. TRP domain integrity determines gating properties of TRPV1 since modest changes in this sequence severely affect coupling properties of channel gating between the voltage and temperature sensors and with the channel pore.
6. TRP domain plays an important role in channel expression and folding since mutations within this sequence dramatically altered protein expression pattern and glycosylation process.

TRPV1 STRUCTURE-FUNCTION STUDY: ROLE OF THE TRP DOMAIN IN TRPV1 ALLOSTERIC GATING

DOCTORAL THESIS

LUCIA GREGORIO TERUEL





6. MATERIAL AND METHODS

TRPV1 STRUCTURE-FUNCTION STUDY: ROLE OF THE TRP DOMAIN IN TRPV1 ALLOSTERIC GATING

DOCTORAL THESIS

LUCIA GREGORIO TERUEL



TRPV1 STRUCTURE-FUNCTION STUDY: ROLE OF THE TRP DOMAIN IN TRPV1 ALLOSTERIC GATING

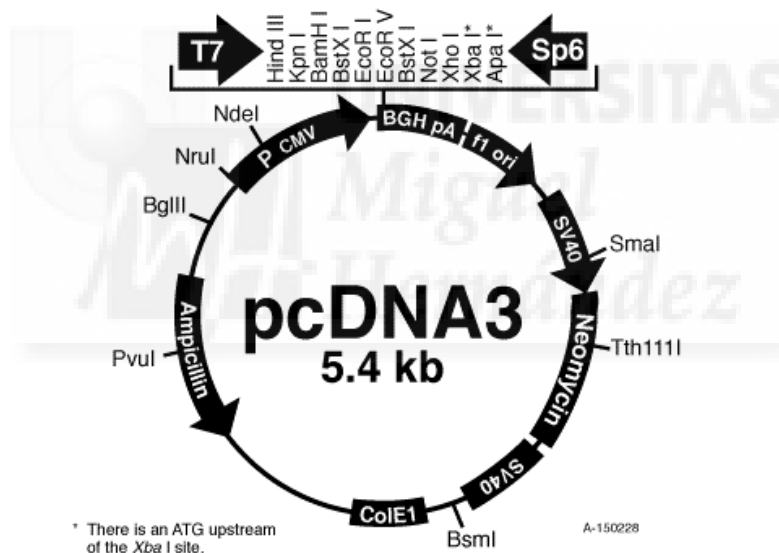
DOCTORAL THESIS

LUCIA GREGORIO TERUEL

MOLECULAR BIOLOGY

PLASMIDS AND CHIMERIC CONSTRUCTS

There are two main plasmidic constructs which have been used in this work. One of them contains the rat TRPV1 cDNA as inserted gene. The other one includes the TRPV1 chimeric channel TRPV1-AD2 [referred to as association domain (AD)] in which has been previously deleted the TRP domain sequence of TRPV1 ($\Delta 684-721$) and inserted the cognate sequence of human TRPV2 (645-683). Both constructs are both cloned into the pcDNA3 vector (Invitrogen).



SITE-DIRECTED MUTAGENESIS

Site-directed mutagenesis of the residues in TRPV1 and TRPV1-AD2 chimera were carried out by PCR. We amplified the complete plasmid using a pair of primers which included the designed mutation in the template DNA. We used the Pfu Turbo DNA polymerase (Stratagene) following the manufacturer's recommendations. For punctual mutations in TRP box we designed a pair of degenerate primers for each residue obtaining the 19 mutants (Ile

for 696 and Trp for 697 were introduced as internal controls) from an only PCR reaction. To confirm the correct amplification we loaded the PCR products in an agarose gel. The electrophoresis of nucleic acids is used for identifying and separating individual molecules or fragments of DNA. The DNA molecules are negatively charged because of the phosphate group. This property allows the electrophoresis technique to separate them only attending to their size. The gel was prepared at 0.8% agarose (m/v) in TAE buffer. We used 35 ml of 0.8% agarose for one gel where 3 μ l of GelRed (Biotium) was added to the mixture. GelRed is an environmentally safe fluorescent nucleic acid dye for staining dsDNA, ssDNA or RNA in agarose gels which can be detected by ultraviolet light transillumination of the gel. For the gel running we used the Mini SubCell GT system (BIO-RAD) applying a voltage of 100V. Once we determined the correct size of the PCR products the mutant channels were confirmed by DNA sequencing. The PCR products was digested with DpnI for 1h at 37°C to eliminate the methylated plasmid fraction and transformed in bacteria. For mutants' identification, the number indicates the position of the residue in the protein sequence; the first letter is the original amino acid in the wild-type protein, and the second is the residue that substitutes it.

TRANSFORMATION AND PLASMIDIC DNA EXTRACTION

We included the plasmidic DNA in XL1-Blue strain of *Escherichia coli* employing the heat shock protocol (Molecular cloning, Maniatis). Previously bacteria were chemically prepared as competent cells using calcium chloride procedure (Maniatis). Afterwards, the cells were seeded in a LB-Agar (2%)-Ampicilin (100mg/ml) plate and grew over night at 37°C. For the plasmidic DNA extraction we used QIAGEN Plasmid MINI kit and QIAGEN Plasmid MIDI kit following manufacturer's instructions.

FUNCTIONAL ASSESMENT

CELL CULTURE AND TRANSFECTION

Human embryonic Kidney (HEK) 293 cells were cultured and maintained in DMEM-Glutamax supplemented with 10% fetal bovine serum and 1% penicillin-streptomycin solution, pH 7.6 in a 5% CO₂ incubator at 37 °C. The cells were seeded according to the experiment were going to be used for. It will be describe in detail in the corresponding paragraph. We used two transfection methods depending on the experiment:

- Lipofectamine 2000 (Invitrogen, Carlsbad, CA, USA) following the recommendations of the manufacturer.
- Calcium phosphate precipitation. This technique is based on the precipitation of the complex formed between DNA and salt. These precipitates layer directly onto the cells facilitating the entrance into the cells by endocytotic uptake. The solution contained: 2x HEPES, 0.25 M CaCl₂ and sterile distilled water. The amount of DNA used for this transfection protocol was ≈ 0.5 µg per 35mm plate. For all the experiments we used the plasmid containing the cDNA encoding rat TRPV1 as a positive control and the empty vector pcDNA3 as a negative control.

CALCIUM MICROFLUOROGRAPHIC ASSAY

Cells were seeded in black 96 well-plate with clear flat bottom at 10000-20000 cells per well and transfected between 24-48h after seed with Lipofectamine 2000. This experiment was performed 48h after transfection. We used the fluorescence calcium indicator Fluo4-NW (Molecular Probes) for detecting channel's activity. Cells were incubated with 100µl of dye loading solution (1X HBSS, 20mM HEPES, pH 7.4) in the presence of 2.5mM probenecid for 45 min at 37°C and 10 min at room temperature. For fluorescence detection we used the microplate reader POLARstar Omega (BMG Labtech). The protocol used measured the Fluo-4 fluorescence signal (Excitation at 494nm and emission at 516nm) during 18 cycles. TRPV1 and mutants activity was evoked by the addition of capsaicin 100µM in the fifth cycle using the injection system of the plate reader. We quantified the response to capsaicin by calculating the

Area under the curve (AUC) between the fifth and the eighteenth cycles, generated by the increase of fluorescence signal induced by the response to capsaicin.

PATCH-CLAMP RECORDINGS, DATA ACQUISITION AND ANALYSIS

This procedure was used for the study of the response of TRPV1 and mutants to capsaicin and depolarizing voltages. Cells were seeded in Poly-D-lysine coated 30 mm dishes at 40000-80000 cells per plate and transfected between 24-48h after seed with Lipofectamine 2000. Whole-cell patch-clamp recordings were made from transfected cells 48 h after transfection [62]. Specifically, HEK293 cells were cotransfected with channel under study (TRPV1 or Mutants) and EYFP protein as reporter (pEYFP, Clontech, Palo Alto, CA, USA). Cells transfected with pcDNA3 empty vector were used as negative control. Patch pipettes were prepared from thin-borosilicate glass (World Precision Instruments, Sarasota, FL), pulled (P-97 horizontal puller, Sutter Instruments) and fire-polished to have a final resistance of 2-4 M Ω when filled with standard internal solution. Data were sampled at 10 kHz (EPC-10 amplifier with Pulse software; HEKA Electronic, Lambrecht, Germany) and low-pass filtered at 3 kHz for analysis (Pulse Fit 8.54; HEKA Electronic). Recordings with leak currents >100 pA or series resistance >10 M Ω were discarded.

For whole cells recordings pipettes were filled with Standard Internal Solution contained (in mM): 150 NaCl, 3 MgCl₂, 5 EGTA and 10 HEPES, pH 7.2 with CsOH, and perfused with Standard Extracellular Solution contained (in mM): 150 NaCl, 6 CsCl, 1 MgCl₂, 1.5 CaCl₂, 10 glucose and 10 HEPES, pH 7.4 with NaOH. The different saline solutions were applied with a gravity-driven local microperfusion system with a rate flow of about 200 μ l/min, located within about 100 μ m of cell under study. Capsaicin stocks (Fluka) (10 mM and 100 mM) were prepared in dimethylsulfoxide and diluted as indicated for the experiments in bath solution the day of the experiment. All recordings were performed at room temperature of 22-24 °C.

Voltage-step protocols consisting of 100 ms depolarizing pulses from -120 mV to +240 mV in steps of 20 mV were used. The holding potential was 0 mV and the time interval between each pulse was 5s. I-V relationships were studied using a ramp protocol consisting of a voltage step of 300 ms from the holding potential of 0 mV to -80 mV, followed by 350 ms

TRPV1 STRUCTURE-FUNCTION STUDY: ROLE OF THE TRP DOMAIN IN TRPV1 ALLOSTERIC GATING

DOCTORAL THESIS

LUCIA GREGORIO TERUEL

linear ramp up to +80 or +160 mV. Time interval between each pulse was 5 s for voltage activation and 3 s when experiments with capsaicin were performed. The series resistance was usually less than 10 M Ω and to minimize voltage errors was compensated to 70-90%.

The conductance-voltage (G-V) curves were obtained by converting the maximal current values from the voltage step protocol to conductance using the relation $G=I/(V-V_R)$, where G is the conductance, I is the peak current, V is the command pulse potential, and V_R is the reversal potential of the ionic current. G-V curves for each cell were fitted to the Boltzmann equation: $G=G_{min} + (G_{max} - G_{min}) / \{1 + \exp [(V-V_{0.5})/a_n]\}$ where G_{max} is the maximal conductance, G_{min} is the minimal conductance at hyperpolarized potentials, $V_{0.5}$ is the voltage required to activate the half-maximal conductance, and a_n is the slope of the G-V curve. Thereafter, estimated G_{max} values were used to obtain the normalized G/ G_{max} -V curves. Free energy difference between the closed and the open states at 0 mV (ΔG_0) was calculated using $\Delta G_0 = z_g F V_{0.5}$ equation, where F is the Faraday constant (0.023 Kcal/mol⁻¹.mV⁻¹) and z_g is the apparent gating valence obtained from $z_g = 25.69 \text{ mV}/a_n$. For channels that displayed voltage-dependent and -independent components in the G-V curve in the presence of capsaicin, the free energy of the activation process was obtained using $\Delta G_0 = \Delta G_0(V) + \Delta G_0(I)$, where $\Delta G_0(V)$ denoted free energy of the voltage dependent component, and $\Delta G_0(I)$ indicated the free energy of the voltage-independent part. This energy was calculated using $\Delta G_0(I) = -RT \ln(P_o/1-P_o)$ [173], where P_o denoted the probability of channel opening at hyperpolarized potentials. P_o was calculated as the value obtained from the Boltzmann fitting for the bottom horizontal asymptote.

Data were visualized and analyzed using PulseFit 8.11 (HEKA Elektronik), GraphPad Prism 5 statistical software (GraphPad Software, Inc., CA, USA) and Origin 8.0 (Microcal Software, Northampton, MA). All data were expressed as mean \pm SEM with n=number of cells tested for electrophysiological data. Statistical analysis was performed with One-way ANOVA and significance level was preset to $p < 0.05$

PATCH-CLAMP RECORDINGS AND LASER DIODE HEATING (Yao et al., 2009, 121)

This procedure was used for the study of the response of representative chimeric mutants to heating temperatures. Cells were seeded in Poly-D-lysine coated 30 mm dishes at 40000-80000 cells per plate and transfected between 24-48h after seed by using calcium phosphate precipitation method. Specifically, HEK293 cells were cotransfected with channel under study and GFP protein as reporter (pGFP, Clontech, Palo Alto, CA, USA).

Patch-clamp recording of channel currents was made in whole-cell configuration. Currents were amplified using an Axopatch 200B amplifier (Axon Instruments, Foster City, CA), low-pass filtered at 5-10 kHz through the built-in 8-pole Bessel filter, and sampled at 10-20 kHz with a multifunctional data acquisition card (National Instruments, Austin, TX). Data acquisition was controlled by custom-made software, which was capable of synchronous I/O and simultaneous control of laser and patch-clamp amplifier. Patch pipettes were fabricated from borosilicate glass capillary (Sutter Instrument, Novato, CA) and fire-polished to a resistance $<5\text{ M}\Omega$ when filled with 150 mM NaCl solution. Pipette series resistance and capacitance were compensated using the built-in circuitry of the amplifier (50-70%), and the liquid junction potential between the pipette and bath solutions was zeroed prior to seal formation. Currents were normally evoked from a holding potential of either -60 mV (inward) or +60 mV (outward). All voltages were defined as membrane potentials with respect to extracellular solutions. Bath solutions consisted of (mM): 150 NaCl, 5 EGTA, 10 HEPES, pH 7.4 (adjusted with NaOH). Electrodes were filled with (mM): 140 CsCl, 10 HEPES, 1 EGTA, pH 7.4 (adjusted with CsOH). All chemicals were purchased from Sigma (St. Louis, MO).

Temperature jumps were produced using a single emitter laser diode as the heat source. The fiber was mounted on a micromanipulator with the tip placed close to cells as the perfusion pipette normally was. The laser diode was driven by a pulsed quasi-CW current power supply (Lumina Power, Bradford, MA). Pulsing of the controller was controlled from computer through the data acquisition card using a custom program. A visible laser line (532 nm) was coupled to the fiber to aid alignment. Constant temperature steps were generated by irradiating the tip of an open pipette and using the current of the electrode as a readout for feedback control. The laser was first powered on for a brief duration to reach the set temperature and was then modulated to maintain a constant pipette current. Temperature

TRPV1 STRUCTURE-FUNCTION STUDY: ROLE OF THE TRP DOMAIN IN TRPV1 ALLOSTERIC GATING

DOCTORAL THESIS

LUCIA GREGORIO TERUEL

was calibrated offline from the pipette current and the temperature dependence of electrolyte conductivity. Temperature for every step was calculated as follow:

$$T = \frac{1}{\frac{1}{T_0} - \frac{R}{Ea} \log\left(\frac{I}{I_0}\right)}$$

Where T_0 corresponded to the initial (room) temperature, R denoted gases constant (1.98 cal/K.mol), I_0 and I are initial current (at T_0) and current induced by the pulse (at T) and Ea refers to a constant activation energy for the solution going through the open pipette.

Temperature-step protocols consisting of 9 steps of 100 ms from ≈ 36 °C to ≈ 60 °C were used. Previous to every step, a room temperature step (23°C) was applied for 50 ms, followed by a rapid ramp of 0.75 ms to reach the temperature set. At the end of the step, a slow ramp (200 ms) was performed for recovering room temperature.

The conductance-temperature (G-T) curves were obtained by converting the maximal current values from the temperature step protocol to conductance using the relation $G=I/(V-V_R)$. G-T curves for each cell were fitted to the Boltzmann equation: $G=G_{min} + (G_{max} - G_{min}) / \{1 + \exp [(-\Delta H/R) * ((1/T) - (1/T_{0.5}))]\}$ where G_{max} is the maximal conductance, G_{min} is the minimal conductance at low temperatures, $T_{0.5}$ is the temperature required to activate the half-maximal conductance, and ΔH is the slope of the G-T curve. Thereafter, estimated G_{max} values were used to obtain the normalized G/G_{max} -T curves. Thermodynamical parameters for determining the temperature dependence of channel opening were calculated using Van't Hoff equation: $\ln Keq = \{(-\Delta H/RT) + (\Delta S/R)\}$ where ΔH and ΔS corresponds to enthalpy (cal/mol) and entropy (cal.mol⁻¹.K⁻¹) of gating process between closed and open state, T is the temperature applied in every step, R is the gas constant and Keq refers the equilibrium constant of the channel opening process obtained from $Keq = \{G/G_{max} / (1 - G/G_{max})\}$. Free energy difference between closed and open state was calculated from $\Delta G = RT \ln(Keq)$. Temperature sensitivity was estimated with Q_{10} parameter from macroscopic currents, obtained from $Q_{10} = \{(I_2/I_1) \exp(10/(T_2 - T_1))\}$, I_2 represented the maximum current obtained for each cell measured at temperature T_2 , and I_1 represented the current value obtained for each pulse of temperature T_1 .

Data were visualized and analyzed using a custom-made software (Q-studio), GraphPad Prism 5 statistical software (GraphPad Software, Inc., CA, USA), Origin 8.0 (Microcal Software, Northampton, MA) and pCLAMP 10.3 (Axon Instruments, Foster City, CA). All data were expressed as mean \pm SEM with n=number of cells tested for electrophysiological data



BIOCHEMICAL APPROACHES

BIOTINYLATION ASSAY

This procedure was used for detecting the plasma membrane protein level. Cells were plated onto 6-well plates at 250000-400000 cells per well and transfected with Lipofectamine 2000 between 24-48h after seeding (we used one well for each DNA). The experiment was carried out 48 h after transfection. It is important to keep the temperature down during the whole process to avoid the internalization of membrane proteins. Firstly, we washed the cells twice with pre-chilled PBS to eliminate the rest of serum. Then, we incubated the cells with 1 ml of biotin (Thermo Scientific Pierce) solution at 0.9 mg/ml diluted in PBS for 30 min at 4°C with gentle agitation. Afterwards, we added 1 ml of Quench Biotinylation buffer [Tris-buffered saline (in mM: 10 Tris pH 7.4, 154 NaCl)] to stop the reaction and incubated the cells for 30 min at 4°C with agitation. Then, we scrapped the cells and centrifuged them to remove the supernatant and the extra-biotin has been not bound to the plasma membrane proteins. We proceed to lysate the cells using lysis buffer (150 µl per well) having the following composition: in mM, 50 HEPES pH 7.4; 140 NaCl; 10% Glycerol; 1% v/v Triton X-100; 1 EDTA; 2 EGTA; 0.5% Deoxycholate; proteases inhibitor cocktail (Sigma) 1:100. Cells were maintained in lysis buffer for 40 min at 25°C with gentle agitation. Solubilized proteins were recovered by centrifugation at 10000rpm for 15 min. Then, we discarded the pellet and quantified the supernatant by using BCA kit procedure (Pierce) following manufacturer's instructions. After the lysate procedure, we kept the solubilised proteins as a reference of the total amount of protein we started from and proceeded to denature them with SDS-PAGE sample buffer (4X: 0.25 mM Tris-HCl pH 6.8, 80 mg/ml SDS, 4 mg/ml bromophenol blue, 40 % Glycerol and 0.2 M DTT) boiling the samples at 100 °C for 5min. From the total extract we added 150 µg of protein sample to the Streptavidin-Agarose resin (Sigma) in over resin capacity to make sure all the biotin-labelled proteins are getting bound to the resin. We incubated the mix over night at 4°C. Next day we centrifuged the resin at 5000 rpm for 15 min and removed the supernatant very carefully. Then, we washed the resin twice with lysis buffer by centrifugation and denatured the samples as we have already described.

SODIUM DODECYL SULFATE POLYACRYLAMIDE GEL ELECTROPHORESIS (SDS-PAGE)

This electrophoretic technique allows us to separate proteins using an electric field. SDS confers negative charge to the proteins and permits them to be separated by their molecular weight. We used this technique for detecting TRPV1 and mutants obtained as from total protein extracts as from biotinylation. The polyacrylamide gels (1.5 mm thickness) were made as follow:

Composition	Resolving gel (10%)	Composition	Stacking gel (4%)
Distilled water	4 ml	Distilled water	3 ml
Tris base 1.5 M pH 8.8	2.5 ml	Tris base 0.5 M pH 6.8	1.25 ml
SDS	100 µl	SDS	50 µl
30% Acril: 8% bisacril *	3.3 ml	30% Acril: 8% bisacril*	0.65 ml
PSA (10%)	70 µl	PSA (10%)	60 µl
TEMED	7 µl	TEMED	7 µl

* (Protogel)

We used the MiniProtean III system (BIORAD) with a running buffer containing 0.3% Tris base, glycine 1.44% and SDS 0.1%. We gel was run at 100mV for 1h 30min at room temperature.

WESTERN IMMUNOBLOTTING

Western blotting identifies with specific antibodies proteins that have been separated from a pull. We used this technique to detect and quantify the amount of TRPV1 and mutant channels we have obtained by different methods. First of all, we transferred the proteins to a 0.45µm nitrocellulose membrane (BIORAD) using the Trans-Blot SD Semi-Dry Transfer Cell System (BIORAD) following manufacturer's conditions. The transfer buffer contained: 200 mM Glycine, 25 mM Tris base and 20% Methanol, pH 8.5. The proteins were transferred to the membrane for 45 min at 0.27 or 0.52 A for one or two gels respectively. Afterwards, the membrane was blockade with non-fat milk at 5% in PBS-0.05% Tween for 1h at room temperature with agitation. Blocking the membrane prevents non-specific background binding of the primary and/or secondary antibodies to the membrane. Then, we separately incubated

TRPV1 STRUCTURE-FUNCTION STUDY: ROLE OF THE TRP DOMAIN IN TRPV1 ALLOSTERIC GATING

DOCTORAL THESIS

LUCIA GREGORIO TERUEL

the membrane for the staining of primary antibodies. The antibodies used were anti-TRPV1 antibody (1:30000, Allomone labs) and anti-actin antibody (1:10000, Sigma. Actin was used as a loading control protein) and were incubated over night at 4°C with agitation. The next day membranes were washed out with PBS-0.05% Tween three times for 10 min each one. Following, we incubated them with the secondary antibody anti-Rabbit IgG Peroxidase conjugate (1:50000, Sigma) for 1 h at room temperature while agitating (all the antibodies were prepared in non-fat milk at 5% in PBS-0.05% Tween). Immunoreactive bands were visualized using the ECL method (ECL-Select, GE-Healthcare) and manually developed using X-ray films. Protein bands quantification was calculated using TotalLab QUANT software. Data were expressed as means \pm SEM for number of experiments (n) in different conditions. Statistical analysis was performed with One-way Analysis of Variance and significance level was preset to $p < 0.05$.



BIONFORMATICS

SECONDARY STRUCTURE PREDICTION

We investigated the presence of several secondary structures predicted in TRP domain region of TRPV1 and some representative AD2 chimeras. Analysis was performed with the server GOR IV (http://npsa-pbil.ibcp.fr/cgi-bin/npsa_automat.pl?page=npsa_gor4.html). We studied TRP domain sequence (M682-F721 corresponding with rat TRPV1) of wild type protein, AD2, AD2-17, AD2-18, AD2-19 and AD2-20. Secondary structure forms considered are alpha helix (h), 3_{10} helix (g), Pi helix (i), beta bridge (b), extended strand (e), beta turn (t), bend region (s) and random coil (c). An estimated percentage is calculated for each structure.

MODELLING FULL-LENGTH TRPV1 CHANNEL

The multiple sequence alignment of the different parts of the protein was made with CLUSTALW [174] at the European Bioinformatics Institute site (<http://www.ebi.ac.uk>) using Gonnet matrices [175]. The protein was modeled by homology [163] using the templates of remote or close homologues available with the highest resolution possible at the Brookhaven Protein Data Bank (<http://www.rcsb.org/pdb>). Briefly, the transmembrane region was cast with the spatial coordinates of the atomic structure of the eukaryotic, voltage-gated Kv1.2 K⁺ channel [176] (PDB code 2R9R at 2.4Å resolution). The N-end domain of N-terminus was modeled using the human thymidylate kinase (PDB code 1E9C at 1.6Å resolution) as a template, while the ankyrin domain was modeled using its solved atomic structure (PDB code 2PNN at 2.7Å resolution) by Lishko et al. (2007) [177]. The C-terminal domain was modeled as two different domains: i) the coiled-coil TRP domain near the channel gate was previously cast using the coordinates of a parallel tetrameric four helix bundle ([61], [178]) (PDB code 1WL5 at 2.17Å resolution); and, ii) the regulatory domain was modeled using the C-terminal region of the hyperpolarized, cyclic nucleotide-gated channel HCN2 in the presence of cGMP [60] (PDB code 1Q3E at 1.9Å resolution).

TRPV1 STRUCTURE-FUNCTION STUDY: ROLE OF THE TRP DOMAIN IN TRPV1 ALLOSTERIC GATING

DOCTORAL THESIS

LUCIA GREGORIO TERUEL

The homology modeling of the individual domains was performed in the Swiss-Model Protein Modeling Server [179] at ExPASy Molecular Biology site (<http://kr.expasy.org/>). To construct the whole model, the assembly of the entire TRPV1 was made following the physical, biochemical, and functional information available. Peptide bond connection as well as structure visualization and checking were made using WHAT IF [180], Swiss PDB viewer version 3.7 [181] and Yasara (<http://www.yasara.org>). The final molecular graphic representations were created by Pymol 0.99rc6 (<http://www.pymol.org>).

The orientation and optimization of the side chains were carried out in two steps: first, those residues making van der Waals clashes were selected and fitted with “Quick and Dirty” algorithms (DeepView); second, models were energy minimized in vacuum (100 steps of steepest descent and 100 conjugate gradient, cutoff of 10 Å for nonbonded interactions) with Insight II (Biosym/MSI). The edition of the structure was accomplished with Swiss PDB viewer [181] and Insight II (Accelrys Software Inc., <http://www.accelrys.com/>). In addition, the model was tested in terms of energy with FoldX ([182], [183]) at the CRG site: <http://foldx.crg.es> The force field of FoldX evaluated the properties of the structure, such as its atomic contact map, the accessibility of the atoms and residues, the backbone dihedral angles, and the hydrogen bond and electrostatic networks of the protein.

The entire system was subjected to an equilibration process previous to the molecular dynamics simulation. The equilibration consisted in an initial minimization with fixed backbone atoms, followed by a minimization with restrained carbon alpha atoms and a short molecular dynamics (10 ps), to reduce initial bad contacts and to fill empty cavities. Then, the full system, under periodic boundary conditions in the three coordinate directions, was simulated at 310°K for 1 ns. All dynamic simulations were done by using NAMD [184] with the force field CHARMM27 [185]. The cutoff used for long range interactions was 10 Å.

TRPV1 STRUCTURE-FUNCTION STUDY: ROLE OF THE TRP DOMAIN IN TRPV1 ALLOSTERIC GATING

DOCTORAL THESIS

LUCIA GREGORIO TERUEL





7. REFERENCES



TRPV1 STRUCTURE-FUNCTION STUDY: ROLE OF THE TRP DOMAIN IN TRPV1 ALLOSTERIC GATING

DOCTORAL THESIS

LUCIA GREGORIO TERUEL

Reference List

1. Julius D, Basbaum AI (2001) Molecular mechanisms of nociception. *Nature* 413: 203-210.
2. Baron R (2006) Mechanisms of disease: neuropathic pain--a clinical perspective. *Nat Clin Pract Neurol* 2: 95-106. ncpneuro0113 [pii];10.1038/ncpneuro0113 [doi].
3. Baron R (2000) Peripheral neuropathic pain: from mechanisms to symptoms. *Clin J Pain* 16: S12-S20.
4. Patapoutian A, Tate S, Woolf CJ (2009) Transient receptor potential channels: targeting pain at the source. *Nat Rev Drug Discov* 8: 55-68.
5. Dubin AE, Patapoutian A (2010) Nociceptors: the sensors of the pain pathway. *J Clin Invest* 120: 3760-3772. 42843 [pii];10.1172/JCI42843 [doi].
6. Hucho T, Levine JD (2007) Signaling pathways in sensitization: toward a nociceptor cell biology. *Neuron* 55: 365-376.
7. Cortright DN, Szallasi A (2009) TRP channels and pain. *Curr Pharm Des* 15: 1736-1749.
8. Basbaum AI, Bautista DM, Scherrer G, Julius D (2009) Cellular and molecular mechanisms of pain. *Cell* 139: 267-284. S0092-8674(09)01243-4 [pii];10.1016/j.cell.2009.09.028 [doi].
9. Belmonte C, Viana F (2008) Molecular and cellular limits to somatosensory specificity. *Mol Pain* 4: 14.
10. Woolf CJ, Ma Q (2007) Nociceptors--noxious stimulus detectors. *Neuron* 55: 353-364.
11. Caterina MJ, Schumacher MA, Tominaga M, Rosen TA, Levine JD, Julius D (1997) The capsaicin receptor: a heat-activated ion channel in the pain pathway. *Nature* 389: 816-824.
12. Alloui A, Zimmermann K, Mamet J, Duprat F, Noel J, Chemin J, Guy N, Blondeau N, Voilley N, Rubat-Coudert C, Borsetto M, Romey G, Heurteaux C, Reeh P, Eschaliier A, Lazdunski M (2006) TREK-1, a K⁺ channel involved in polymodal pain perception. *EMBO J* 25: 2368-2376. 7601116 [pii];10.1038/sj.emboj.7601116 [doi].
13. Cohen A, Sagron R, Somech E, Segal-Hayoun Y, Zilberberg N (2009) Pain-associated signals, acidosis and lysophosphatidic acid, modulate the neuronal K(2P)2.1 channel. *Mol Cell Neurosci* 40: 382-389. S1044-7431(08)00314-X [pii];10.1016/j.mcn.2008.12.004 [doi].

7. REFERENCES

14. Noel J, Zimmermann K, Busserolles J, Deval E, Alloui A, Diochot S, Guy N, Borsotto M, Reeh P, Eschalié A, Lazdunski M (2009) The mechano-activated K⁺ channels TRAAK and TREK-1 control both warm and cold perception. *EMBO J* 28: 1308-1318. [emboj200957 \[pii\]](#);10.1038/emboj.2009.57 [doi].
15. Chien LY, Cheng JK, Chu D, Cheng CF, Tsaur ML (2007) Reduced expression of A-type potassium channels in primary sensory neurons induces mechanical hypersensitivity. *J Neurosci* 27: 9855-9865. 27/37/9855 [pii];10.1523/JNEUROSCI.0604-07.2007 [doi].
16. Binshtok AM (2011) Mechanisms of nociceptive transduction and transmission: a machinery for pain sensation and tools for selective analgesia. *Int Rev Neurobiol* 97: 143-177. B978-0-12-385198-7.00006-0 [pii];10.1016/B978-0-12-385198-7.00006-0 [doi].
17. Moran MM, McAlexander MA, Biro T, Szallasi A (2011) Transient receptor potential channels as therapeutic targets. *Nat Rev Drug Discov* 10: 601-620. nrd3456 [pii];10.1038/nrd3456 [doi].
18. Cosens DJ, Manning A (1969) Abnormal electroretinogram from a *Drosophila* mutant. *Nature* 224: 285-287.
19. Montell C, Birnbaumer L, Flockerzi V, Bindels RJ, Bruford EA, Caterina MJ, Clapham DE, Harteneck C, Heller S, Julius D, Kojima I, Mori Y, Penner R, Prawitt D, Scharenberg AM, Schultz G, Shimizu N, Zhu MX (2002) A unified nomenclature for the superfamily of TRP cation channels. *Mol Cell* 9: 229-231. S1097276502004483 [pii].
20. Clapham DE (2003) TRP channels as cellular sensors. *Nature* 426: 517-524.
21. Pedersen SF, Owsianik G, Nilius B (2005) TRP channels: an overview. *Cell Calcium* 38: 233-252.
22. Venkatachalam K, Montell C (2007) TRP channels. *Annu Rev Biochem* 76: 387-417.
23. Clapham DE, Runnels LW, Strubing C (2001) The TRP ion channel family. *Nat Rev Neurosci* 2: 387-396. 10.1038/35077544 [doi];35077544 [pii].
24. Gaudet R (2008) A primer on ankyrin repeat function in TRP channels and beyond. *Mol Biosyst* 4: 372-379. 10.1039/b801481g [doi].
25. Montell C, Birnbaumer L, Flockerzi V (2002) The TRP channels, a remarkably functional family. *Cell* 108: 595-598. S0092867402006700 [pii].
26. Ramsey IS, Delling M, Clapham DE (2006) An introduction to TRP channels. *Annu Rev Physiol* 68: 619-647. 10.1146/annurev.physiol.68.040204.100431 [doi].
27. Nilius B, Owsianik G, Voets T, Peters JA (2007) Transient receptor potential cation channels in disease. *Physiol Rev* 87: 165-217.

TRPV1 STRUCTURE-FUNCTION STUDY: ROLE OF THE TRP DOMAIN IN TRPV1 ALLOSTERIC GATING

DOCTORAL THESIS

LUCIA GREGORIO TERUEL

28. Sun M, Goldin E, Stahl S, Falardeau JL, Kennedy JC, Acierno JS, Jr., Bove C, Kaneski CR, Nagle J, Bromley MC, Colman M, Schiffmann R, Slaughter SA (2000) Mucopolidosis type IV is caused by mutations in a gene encoding a novel transient receptor potential channel. *Hum Mol Genet* 9: 2471-2478.
29. Lee G, Abdi K, Jiang Y, Michaely P, Bennett V, Marszalek PE (2006) Nanospring behaviour of ankyrin repeats. *Nature* 440: 246-249. [nature04437 \[pii\];10.1038/nature04437 \[doi\]](#).
30. Nilius B, Owsianik G (2011) The transient receptor potential family of ion channels. *Genome Biol* 12: 218. [gb-2011-12-3-218 \[pii\];10.1186/gb-2011-12-3-218 \[doi\]](#).
31. Bandell M, Story GM, Hwang SW, Viswanath V, Eid SR, Petrus MJ, Earley TJ, Patapoutian A (2004) Noxious cold ion channel TRPA1 is activated by pungent compounds and bradykinin. *Neuron* 41: 849-857. [S0896627304001503 \[pii\]](#).
32. Jordt SE, Bautista DM, Chuang HH, McKemy DD, Zygmunt PM, Hogestatt ED, Meng ID, Julius D (2004) Mustard oils and cannabinoids excite sensory nerve fibres through the TRP channel ANKTM1. *Nature* 427: 260-265. [10.1038/nature02282 \[doi\];nature02282 \[pii\]](#).
33. Bautista DM, Jordt SE, Nikai T, Tsuruda PR, Read AJ, Poblete J, Yamoah EN, Basbaum AI, Julius D (2006) TRPA1 mediates the inflammatory actions of environmental irritants and proalgesic agents. *Cell* 124: 1269-1282. [S0092-8674\(06\)00240-6 \[pii\];10.1016/j.cell.2006.02.023 \[doi\]](#).
34. Hinman A, Chuang HH, Bautista DM, Julius D (2006) TRP channel activation by reversible covalent modification. *Proc Natl Acad Sci U S A* 103: 19564-19568. [0609598103 \[pii\];10.1073/pnas.0609598103 \[doi\]](#).
35. Macpherson LJ, Dubin AE, Evans MJ, Marr F, Schultz PG, Cravatt BF, Patapoutian A (2007) Noxious compounds activate TRPA1 ion channels through covalent modification of cysteines. *Nature* 445: 541-545. [nature05544 \[pii\];10.1038/nature05544 \[doi\]](#).
36. Chen J, Zhang XF, Kort ME, Huth JR, Sun C, Miesbauer LJ, Cassar SC, Neelands T, Scott VE, Moreland RB, Reilly RM, Hajduk PJ, Kym PR, Hutchins CW, Faltynek CR (2008) Molecular determinants of species-specific activation or blockade of TRPA1 channels. *J Neurosci* 28: 5063-5071. [28/19/5063 \[pii\];10.1523/JNEUROSCI.0047-08.2008 \[doi\]](#).
37. Zurborg S, Yurgionas B, Jira JA, Caspani O, Heppenstall PA (2007) Direct activation of the ion channel TRPA1 by Ca²⁺. *Nat Neurosci* 10: 277-279. [nn1843 \[pii\];10.1038/nn1843 \[doi\]](#).
38. Banke TG, Wickenden AD (2009) Intracellular zinc irritates TRPA1. *Nat Chem Biol* 5: 141-142. [nchembio0309-141 \[pii\];10.1038/nchembio0309-141 \[doi\]](#).

39. Peyrot des GC, Uchida K, Bryant B, Shima A, Sperry JB, Dankulich-Nagrudny L, Tominaga M, Smith AB, III, Beauchamp GK, Breslin PA (2011) Unusual pungency from extra-virgin olive oil is attributable to restricted spatial expression of the receptor of oleocanthal. *J Neurosci* 31: 999-1009. 31/3/999 [pii];10.1523/JNEUROSCI.1374-10.2011 [doi].
40. Gracheva EO, Ingolia NT, Kelly YM, Cordero-Morales JF, Hollopeter G, Chesler AT, Sanchez EE, Perez JC, Weissman JS, Julius D (2010) Molecular basis of infrared detection by snakes. *Nature* 464: 1006-1011. nature08943 [pii];10.1038/nature08943 [doi].
41. Story GM, Peier AM, Reeve AJ, Eid SR, Mosbacher J, Hricik TR, Earley TJ, Hergarden AC, Andersson DA, Hwang SW, McIntyre P, Jegla T, Bevan S, Patapoutian A (2003) ANKTM1, a TRP-like channel expressed in nociceptive neurons, is activated by cold temperatures. *Cell* 112: 819-829. S0092867403001582 [pii].
42. Kwan KY, Allchorne AJ, Vollrath MA, Christensen AP, Zhang DS, Woolf CJ, Corey DP (2006) TRPA1 contributes to cold, mechanical, and chemical nociception but is not essential for hair-cell transduction. *Neuron* 50: 277-289. S0896-6273(06)00269-8 [pii];10.1016/j.neuron.2006.03.042 [doi].
43. Karashima Y, Talavera K, Everaerts W, Janssens A, Kwan KY, Vennekens R, Nilius B, Voets T (2009) TRPA1 acts as a cold sensor in vitro and in vivo. *Proc Natl Acad Sci U S A* 106: 1273-1278. 0808487106 [pii];10.1073/pnas.0808487106 [doi].
44. Nilius B, Talavera K, Owsianik G, Prenen J, Droogmans G, Voets T (2005) Gating of TRP channels: a voltage connection? *J Physiol* 567: 35-44.
45. Fleig A, Penner R (2004) The TRPM ion channel subfamily: molecular, biophysical and functional features. *Trends Pharmacol Sci* 25: 633-639. S0165-6147(04)00282-2 [pii];10.1016/j.tips.2004.10.004 [doi].
46. Nadler MJ, Hermosura MC, Inabe K, Perraud AL, Zhu Q, Stokes AJ, Kurotaki T, Kinet JP, Penner R, Scharenberg AM, Fleig A (2001) LTRPC7 is a Mg²⁺-ATP-regulated divalent cation channel required for cell viability. *Nature* 411: 590-595. 10.1038/35079092 [doi];35079092 [pii].
47. Voets T, Nilius B, Hoefs S, van der Kemp AW, Droogmans G, Bindels RJ, Hoenderop JG (2004) TRPM6 forms the Mg²⁺ influx channel involved in intestinal and renal Mg²⁺ absorption. *J Biol Chem* 279: 19-25. 10.1074/jbc.M311201200 [doi];M311201200 [pii].
48. Perraud AL, Fleig A, Dunn CA, Bagley LA, Launay P, Schmitz C, Stokes AJ, Zhu Q, Bessman MJ, Penner R, Kinet JP, Scharenberg AM (2001) ADP-ribose gating of the calcium-permeable LTRPC2 channel revealed by Nudix motif homology. *Nature* 411: 595-599. 10.1038/35079100 [doi];35079100 [pii].
49. Kuhn FJ, Heiner I, Luckhoff A (2005) TRPM2: a calcium influx pathway regulated by oxidative stress and the novel second messenger ADP-ribose. *Pflugers Arch* 451: 212-219. 10.1007/s00424-005-1446-y [doi].

TRPV1 STRUCTURE-FUNCTION STUDY: ROLE OF THE TRP DOMAIN IN TRPV1 ALLOSTERIC GATING

DOCTORAL THESIS

LUCIA GREGORIO TERUEL

50. McKemy DD, Neuhausser WM, Julius D (2002) Identification of a cold receptor reveals a general role for TRP channels in thermosensation. *Nature* 416: 52-58. 10.1038/nature719 [doi];nature719 [pii].
51. Patapoutian A, Peier AM, Story GM, Viswanath V (2003) ThermoTRP channels and beyond: mechanisms of temperature sensation. *Nat Rev Neurosci* 4: 529-539. 10.1038/nrn1141 [doi];nrn1141 [pii].
52. Voets T, Droogmans G, Wissenbach U, Janssens A, Flockerzi V, Nilius B (2004) The principle of temperature-dependent gating in cold- and heat-sensitive TRP channels. *Nature* 430: 748-754.
53. Brauchi S, Orio P, Latorre R (2004) Clues to understanding cold sensation: thermodynamics and electrophysiological analysis of the cold receptor TRPM8. *Proc Natl Acad Sci U S A* 101: 15494-15499. 0406773101 [pii];10.1073/pnas.0406773101 [doi].
54. Andersson DA, Chase HW, Bevan S (2004) TRPM8 activation by menthol, icilin, and cold is differentially modulated by intracellular pH. *J Neurosci* 24: 5364-5369. 10.1523/JNEUROSCI.0890-04.2004 [doi];24/23/5364 [pii].
55. Liu B, Qin F (2005) Functional control of cold- and menthol-sensitive TRPM8 ion channels by phosphatidylinositol 4,5-bisphosphate. *J Neurosci* 25: 1674-1681. 25/7/1674 [pii];10.1523/JNEUROSCI.3632-04.2005 [doi].
56. Rohacs T, Lopes CM, Michailidis I, Logothetis DE (2005) PI(4,5)P2 regulates the activation and desensitization of TRPM8 channels through the TRP domain. *Nat Neurosci* 8: 626-634. nn1451 [pii];10.1038/nn1451 [doi].
57. Colbert HA, Smith TL, Bargmann CI (1997) OSM-9, a novel protein with structural similarity to channels, is required for olfaction, mechanosensation, and olfactory adaptation in *Caenorhabditis elegans*. *J Neurosci* 17: 8259-8269.
58. Kim J, Chung YD, Park DY, Choi S, Shin DW, Soh H, Lee HW, Son W, Yim J, Park CS, Kernan MJ, Kim C (2003) A TRPV family ion channel required for hearing in *Drosophila*. *Nature* 424: 81-84. 10.1038/nature01733 [doi];nature01733 [pii].
59. Vennekens R, Owsianik G, Nilius B (2008) Vanilloid transient receptor potential cation channels: an overview. *Curr Pharm Des* 14: 18-31.
60. Garcia-Sanz N, Fernandez-Carvajal A, Morenilla-Palao C, Planells-Cases R, Fajardo-Sanchez E, Fernandez-Ballester G, Ferrer-Montiel A (2004) Identification of a tetramerization domain in the C terminus of the vanilloid receptor. *J Neurosci* 24: 5307-5314.
61. Garcia-Sanz N, Valente P, Gomis A, Fernandez-Carvajal A, Fernandez-Ballester G, Viana F, Belmonte C, Ferrer-Montiel A (2007) A role of the transient receptor potential domain of vanilloid receptor I in channel gating. *J Neurosci* 27: 11641-11650.

7. REFERENCES

62. Valente P, Garcia-Sanz N, Gomis A, Fernandez-Carvajal A, Fernandez-Ballester G, Viana F, Belmonte C, Ferrer-Montiel A (2008) Identification of molecular determinants of channel gating in the transient receptor potential box of vanilloid receptor I. *FASEB J* .
63. Gunthorpe MJ, Benham CD, Randall A, Davis JB (2002) The diversity in the vanilloid (TRPV) receptor family of ion channels. *Trends Pharmacol Sci* 23: 183-191. S0165-6147(02)01999-5 [pii].
64. Benham CD, Davis JB, Randall AD (2002) Vanilloid and TRP channels: a family of lipid-gated cation channels. *Neuropharmacology* 42: 873-888. S0028390802000473 [pii].
65. Montell C (2005) The TRP superfamily of cation channels. *Sci STKE* 2005: re3.
66. Nilius B, Vennekens R, Prenen J, Hoenderop JG, Droogmans G, Bindels RJ (2001) The single pore residue Asp542 determines Ca²⁺ permeation and Mg²⁺ block of the epithelial Ca²⁺ channel. *J Biol Chem* 276: 1020-1025. 10.1074/jbc.M006184200 [doi];M006184200 [pii].
67. den DE, Hoenderop JG, Nilius B, Bindels RJ (2003) The epithelial calcium channels, TRPV5 & TRPV6: from identification towards regulation. *Cell Calcium* 33: 497-507. S0143416003000654 [pii].
68. Voets T, Janssens A, Prenen J, Droogmans G, Nilius B (2003) Mg²⁺-dependent gating and strong inward rectification of the cation channel TRPV6. *J Gen Physiol* 121: 245-260.
69. Hoenderop JG, Voets T, Hoefs S, Weidema F, Prenen J, Nilius B, Bindels RJ (2003) Homo- and heterotetrameric architecture of the epithelial Ca²⁺ channels TRPV5 and TRPV6. *EMBO J* 22: 776-785. 10.1093/emboj/cdg080 [doi].
70. Bianco SD, Peng JB, Takanaga H, Suzuki Y, Crescenzi A, Kos CH, Zhuang L, Freeman MR, Gouveia CH, Wu J, Luo H, Mauro T, Brown EM, Hediger MA (2007) Marked disturbance of calcium homeostasis in mice with targeted disruption of the Trpv6 calcium channel gene. *J Bone Miner Res* 22: 274-285. 10.1359/jbmr.061110 [doi].
71. Hoenderop JG, van Leeuwen JP, van der Eerden BC, Kersten FF, van der Kemp AW, Merillat AM, Waarsing JH, Rossier BC, Vallon V, Hummler E, Bindels RJ (2003) Renal Ca²⁺ wasting, hyperabsorption, and reduced bone thickness in mice lacking TRPV5. *J Clin Invest* 112: 1906-1914. 10.1172/JCI19826 [doi];112/12/1906 [pii].
72. Tillman DB, Treede RD, Meyer RA, Campbell JN (1995) Response of C fibre nociceptors in the anaesthetized monkey to heat stimuli: correlation with pain threshold in humans. *J Physiol* 485 (Pt 3): 767-774.

TRPV1 STRUCTURE-FUNCTION STUDY: ROLE OF THE TRP DOMAIN IN TRPV1 ALLOSTERIC GATING

DOCTORAL THESIS

LUCIA GREGORIO TERUEL

73. Caterina MJ, Rosen TA, Tominaga M, Brake AJ, Julius D (1999) A capsaicin-receptor homologue with a high threshold for noxious heat. *Nature* 398: 436-441. 10.1038/18906 [doi].
74. Xu H, Ramsey IS, Kotecha SA, Moran MM, Chong JA, Lawson D, Ge P, Lilly J, Silos-Santiago I, Xie Y, DiStefano PS, Curtis R, Clapham DE (2002) TRPV3 is a calcium-permeable temperature-sensitive cation channel. *Nature* 418: 181-186. 10.1038/nature00882 [doi];nature00882 [pii].
75. Smith GD, Gunthorpe MJ, Kelsell RE, Hayes PD, Reilly P, Facer P, Wright JE, Jerman JC, Walhin JP, Ooi L, Egerton J, Charles KJ, Smart D, Randall AD, Anand P, Davis JB (2002) TRPV3 is a temperature-sensitive vanilloid receptor-like protein. *Nature* 418: 186-190. 10.1038/nature00894 [doi];nature00894 [pii].
76. Peier AM, Reeve AJ, Andersson DA, Moqrich A, Earley TJ, Hergarden AC, Story GM, Colley S, Hogenesch JB, McIntyre P, Bevan S, Patapoutian A (2002) A heat-sensitive TRP channel expressed in keratinocytes. *Science* 296: 2046-2049. 10.1126/science.1073140 [doi];1073140 [pii].
77. Strotmann R, Harteneck C, Nunnenmacher K, Schultz G, Plant TD (2000) OTRPC4, a nonselective cation channel that confers sensitivity to extracellular osmolarity. *Nat Cell Biol* 2: 695-702. 10.1038/35036318 [doi].
78. Tominaga M, Caterina MJ, Malmberg AB, Rosen TA, Gilbert H, Skinner K, Raumann BE, Basbaum AI, Julius D (1998) The cloned capsaicin receptor integrates multiple pain-producing stimuli. *Neuron* 21: 531-543. S0896-6273(00)80564-4 [pii].
79. Planells-Cases R, Garcia-Sanz N, Morenilla-Palao C, Ferrer-Montiel A (2005) Functional aspects and mechanisms of TRPV1 involvement in neurogenic inflammation that leads to thermal hyperalgesia. *Pflugers Arch* 451: 151-159.
80. Tominaga M, Tominaga T (2005) Structure and function of TRPV1. *Pflugers Arch* 451: 143-150.
81. Jordt SE, Julius D (2002) Molecular basis for species-specific sensitivity to "hot" chili peppers. *Cell* 108: 421-430. S0092867402006372 [pii].
82. Winter Z, Buhala A, Otvos F, Josvay K, Vizler C, Dombi G, Szakonyi G, Olah Z (2013) Functionally important amino acid residues in the transient receptor potential vanilloid 1 (TRPV1) ion channel - an overview of the current mutational data. *Mol Pain* 9: 30. 1744-8069-9-30 [pii];10.1186/1744-8069-9-30 [doi].
83. Van Der Stelt M, Di M, V (2004) Endovanilloids. Putative endogenous ligands of transient receptor potential vanilloid 1 channels. *Eur J Biochem* 271: 1827-1834. 10.1111/j.1432-1033.2004.04081.x [doi];EJB4081 [pii].
84. Caterina MJ, Julius D (2001) The vanilloid receptor: a molecular gateway to the pain pathway. *Annu Rev Neurosci* 24: 487-517. 10.1146/annurev.neuro.24.1.487 [doi];24/1/487 [pii].

85. Matta JA, Ahern GP (2007) Voltage is a partial activator of rat thermosensitive TRP channels. *J Physiol* 585: 469-482.
86. Vlachova V, Teisinger J, Susankova K, Lyfenko A, Ettrich R, Vyklicky L (2003) Functional role of C-terminal cytoplasmic tail of rat vanilloid receptor 1. *J Neurosci* 23: 1340-1350. 23/4/1340 [pii].
87. Mandadi S, Numazaki M, Tominaga M, Bhat MB, Armati PJ, Roufogalis BD (2004) Activation of protein kinase C reverses capsaicin-induced calcium-dependent desensitization of TRPV1 ion channels. *Cell Calcium* 35: 471-478. 10.1016/j.ceca.2003.11.003 [doi];S014341600300232X [pii].
88. Mandadi S, Tominaga T, Numazaki M, Murayama N, Saito N, Armati PJ, Roufogalis BD, Tominaga M (2006) Increased sensitivity of desensitized TRPV1 by PMA occurs through PKCepsilon-mediated phosphorylation at S800. *Pain* 123: 106-116. S0304-3959(06)00098-4 [pii];10.1016/j.pain.2006.02.016 [doi].
89. Messeguer A, Planells-Cases R, Ferrer-Montiel A (2006) Physiology and pharmacology of the vanilloid receptor. *Curr Neuropharmacol* 4: 1-15.
90. Planells-Cases R, Perez-Paya E, Messeguer A, Carreno C, Ferrer-Montiel A (2003) Small molecules targeting the NMDA receptor complex as drugs for neuropathic pain. *Mini Rev Med Chem* 3: 749-756.
91. Huang J, Zhang X, McNaughton PA (2006) Inflammatory pain: the cellular basis of heat hyperalgesia. *Curr Neuropharmacol* 4: 197-206.
92. Morenilla-Palao C, Planells-Cases R, Garcia-Sanz N, Ferrer-Montiel A (2004) Regulated exocytosis contributes to protein kinase C potentiation of vanilloid receptor activity. *J Biol Chem* 279: 25665-25672. 10.1074/jbc.M311515200 [doi];M311515200 [pii].
93. Zhang X, Huang J, McNaughton PA (2005) NGF rapidly increases membrane expression of TRPV1 heat-gated ion channels. *EMBO J* 24: 4211-4223. 7600893 [pii];10.1038/sj.emboj.7600893 [doi].
94. Park U, Vastani N, Guan Y, Raja SN, Koltzenburg M, Caterina MJ (2011) TRP vanilloid 2 knock-out mice are susceptible to perinatal lethality but display normal thermal and mechanical nociception. *J Neurosci* 31: 11425-11436. 31/32/11425 [pii];10.1523/JNEUROSCI.1384-09.2011 [doi].
95. Peralvarez-Marin A, Donate-Macian P, Gaudet R (2013) What do we know about the Transient Receptor Potential Vanilloid 2 (TRPV2) ion channel? *FEBS J* . 10.1111/febs.12302 [doi].
96. Kanzaki M, Zhang YQ, Mashima H, Li L, Shibata H, Kojima I (1999) Translocation of a calcium-permeable cation channel induced by insulin-like growth factor-I. *Nat Cell Biol* 1: 165-170. 10.1038/11086 [doi].
97. Penna A, Juvin V, Chemin J, Compan V, Monet M, Rassendren FA (2006) PI3-kinase promotes TRPV2 activity independently of channel translocation to the plasma

TRPV1 STRUCTURE-FUNCTION STUDY: ROLE OF THE TRP DOMAIN IN TRPV1 ALLOSTERIC GATING

DOCTORAL THESIS

LUCIA GREGORIO TERUEL

- membrane. *Cell Calcium* 39: 495-507. S0143-4160(06)00019-4 [pii];10.1016/j.ceca.2006.01.009 [doi].
98. Moqrich A, Hwang SW, Earley TJ, Petrus MJ, Murray AN, Spencer KS, Andahazy M, Story GM, Patapoutian A (2005) Impaired thermosensation in mice lacking TRPV3, a heat and camphor sensor in the skin. *Science* 307: 1468-1472. 307/5714/1468 [pii];10.1126/science.1108609 [doi].
 99. Asakawa M, Yoshioka T, Matsutani T, Hikita I, Suzuki M, Oshima I, Tsukahara K, Arimura A, Horikawa T, Hirasawa T, Sakata T (2006) Association of a mutation in TRPV3 with defective hair growth in rodents. *J Invest Dermatol* 126: 2664-2672. 5700468 [pii];10.1038/sj.jid.5700468 [doi].
 100. Nilius B, Watanabe H, Vriens J (2003) The TRPV4 channel: structure-function relationship and promiscuous gating behaviour. *Pflugers Arch* 446: 298-303. 10.1007/s00424-003-1028-9 [doi].
 101. Watanabe H, Vriens J, Janssens A, Wondergem R, Droogmans G, Nilius B (2003) Modulation of TRPV4 gating by intra- and extracellular Ca²⁺. *Cell Calcium* 33: 489-495. S0143416003000642 [pii].
 102. Vriens J, Watanabe H, Janssens A, Droogmans G, Voets T, Nilius B (2004) Cell swelling, heat, and chemical agonists use distinct pathways for the activation of the cation channel TRPV4. *Proc Natl Acad Sci U S A* 101: 396-401. 10.1073/pnas.0303329101 [doi];0303329101 [pii].
 103. Nilius B, Vriens J, Prenen J, Droogmans G, Voets T (2004) TRPV4 calcium entry channel: a paradigm for gating diversity. *Am J Physiol Cell Physiol* 286: C195-C205. 10.1152/ajpcell.00365.2003 [doi];286/2/C195 [pii].
 104. Liedtke W, Friedman JM (2003) Abnormal osmotic regulation in *trpv4*^{-/-} mice. *Proc Natl Acad Sci U S A* 100: 13698-13703. 10.1073/pnas.1735416100 [doi];1735416100 [pii].
 105. Suzuki M, Mizuno A, Kodaira K, Imai M (2003) Impaired pressure sensation in mice lacking TRPV4. *J Biol Chem* 278: 22664-22668. 10.1074/jbc.M302561200 [doi];M302561200 [pii].
 106. Caterina MJ, Leffler A, Malmberg AB, Martin WJ, Trafton J, Petersen-Zeit KR, Koltzenburg M, Basbaum AI, Julius D (2000) Impaired nociception and pain sensation in mice lacking the capsaicin receptor. *Science* 288: 306-313.
 107. Szallasi A, Cruz F, Geppetti P (2006) TRPV1: a therapeutic target for novel analgesic drugs? *Trends Mol Med* 12: 545-554. S1471-4914(06)00197-3 [pii];10.1016/j.molmed.2006.09.001 [doi].
 108. Agopyan N, Bhatti T, Yu S, Simon SA (2003) Vanilloid receptor activation by 2- and 10-microm particles induces responses leading to apoptosis in human airway epithelial cells. *Toxicol Appl Pharmacol* 192: 21-35. S0041008X0300259X [pii].

7. REFERENCES

109. Agopyan N, Head J, Yu S, Simon SA (2004) TRPV1 receptors mediate particulate matter-induced apoptosis. *Am J Physiol Lung Cell Mol Physiol* 286: L563-L572. 10.1152/ajplung.00299.2003 [doi];00299.2003 [pii].
110. Apostolidis A, Brady CM, Yiangou Y, Davis J, Fowler CJ, Anand P (2005) Capsaicin receptor TRPV1 in urothelium of neurogenic human bladders and effect of intravesical resiniferatoxin. *Urology* 65: 400-405. S0090-4295(04)01151-3 [pii];10.1016/j.urology.2004.10.007 [doi].
111. Mason L, Moore RA, Derry S, Edwards JE, McQuay HJ (2004) Systematic review of topical capsaicin for the treatment of chronic pain. *BMJ* 328: 991. 10.1136/bmj.38042.506748.EE [doi];bmj.38042.506748.EE [pii].
112. Knotkova H, Pappagallo M, Szallasi A (2008) Capsaicin (TRPV1 Agonist) therapy for pain relief: farewell or revival? *Clin J Pain* 24: 142-154. 10.1097/AJP.0b013e318158ed9e [doi];00002508-200802000-00009 [pii].
113. Karai L, Brown DC, Mannes AJ, Connelly ST, Brown J, Gandal M, Wellisch OM, Neubert JK, Olah Z, Iadarola MJ (2004) Deletion of vanilloid receptor 1-expressing primary afferent neurons for pain control. *J Clin Invest* 113: 1344-1352. 10.1172/JCI20449 [doi].
114. Jeffrey JA, Yu SQ, Sikand P, Parihar A, Evans MS, Premkumar LS (2009) Selective targeting of TRPV1 expressing sensory nerve terminals in the spinal cord for long lasting analgesia. *PLoS One* 4: e7021. 10.1371/journal.pone.0007021 [doi].
115. Li H, Wang S, Chuang AY, Cohen BE, Chuang HH (2011) Activity-dependent targeting of TRPV1 with a pore-permeating capsaicin analog. *Proc Natl Acad Sci U S A* 108: 8497-8502. 1018550108 [pii];10.1073/pnas.1018550108 [doi].
116. Szallasi A, Cortright DN, Blum CA, Eid SR (2007) The vanilloid receptor TRPV1: 10 years from channel cloning to antagonist proof-of-concept. *Nat Rev Drug Discov* 6: 357-372.
117. Wong GY, Gavva NR (2009) Therapeutic potential of vanilloid receptor TRPV1 agonists and antagonists as analgesics: Recent advances and setbacks. *Brain Res Rev* 60: 267-277. S0165-0173(08)00144-6 [pii];10.1016/j.brainresrev.2008.12.006 [doi].
118. Chizh BA, O'Donnell MB, Napolitano A, Wang J, Brooke AC, Aylott MC, Bullman JN, Gray EJ, Lai RY, Williams PM, Appleby JM (2007) The effects of the TRPV1 antagonist SB-705498 on TRPV1 receptor-mediated activity and inflammatory hyperalgesia in humans. *Pain* 132: 132-141. S0304-3959(07)00308-9 [pii];10.1016/j.pain.2007.06.006 [doi].
119. Gavva NR, Bannon AW, Surapaneni S, Hovland DN, Jr., Lehto SG, Gore A, Juan T, Deng H, Han B, Klionsky L, Kuang R, Le A, Tamir R, Wang J, Youngblood B, Zhu D, Norman MH, Magal E, Treanor JJ, Louis JC (2007) The vanilloid receptor TRPV1 is tonically activated in vivo and involved in body temperature regulation. *J*

TRPV1 STRUCTURE-FUNCTION STUDY: ROLE OF THE TRP DOMAIN IN TRPV1 ALLOSTERIC GATING

DOCTORAL THESIS

LUCIA GREGORIO TERUEL

- Neurosci 27: 3366-3374. 27/13/3366 [pii];10.1523/JNEUROSCI.4833-06.2007 [doi].
120. Gavva NR (2008) Body-temperature maintenance as the predominant function of the vanilloid receptor TRPV1. *Trends Pharmacol Sci* 29: 550-557. S0165-6147(08)00183-1 [pii];10.1016/j.tips.2008.08.003 [doi].
 121. Vidal-Mosquera M, Fernandez-Carvajal A, Moure A, Valente P, Planells-Cases R, Gonzalez-Ros JM, Bujons J, Ferrer-Montiel A, Messeguer A (2011) Triazine-based vanilloid 1 receptor open channel blockers: design, synthesis, evaluation, and SAR analysis. *J Med Chem* 54: 7441-7452. 10.1021/jm200981s [doi].
 122. Meyers JR, MacDonald RB, Duggan A, Lenzi D, Standaert DG, Corwin JT, Corey DP (2003) Lighting up the senses: FM1-43 loading of sensory cells through nonselective ion channels. *J Neurosci* 23: 4054-4065. 23/10/4054 [pii].
 123. Chung MK, Guler AD, Caterina MJ (2008) TRPV1 shows dynamic ionic selectivity during agonist stimulation. *Nat Neurosci* 11: 555-564.
 124. Binshtok AM, Gerner P, Oh SB, Puopolo M, Suzuki S, Roberson DP, Herbert T, Wang CF, Kim D, Chung G, Mitani AA, Wang GK, Bean BP, Woolf CJ (2009) Coapplication of lidocaine and the permanently charged sodium channel blocker QX-314 produces a long-lasting nociceptive blockade in rodents. *Anesthesiology* 111: 127-137. 10.1097/ALN.0b013e3181a915e7 [doi].
 125. Camprubi-Robles M, Planells-Cases R, Ferrer-Montiel A (2009) Differential contribution of SNARE-dependent exocytosis to inflammatory potentiation of TRPV1 in nociceptors. *FASEB J* 23: 3722-3733. fj.09-134346 [pii];10.1096/fj.09-134346 [doi].
 126. Blanes-Mira C, Merino JM, Valera E, Fernandez-Ballester G, Gutierrez LM, Viniegra S, Perez-Paya E, Ferrer-Montiel A (2004) Small peptides patterned after the N-terminus domain of SNAP25 inhibit SNARE complex assembly and regulated exocytosis. *J Neurochem* 88: 124-135. 2133 [pii].
 127. Moiseenkova-Bell VY, Stanciu LA, Serysheva II, Tobe BJ, Wensel TG (2008) Structure of TRPV1 channel revealed by electron cryomicroscopy. *Proc Natl Acad Sci U S A* 105: 7451-7455.
 128. Pingle SC, Matta JA, Ahern GP (2007) Capsaicin receptor: TRPV1 a promiscuous TRP channel. *Handb Exp Pharmacol* 155-171.
 129. Garcia-Martinez C, Morenilla-Palao C, Planells-Cases R, Merino JM, Ferrer-Montiel A (2000) Identification of an aspartic residue in the P-loop of the vanilloid receptor that modulates pore properties. *J Biol Chem* 275: 32552-32558.
 130. Voets T, Prenen J, Vriens J, Watanabe H, Janssens A, Wissenbach U, Boddling M, Droogmans G, Nilius B (2002) Molecular determinants of permeation through

- the cation channel TRPV4. *J Biol Chem* 277: 33704-33710. 10.1074/jbc.M204828200 [doi];M204828200 [pii].
131. Jahnel R, Dreger M, Gillen C, Bender O, Kurreck J, Hucho F (2001) Biochemical characterization of the vanilloid receptor 1 expressed in a dorsal root ganglia derived cell line. *Eur J Biochem* 268: 5489-5496. 2500 [pii].
 132. Wirkner K, Hognestad H, Jahnel R, Hucho F, Illes P (2005) Characterization of rat transient receptor potential vanilloid 1 receptors lacking the N-glycosylation site N604. *Neuroreport* 16: 997-1001. 00001756-200506210-00023 [pii].
 133. Veldhuis NA, Lew MJ, Abogadie FC, Poole DP, Jennings EA, Ivanusic JJ, Eilers H, Bunnett NW, McIntyre P (2012) N-glycosylation determines ionic permeability and desensitization of the TRPV1 capsaicin receptor. *J Biol Chem* 287: 21765-21772. M112.342022 [pii];10.1074/jbc.M112.342022 [doi].
 134. Jordt SE, Tominaga M, Julius D (2000) Acid potentiation of the capsaicin receptor determined by a key extracellular site. *Proc Natl Acad Sci U S A* 97: 8134-8139. 10.1073/pnas.100129497 [doi];100129497 [pii].
 135. Yang F, Cui Y, Wang K, Zheng J (2010) Thermosensitive TRP channel pore turret is part of the temperature activation pathway. *Proc Natl Acad Sci U S A* 107: 7083-7088. 1000357107 [pii];10.1073/pnas.1000357107 [doi].
 136. Grandl J, Kim SE, Uzzell V, Bursulaya B, Petrus M, Bandell M, Patapoutian A (2010) Temperature-induced opening of TRPV1 ion channel is stabilized by the pore domain. *Nat Neurosci* 13: 708-714. nn.2552 [pii];10.1038/nn.2552 [doi].
 137. Yao J, Liu B, Qin F (2010) Pore turret of thermal TRP channels is not essential for temperature sensing. *Proc Natl Acad Sci U S A* 107: E125-E127. 1008272107 [pii];10.1073/pnas.1008272107 [doi].
 138. Grandl J, Hu H, Bandell M, Bursulaya B, Schmidt M, Petrus M, Patapoutian A (2008) Pore region of TRPV3 ion channel is specifically required for heat activation. *Nat Neurosci* .
 139. Szallasi A, Blumberg PM (1999) Vanilloid (Capsaicin) receptors and mechanisms. *Pharmacol Rev* 51: 159-212.
 140. Brauchi S, Orta G, Salazar M, Rosenmann E, Latorre R (2006) A hot-sensing cold receptor: C-terminal domain determines thermosensation in transient receptor potential channels. *J Neurosci* 26: 4835-4840.
 141. Clapham DE, Miller C (2011) A thermodynamic framework for understanding temperature sensing by transient receptor potential (TRP) channels. *Proc Natl Acad Sci U S A* 108: 19492-19497. 1117485108 [pii];10.1073/pnas.1117485108 [doi].
 142. Bhave G, Zhu W, Wang H, Brasier DJ, Oxford GS, Gereau RW (2002) cAMP-dependent protein kinase regulates desensitization of the capsaicin receptor (VR1) by direct phosphorylation. *Neuron* 35: 721-731. S0896627302008024 [pii].

TRPV1 STRUCTURE-FUNCTION STUDY: ROLE OF THE TRP DOMAIN IN TRPV1 ALLOSTERIC GATING

DOCTORAL THESIS

LUCIA GREGORIO TERUEL

143. Bhawe G, Hu HJ, Glauner KS, Zhu W, Wang H, Brasier DJ, Oxford GS, Gereau RW (2003) Protein kinase C phosphorylation sensitizes but does not activate the capsaicin receptor transient receptor potential vanilloid 1 (TRPV1). *Proc Natl Acad Sci U S A* 100: 12480-12485. 10.1073/pnas.2032100100 [doi];2032100100 [pii].
144. Jung J, Shin JS, Lee SY, Hwang SW, Koo J, Cho H, Oh U (2004) Phosphorylation of vanilloid receptor 1 by Ca²⁺/calmodulin-dependent kinase II regulates its vanilloid binding. *J Biol Chem* 279: 7048-7054. 10.1074/jbc.M311448200 [doi];M311448200 [pii].
145. Mohapatra DP, Nau C (2003) Desensitization of capsaicin-activated currents in the vanilloid receptor TRPV1 is decreased by the cyclic AMP-dependent protein kinase pathway. *J Biol Chem* 278: 50080-50090. 10.1074/jbc.M306619200 [doi];M306619200 [pii].
146. Rosenbaum T, Gordon-Shaag A, Munari M, Gordon SE (2004) Ca²⁺/calmodulin modulates TRPV1 activation by capsaicin. *J Gen Physiol* 123: 53-62. 10.1085/jgp.200308906 [doi];123/1/53 [pii].
147. Lainez S, Valente P, Ontoria-Oviedo I, Estevez-Herrera J, Camprubi-Robles M, Ferrer-Montiel A, Planells-Cases R (2010) GABAA receptor associated protein (GABARAP) modulates TRPV1 expression and channel function and desensitization. *FASEB J* 24: 1958-1970. fj.09-151472 [pii];10.1096/fj.09-151472 [doi].
148. Numazaki M, Tominaga T, Takeuchi K, Murayama N, Toyooka H, Tominaga M (2003) Structural determinant of TRPV1 desensitization interacts with calmodulin. *Proc Natl Acad Sci U S A* 100: 8002-8006. 10.1073/pnas.1337252100 [doi];1337252100 [pii].
149. Kim AY, Tang Z, Liu Q, Patel KN, Maag D, Geng Y, Dong X (2008) Pirt, a phosphoinositide-binding protein, functions as a regulatory subunit of TRPV1. *Cell* 133: 475-485.
150. Prescott ED, Julius D (2003) A modular PIP2 binding site as a determinant of capsaicin receptor sensitivity. *Science* 300: 1284-1288. 10.1126/science.1083646 [doi];300/5623/1284 [pii].
151. Ferrer-Montiel A, Garcia-Martinez C, Morenilla-Palao C, Garcia-Sanz N, Fernandez-Carvajal A, Fernandez-Ballester G, Planells-Cases R (2004) Molecular architecture of the vanilloid receptor. *Insights for drug design. Eur J Biochem* 271: 1820-1826.
152. Nieto-Posadas A, Picazo-Juarez G, Llorente I, Jara-Oseguera A, Morales-Lazaro S, Escalante-Alcalde D, Islas LD, Rosenbaum T (2012) Lysophosphatidic acid directly activates TRPV1 through a C-terminal binding site. *Nat Chem Biol* 8: 78-85. nchembio.712 [pii];10.1038/nchembio.712 [doi].

7. REFERENCES

153. Minke B, Cook B (2002) TRP channel proteins and signal transduction. *Physiol Rev* 82: 429-472. 10.1152/physrev.00001.2002 [doi].
154. Birnbaumer L, Yildirim E, Abramowitz J (2003) A comparison of the genes coding for canonical TRP channels and their M, V and P relatives. *Cell Calcium* 33: 419-432. S014341600300068X [pii].
155. Jenke M, Sanchez A, Monje F, Stuhmer W, Weseloh RM, Pardo LA (2003) C-terminal domains implicated in the functional surface expression of potassium channels. *EMBO J* 22: 395-403. 10.1093/emboj/cdg035 [doi].
156. Voets T (2012) Quantifying and Modeling the Temperature-Dependent Gating of TRP Channels. *Rev Physiol Biochem Pharmacol* . 10.1007/112_2011_5 [doi].
157. Hui K, Liu B, Qin F (2003) Capsaicin activation of the pain receptor, VR1: multiple open states from both partial and full binding. *Biophys J* 84: 2957-2968. S0006-3495(03)70022-8 [pii];10.1016/S0006-3495(03)70022-8 [doi].
158. Altomare C, Bucchi A, Camatini E, Baruscotti M, Viscomi C, Moroni A, DiFrancesco D (2001) Integrated allosteric model of voltage gating of HCN channels. *J Gen Physiol* 117: 519-532.
159. Horrigan FT, Aldrich RW (2002) Coupling between voltage sensor activation, Ca²⁺ binding and channel opening in large conductance (BK) potassium channels. *J Gen Physiol* 120: 267-305.
160. Chowdhury S, Chanda B (2013) Free-energy relationships in ion channels activated by voltage and ligand. *J Gen Physiol* 141: 11-28. jgp.201210860 [pii];10.1085/jgp.201210860 [doi].
161. Yao J, Liu B, Qin F (2010) Kinetic and energetic analysis of thermally activated TRPV1 channels. *Biophys J* 99: 1743-1753. S0006-3495(10)00894-5 [pii];10.1016/j.bpj.2010.07.022 [doi].
162. Yao J, Liu B, Qin F (2009) Rapid temperature jump by infrared diode laser irradiation for patch-clamp studies. *Biophys J* 96: 3611-3619. S0006-3495(09)00569-4 [pii];10.1016/j.bpj.2009.02.016 [doi].
163. Fernandez-Ballester G, Ferrer-Montiel A (2008) Molecular modeling of the full-length human TRPV1 channel in closed and desensitized states. *J Membr Biol* 223: 161-172. 10.1007/s00232-008-9123-7 [doi].
164. Labro AJ, Raes AL, Grottesi A, Van HD, Sansom MS, Snyders DJ (2008) Kv channel gating requires a compatible S4-S5 linker and bottom part of S6, constrained by non-interacting residues. *J Gen Physiol* 132: 667-680. jgp.200810048 [pii];10.1085/jgp.200810048 [doi].
165. Labro AJ, Boulet IR, Choveau FS, Mayeur E, Bruyins T, Loussouarn G, Raes AL, Snyders DJ (2011) The S4-S5 linker of KCNQ1 channels forms a structural scaffold with the S6 segment controlling gate closure. *J Biol Chem* 286: 717-725. M110.146977 [pii];10.1074/jbc.M110.146977 [doi].

TRPV1 STRUCTURE-FUNCTION STUDY: ROLE OF THE TRP DOMAIN IN TRPV1 ALLOSTERIC GATING

DOCTORAL THESIS

LUCIA GREGORIO TERUEL

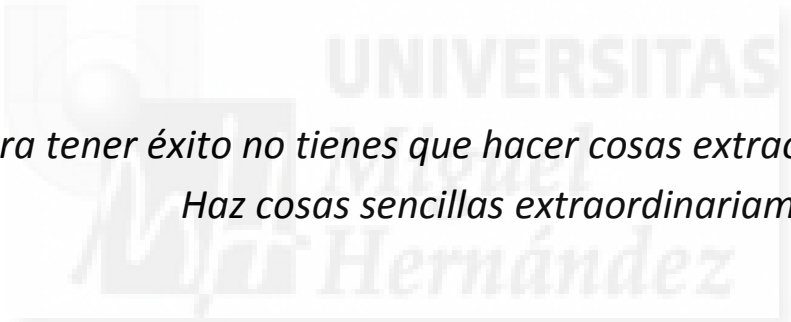
166. Brauchi S, Orta G, Mascayano C, Salazar M, Raddatz N, Urbina H, Rosenmann E, Gonzalez-Nilo F, Latorre R (2007) Dissection of the components for PIP2 activation and thermosensation in TRP channels. *Proc Natl Acad Sci U S A* 104: 10246-10251. 0703420104 [pii];10.1073/pnas.0703420104 [doi].
167. Ufret-Vincenty CA, Klein RM, Hua L, Angueyra J, Gordon SE (2011) Localization of the PIP2 sensor of TRPV1 ion channels. *J Biol Chem* 286: 9688-9698. M110.192526 [pii];10.1074/jbc.M110.192526 [doi].
168. Hellwig N, Albrecht N, Harteneck C, Schultz G+, Schaefer M (2005) Homo- and heteromeric assembly of TRPV channel subunits. *Journal of Cell Science* 118: 917-928.
169. Zhang F, Liu S, Yang F, Zheng J, Wang K (2011) Identification of a tetrameric assembly domain in the C-terminus of heat-activated TRPV1 channels. *J Biol Chem* . M111.223941 [pii];10.1074/jbc.M111.223941 [doi].
170. Grycova L, Holendova B, Bumba L, Bily J, Jirku M, Lansky Z, Teisinger J (2012) Integrative binding sites within intracellular termini of TRPV1 receptor. *PLoS One* 7: e48437. 10.1371/journal.pone.0048437 [doi];PONE-D-12-07328 [pii].
171. Lin Z, Chen Q, Lee M, Cao X, Zhang J, Ma D, Chen L, Hu X, Wang H, Wang X, Zhang P, Liu X, Guan L, Tang Y, Yang H, Tu P, Bu D, Zhu X, Wang K, Li R, Yang Y (2012) Exome sequencing reveals mutations in TRPV3 as a cause of Olmsted syndrome. *Am J Hum Genet* 90: 558-564. S0002-9297(12)00091-2 [pii];10.1016/j.ajhg.2012.02.006 [doi].
172. Valente P, Fernandez-Carvajal A, Camprubi-Robles M, Gomis A, Quirce S, Viana F, Fernandez-Ballester G, Gonzalez-Ros JM, Belmonte C, Planells-Cases R, Ferrer-Montiel A (2011) Membrane-tethered peptides patterned after the TRP domain (TRPducins) selectively inhibit TRPV1 channel activity. *FASEB J* 25: 1628-1640. fj.10-174433 [pii];10.1096/fj.10-174433 [doi].
173. Liu B, Hui K, Qin F (2003) Thermodynamics of heat activation of single capsaicin ion channels VR1. *Biophys J* 85: 2988-3006. S0006-3495(03)74719-5 [pii];10.1016/S0006-3495(03)74719-5 [doi].
174. Labarga A, Valentin F, Anderson M, Lopez R (2007) Web services at the European bioinformatics institute. *Nucleic Acids Res* 35: W6-11. gkm291 [pii];10.1093/nar/gkm291 [doi].
175. Gonnet GH, Cohen MA, Benner SA (1992) Exhaustive matching of the entire protein sequence database. *Science* 256: 1443-1445.
176. Long SB, Tao X, Campbell EB, MacKinnon R (2007) Atomic structure of a voltage-dependent K⁺ channel in a lipid membrane-like environment. *Nature* 450: 376-382. nature06265 [pii];10.1038/nature06265 [doi].

177. Lishko PV, Procko E, Jin X, Phelps CB, Gaudet R (2007) The ankyrin repeats of TRPV1 bind multiple ligands and modulate channel sensitivity. *Neuron* 54: 905-918.
178. Yadav MK, Leman LJ, Price DJ, Brooks CL, III, Stout CD, Ghadiri MR (2006) Coiled coils at the edge of configurational heterogeneity. Structural analyses of parallel and antiparallel homotetrameric coiled coils reveal configurational sensitivity to a single solvent-exposed amino acid substitution. *Biochemistry* 45: 4463-4473. 10.1021/bi060092q [doi].
179. Schwede T, Kopp J, Guex N, Peitsch MC (2003) SWISS-MODEL: An automated protein homology-modeling server. *Nucleic Acids Res* 31: 3381-3385.
180. Vriend G (1990) WHAT IF: a molecular modeling and drug design program. *J Mol Graph* 8: 52-6, 29.
181. Guex N, Peitsch MC (1997) SWISS-MODEL and the Swiss-PdbViewer: an environment for comparative protein modeling. *Electrophoresis* 18: 2714-2723. 10.1002/elps.1150181505 [doi].
182. Guerois R, Nielsen JE, Serrano L (2002) Predicting changes in the stability of proteins and protein complexes: a study of more than 1000 mutations. *J Mol Biol* 320: 369-387. 10.1016/S0022-2836(02)00442-4 [doi];S0022-2836(02)00442-4 [pii].
183. Schymkowitz J, Borg J, Stricher F, Nys R, Rousseau F, Serrano L (2005) The FoldX web server: an online force field. *Nucleic Acids Res* 33: W382-W388. 33/suppl_2/W382 [pii];10.1093/nar/gki387 [doi].
184. Phillips JC, Braun R, Wang W, Gumbart J, Tajkhorshid E, Villa E, Chipot C, Skeel RD, Kale L, Schulten K (2005) Scalable molecular dynamics with NAMD. *J Comput Chem* 26: 1781-1802. 10.1002/jcc.20289 [doi].
185. Mackerell AD, Jr., Feig M, Brooks CL, III (2004) Extending the treatment of backbone energetics in protein force fields: limitations of gas-phase quantum mechanics in reproducing protein conformational distributions in molecular dynamics simulations. *J Comput Chem* 25: 1400-1415. 10.1002/jcc.20065 [doi].

TRPV1 STRUCTURE-FUNCTION STUDY: ROLE OF THE TRP DOMAIN IN TRPV1 ALLOSTERIC GATING

DOCTORAL THESIS

LUCIA GREGORIO TERUEL



*Para tener éxito no tienes que hacer cosas extraordinarias.
Haz cosas sencillas extraordinariamente bien.*

Jim Rohn.





8. ACKNOWLEDGMENT



TRPV1 STRUCTURE-FUNCTION STUDY: ROLE OF THE TRP DOMAIN IN TRPV1 ALLOSTERIC GATING

DOCTORAL THESIS

LUCIA GREGORIO TERUEL

Bueno, después de este largo camino hay muchísima gente a la que tengo que agradecer muchas cosas. Así es que, pido perdón de antemano por si se me olvida alguna de esas personas que, en mayor o menor medida, me han ayudado, apoyado, acompañado y compartido algo conmigo durante estos 6 años.

En primer lugar, me gustaría agradecer al Prof. Antonio Ferrer que me diera la oportunidad de haber hecho esta tesis. Que después de ver una charla de “su eminencia” Ramón Latorre, fui de cabeza a su despacho y le dije...”Antonio, yo quiero trabajar en esto de los TRPs” y él me acogió, me enseñó y me ayudó a querer un poco más la ciencia. De nuevo, gracias. También a Grego; gracias por tu ayuda con esos modelos estructurales que tanto me cuesta visualizar...jeje. Pero más por la disposición que siempre has mostrado para ayudarme ante cualquier problema. Gracias. En este grupo también quisiera añadir a unas personas que, nos ayudan mucho más de lo que nos pensamos y valoramos, y siempre pasan injustamente desapercibidos en estos momentos. A mi secretaria favorita, May, Carmen, Javier y Raquelita. Sois lo más. Gracias.

Los siguientes en la lista, sin dudarlo ni un momento, son mi familia. Ese apoyo incondicional que solo unos padres pueden dar no es comparable con ninguna otra cosa. Mamá, que siempre has creído en mí y en “mi estrella”. Y papá, porque siempre me haces reír y por tus abrazos de “energía positiva”. GRACIAS. Y, por supuesto, mi hermana María. SIIIIIST!!! Mia sorellina!! Por fin! Una etapa menos y un pasito más. ¿Y ahora qué?... ¿ves? Nos pasa a todos ;). Tú que siempre, con tus sabias palabras, me has apoyado y hecho feliz en cada paso importante de mi vida, espero que nunca dejes de hacerlo. Y que, cuando más lo necesites, pueda devolverte todo el bien y la felicidad que has añadido a mi vida durante todos estos años. A todos, aunque pronto estaremos lejos de nuevo, sabéis que SIEMPRE os tengo en mi pensamiento. Gracias a los tres, os quiero.

Los siguientes en la lista, como no podrían ser otros, son mis “papás” científicos Núria y Pier. A mi “mamá” científica le quiero agradecer el legado (aunque ella piense que es más un castigo) y el haberme enseñado taaaanto en estos años, y no sólo en lo que a ciencia se refiere. Y a mi “papá” científico Pier...no sé ni por dónde empezar. Quizá por todo lo que me has enseñado, por las risas, por las charlas, por las fiestas...no lo sé. Pero creo que hay una frase que lo resume bastante bien: porque sin ti a mi lado en estos 6 años, no habría llegado donde estoy hoy. Por todo eso y mucho más, gracias.

Ay mis ferrerines... ¿qué voy a decir de ellos? Creo que no sé tantos adjetivos bonitos para describirlos. A toooodos los que son y fueron ferrerines, muchas gracias por compartir conmigo grandes momentos. Lo que yo creo más importante y siempre llevaré en mi memoria, es el compañerismo que nos caracteriza. Cuando algo fallaba (bien sea experimental o no) siempre había alguien de vosotros ahí para arreglarlo. Lo nuestro es increíble. Y, como siempre decimos, sé que ésto no lo encontraremos en ningún otro sitio. Ahora, permitidme hacer alguna mención especial. Aaron, gran compañero de batallas, de largos días de laboratorio y de muchas otras cosas. Gracias a ti, descubrí que las manías están sobreestimadas y que “la boquica es muy castigá”. Pero siempre, siempre, tus lecciones venían acompañadas de tu sonrisa que me encanta. ¡Has sido totalmente mi equilibrio! Y al Rober (sp), aaaaaayyyyyy, como te voy a echar de menos, jodío!! Espero que encuentres a alguien a quien llorarle y contarle los marujeos. Pero yo tengo clarísimo que no encontraré a nadie como tú, porque eres único. Genio, que eres un p..o genio!!!! Y, por supuesto, a todos los demás. Aunque,

desafortunadamente, no me cabe todo lo que os quiero decir! Cloti, Gemi, MeryGrace, Ainara, Rober cp, Isa, Paco, Sakthi, Vero, Christoph, Antonio, Maite, Wen, Efrén... gracias a todos!!

A continuación, no puedo dejar de agradecer a mis “comadres” el haberme acompañado en esta etapa. Desde los últimos años de carrera habéis sido un pilar fundamental para mí en los buenos y malos momentos. Hemos compartido horas de estudio, comidas, viajes, crisis (experimentales o no)...y no cambiaría ni un solo minuto de todo lo vivido con vosotras. Os quiero nenis!

También quiero agradecer a mis amigos “no científicos” su compañía y apoyo en esta andadura. A los “Outtrépidos”, que por fin creo que voy a completar una aventura... Y a mis “bereberes”, mis chicas, más de 15 años ya ha vuestro lado. Porque todos y cada uno de vosotros lo habéis hecho más fácil en algún momento. Gracias.

Y Por último, como dicen los ingleses “the last but not the least”, debo dar infinitas gracias a mi marido, Roberto. Porque nunca has tenido una mala cara cuando llegaba tarde del labo. Porque siempre has creído en mí y en lo que hacía. Porque tu apoyo y confianza han ido siempre más allá de lo que cualquier persona cabe esperar. Y porque si yo te digo ven, estás dispuesto a dejarlo todo...GRACIAS. Te quiero.



**TRPV1 STRUCTURE-FUNCTION STUDY: ROLE OF THE TRP DOMAIN IN
TRPV1 ALLOSTERIC GATING**

DOCTORAL THESIS

LUCIA GREGORIO TERUEL







9. APPENDIX



9.1 ABBREVIATION LIST

cAMP: Cyclic adenosine monophosphate
2-APB: 2-Aminoethoxydiphenyl borate
ATP: Adenosín triphosphate
DNA: Desoxyribonucleic acid
RNA: Ribonucleic acid
CaM: Calmoduline
CaMKII: *Ca²⁺ /Calmodulin-Dependent Protein Kinase II*
cDNA: Complementary desoxyribonucleic acid
CGRP: *Calcitonin gene related peptide*
CNG: *Cyclic nucleotide-gated ion channel*
DRG: Dorsal Root Ganglial
DTT: Dithiothreitol
EC50: Effective concentration 50%
Fluo-4 NW: Fluo-4 no-wash
G: Conductance
GABARAP: *Gamma-aminobutyric acid receptor-associated protein*
ΔG_o: Free energy difference between open and closed state at 0 mV and 25°C
G_{max}: Maximum conductance
HCN: *Hyperpolarization-activated cyclic nucleotide-modulated ion channel*
HEK293: *Human Embryonic Kidney 293*
I: current Intensity
I_{max}: maximum current Intensity
IP3: Inositol trisphosphate
Kcs: *A K⁺ channel from Streptomyces lividans*
NaCl: Calcium chloride
PBS: phosphate buffered saline
PIP2: Phosphatidylinositol 4,5-bisphosphate
Pirt: *Posphoinositide interacting regulator of TRP*
PKA: Protein kinase A
PKC: Protein kinase C
PKD: *Polycystic kidney disease*
PLC: Fosfolipase C
Q10: *Temperature coefficient*
RNA: Ribonucleic acid
RTX: Resiniferatoxin
S1-S6: Transmembrane segments 1 to 6
SDS: Sodium dodecyl sulfate
SDS-PAGE: *Sodium dodecyl sulfate polyacrylamide gel electrophoresis*
SNARE: *SNAP (Soluble NSF Attachment Protein) Receptors*
SP: Substance P
TG: Trigeminal ganglia
TRP: *Transient Receptor Potencial*
TRPA: *Transient Receptor Potencial Ankyrin*
TRPC: *Transient Receptor Potencial Canonical*

TRPM: *Transient Receptor Potencial Melastatin*

TRPML: *Transient Receptor Potencial Mucolipin*

TRPN: *Transient Receptor Potencial (NOMPC) No Mechanoreceptor Potencial C*

TRPP: *Transient Receptor Potencial Polycystin*

TRPV: *Transient Receptor Potencial Vanilloid*

TRPY: *Transient Receptor Potencial Yeast*

V: Voltage

V_{0.5}: voltage at which 50% of channels are open

Zg: gating valence

τ : Rate constant of gating process



9.2 ARTICLES

- **Gregorio-Teruel L**, Valente P, González-Ros JM, Fernández-Ballester G, Ferrer-Montiel A. Mutation of I696 and W697 in the TRP box of Vanilloid Receptor Subtype I modulates allosteric channel activation. *J Gen Physiol.* (Submitted)







“...Salí a la impresionante terraza y me fascinaron aquellas excelentes vistas que abarcaban casi toda la costa de Capri. No me había percatado que al subir tantas cuestas nos habíamos situado en una evaluación privilegiada. A veces en la vida pasa lo mismo: la dificultad de la pendiente te hace olvidar que no paras de progresar y subir.”

Albert Espinosa.

